

**MOLECULAR ANALYSIS OF YEAST SPLICEOSOME
COMPONENTS FOR THEIR ROLES IN
AGROBACTERIUM-YEAST DNA TRANSFER**

WANG BINGQING

NATIONAL UNIVERSITY OF SINGAPORE

2014

**MOLECULAR ANALYSIS OF YEAST SPLICEOSOME
COMPONENTS FOR THEIR ROLES IN
AGROBACTERIUM-YEAST DNA TRANSFER**

WANG BINGQING

(M. Sc.)


**A THESIS SUBMITTED
FOR THE DEGREE OF DOCTOR OF PHILOSOPHY
DEPARTMENT OF BIOLOGICAL SCIENCES
NATIONAL UNIVERSITY OF SINGAPORE**

2014

DECLARATION

I hereby declare that this thesis is my original work and it has been written by me in its entirety. I have duly acknowledged all the sources of information which have been used in the thesis.

This thesis has also not been submitted for any degree in any university previously.



Wang Bingqing

11 November 2014

ACKNOWLEDGEMENTS

The research work presented in this thesis was primarily conducted in Associate Professor Pan Shen Quan's group in the Department of Biological Science of National University of Singapore (NUS). During my PhD study, I met many nice friends who gave me great encouragement and kind help. Here I would like to thank them sincerely.

First of all, I would like to express my deep gratitude to my supervisor Associate Professor Pan Shen Quan for his technical advice, professional guidance, patience and support throughout my PhD study. It will not be possible to have this thesis without his encouragement, useful discussions, constant support and practical help to this research project. I am extremely grateful to my supervisor for his invaluable suggestions during the preparation of this thesis. I believe and appreciate that Prof. Pan with his insightful view and highly standard requirements to the research has an extraordinary impact on my future research career.

I would also like to thank Professor Hew Choy Leong, Professor Wong Sek Man, Professor Yu Hao and Assistant Professor Xu Jian for their valuable advice and kind help during my research progress.

My grateful thanks are also extended to my coworkers and team members in our laboratory: Dr. Tu Haitao, Dr. Yang Qinghua, Dr. Li Xiaoyang, Dr. Chen Zikai, Dr. Sun Deying, Dr. Wen Yi, Dr. Niu Shengniao, Dr. Lim Zijie, Peng Ling, for their kind discussions, suggestions and help on my research work. I would like to take this opportunity to express my gratitude to my family and other friends for their support and encouragement during the course of this study. There are many challenges, ups and downs in the past several years of studies, no matter what happens, they are always on

the standby and encourage me, comfort me.

Finally, I would like to thank all who have helped and inspired me during my PhD study. I especially want to thank the China Scholarship Council and National University of Singapore for providing the research scholarship for my research, and I am really grateful.

TABLE OF CONTENTS

ACKNOWLEDGEMENTS	I
TABLE OF CONTENTS.....	III
SUMMARY	VII
MANUSCRIPTS RELATED TO THIS STUDY	IX
LIST OF TABLES.....	X
LIST OF FIGURES	XI
LIST OF ABBREVIATION	XIII
CHAPTER 1 INTRODUCTION.....	1
1.1. <i>Agrobacterium tumefaciens</i> : phytopathogen in genetic applications.....	2
1.2. <i>Agrobacterium</i> -mediated gene transfer and molecular basis	3
1.2.1. Detection of chemical signal	4
1.2.2. Cell-cell contact and host attachment of <i>Agrobacterium</i>	5
1.2.3. T-complex formation and entry into host plant cell	7
1.2.4. Nuclear target and DNA integration.....	8
1.3. Host factors involved in <i>Agrobacterium</i> -mediated gene transfer	11
1.3.1. Host factors involved in the cell attachment and virulence factors transfer ..	11
1.3.2. Host factors involved in nuclear targeting.....	12
1.3.3. Host factors involved in chromatin targeting and T-DNA integration	13
1.4. Objectives of this study.....	14
CHAPTER 2. MATERIALS AND METHODS.....	15
2.1. Stains, plasmids, primers and cultures	15

2.2. DNA manipulations.....	29
2.2.1. General DNA manipulation techniques.....	29
2.2.2. Genomic DNA preparation.....	29
2.2.3. Transformation of <i>A. tumefaciens</i> by electroporation	30
2.2.4. Lithium acetate transformation of yeast.....	30
2.2.5. Real-time PCR.....	31
2.3. RNA manipulations.....	31
2.3.1. Total RNA extraction from yeast cells	31
2.3.2. Total RNA extraction from <i>A. thaliana</i> and <i>N. benthamiana</i>	32
2.3.3. Reverse transcription polymerase chain reaction (RT-PCR).....	32
2.4. Protein analysis	32
2.4.1. Total proteins extraction from yeast cells.....	32
2.4.2. SDS-PAGE gel electrophoresis and Coomassie blue staining	33
2.4.3. Immunofluorescence (IF)	35
2.5. <i>Agrobacterium</i>-mediated transformation (AMT) of yeast.....	35
2.6. Quantitative real-time PCR detection of T-DNA	38
2.7. Visualization of <i>Agrobacterium</i>-delivered VirE2 by Split-GFP assay	38
2.8. Virus induced gene silencing (VIGS).....	39
2.9. Tumorigenesis	40
2.9.1. In planta tumor assay.....	40
2.9.2. Leaf-disk tumorigenesis assay.....	40
2.10. Agroinfiltration	41
2.11. Imaging techniques	42
2.11.1. Sample preparation for microscopy imaging	42
2.11.2. Fluorescent microscopy and confocal microscopy.....	42

CHAPTER 3. INVOLVEMENT OF SPLICEOSOME COMPONENTS IN

AGROBACTERIUM-YEAST GENE TRANSFER	43
3.1. Introduction of BUD31p and NineTeen Complex (NTC)	43
3.1.1. Literature review of <i>BUD31</i> gene	43
3.1.2. Literature review of NineTeen Complex (NTC)	47
3. 2. Yeast <i>BUD31</i> is involved in <i>Agrobacterium</i>-mediated transformation	52
3.2.1. Yeast mutant <i>bud31Δ</i> shows decreased efficiency of <i>Agrobacterium</i> -mediated transformation	52
3.3.2. The effect of yeast <i>BUD31</i> in <i>Agrobacterium</i> -mediated transformation is specific.....	55
3.3. Yeast NineTeen Complex (NTC) is involved in <i>Agrobacterium</i>-mediated transformation	57
3.4. Discussion	62
 CHAPTER 4. EFFECTS OF <i>BUD31</i> AND NTC GENES IN THE	
AGROBACTERIUM-YEAST GENE TRANSFER	68
4.1. Characterization of Yeast Bud31p	68
4.1.1. Yeast Bud31p is a nuclear protein	68
4.1.2. Yeast mutant <i>bud31Δ</i> showed different microtubule structures	68
4.1.3. Total protein profile of yeast mutant <i>bud31Δ</i> and WT	71
4.2. Yeast mutant <i>bud31Δ</i> showed a decreased competency to receive <i>Agrobacterium</i>- delivered T-DNA	71
4.3. Yeast mutant <i>bud31Δ</i> showed a decreased competency to receive <i>Agrobacterium</i>-delivered VirE2	73
4.4. VirD2 nuclear localization process was not affected in yeast mutant <i>bud31Δ</i>	77
4.5. Integration of T-DNA was not affected in yeast mutant <i>bud31Δ</i>	81
4.6. Discussion	83

CHAPTER 5. EFFECTS OF BUD31P PLANT HOMOLOG IN	
<i>AGROBACTERIUM</i>-MEDITATED TRANSFORMATION.....	87
5.1. Bud31p is conserved across eukaryotes	87
5.2. Bud31p Homolog of <i>Arabidopsis thaliana</i>	89
5.3.1. Expression pattern of <i>Arabidopsis AT4G21110</i> upon agroinfection	89
5.3.2. Genotyping of <i>AT4G21110</i> T-DNA insertion lines.....	90
5.3. Bud31p Homolog of <i>Nicotiana benthamiana</i>	92
5.4. Generation of <i>NbBUD31</i>-silencing plant by virus-induced gene silencing	
(VIGS)	95
5.5. Silencing of <i>NbBUD31</i> did not affect tumor formation	98
5.5.1. In planta tumorigenesis on silenced plants	98
5.5.2. Leaf-disk tumorigenesis on silenced plants.....	98
5.6. Silencing of <i>NbBUD31</i> did not affect transient expression and VirE2	
translocation	101
5.6.1. Transient expression on silenced plants	101
5.6.2. VirE2 translocation on silenced plants	104
5.7. <i>NbBUD31</i> did not show specific sub-cellular localization in <i>N. benthamiana</i>.	
.....	106
5.8. Discussion.....	108
CHAPTER 6. GENERAL CONCLUSIONS AND FUTURE PROSPECTS	110
6.1. General conclusions	110
6.2. Future prospects.....	111
BIBLIOGRAPHY	113

SUMMARY

Agrobacterium tumefaciens is a natural plant pathogen that can cause crown gall disease by transferring a single-stranded DNA (T-DNA) into host cells. Under laboratory condition, *A. tumefaciens* can be induced to transfer T-DNA into a wide range of other eukaryotic species, including yeast, fungal and mammalian cells. It has been widely used as a natural genetic engineer in biotechnology. Although bacteria factors involved in the transformation process have been well characterized, host factors that facilitate the process remain ambiguous. In this study, *Saccharomyces cerevisiae* was used as a model organism to investigate host factors involved in transformation process due to its small genome size and easy manipulation.

In this study, yeast spliceosome component Bud31p and its associated NineTeen Complex (NTC) were identified to play important role in *Agrobacterium*-mediated transformation (AMT). Interestingly, Bud31p and other NTC core proteins had opposite effects on AMT. Deletion of yeast *BUD31* and *SNT309* decreased the efficiency of *Agrobacterium*-mediated transformation while deletion of *SYF2* increased the transformation efficiency.

To investigate the role of *BUD31* on *Agrobacterium*-yeast gene transfer, a variety of approaches were adopted, including molecular genetics, biochemistry and bio-imaging. Experimental data showed that the decrease of AMT efficiency of *bud31Δ* probably attributes to the decrease in the competency to receive *Agrobacterium*-delivered T-DNA and virulence protein VirE2. On the other hand, VirD2 nuclear targeting process and T-DNA integration process were not affected in *bud31Δ*.

Sequence analysis showed Bud31p protein is highly conserved across eukaryotes.

To reveal the role of *BUD31* in AMT, the effect of *BUD31* plant homolog on AMT was investigated. *NbBUD31*-silencing *Nicotiana benthamiana* was generated by virus-induced gene silencing (VIGS). Silencing of *NbBUD31* in *N. benthamiana* did not affect tumor formation, transient expression and VirE2 delivery. The different effects of yeast *BUD31* gene and its plant homolog on AMT suggested a different pathway of AMT in natural host plant from the non-natural recipient yeast.

This study is the first to report the involvement of yeast spliceosome component Bud31p and its associated NineTeen Complex in AMT process. A knockout of *BUD31* reduced the competency of yeast cells to receive *Agrobacterium*-delivered T-DNA and VirE2 protein. This paves the way to further study the newly identified host factors in AMT process and the relationship between T-DNA/virulence protein delivery and *Agrobacterium*-mediated transformation efficiency.

MANUSCRIPTS RELATED TO THIS STUDY

Wang B. and Pan S.Q. (2014) A yeast spliceosome component Bud31p regulates *Agrobacterium*-Yeast DNA Transfer. (Manuscript in preparation)

LIST OF TABLES

Table 2.1. Bacterial and yeast stains used in this study	16
Table 2.2. Plasmids used in this study	22
Table 2.3. Media and solutions used in this study	24
Table 2.4. Primers used in this study	26
Table 2.5. Buffers and solutions used in SDS-PAGE gel electrophoresis	34
Table 3.1. Comparison of the effects on AMT efficiency between other proteins and Bud31p.....	65

LIST OF FIGURES

Figure 1.1 Network of interactions between translocated <i>Agrobacterium</i> effectors and host cell proteins.	9
Figure 2.1. Standard protocol for <i>Agrobacterium</i> -mediated transformation of yeast.	37
Figure 3.1. Yeast mutant <i>bud31Δ</i> shows decreased <i>Agrobacterium</i> -mediated transformation efficiency.	54
Figure 3.2. Complementation experiment confirmed the important role of yeast Bud31p in AMT process.	56
Figure 3.3. The involvement of Yeast NineTeen complex (NTC) components in <i>Agrobacterium</i> -mediated transformation.	59
Figure 3.4. Switching off the expression of Prp19p and Cef1p caused decrease in AMT efficiency.	61
Figure 4. 1 Localization of yeast Bud31p with EGFP reporter.	69
Figure 4.2 Characterization of Yeast Bud31p.	70
Figure 4.3. Real-time PCR analysis of T-DNA delivery.	72
Figure 4.4. A split-GFP assay for visualization of VirE2 inside recipient cells.	74
Figure 4.5. Yeast mutant <i>bud31Δ</i> showed a decreased competency to receive <i>Agrobacterium</i> -delivered VirE2.	76
Figure 4.6. VirD2 nucleus targeting process is not affected in yeast mutant <i>bud31Δ</i>	80
Figure 4.7. Integration of T-DNA was not affected in yeast mutant <i>bud31Δ</i>	82
Figure 4.8. Summary of the role of yeast <i>BUD31</i> on AMT.	84
Figure 5.1 Bud31p is conserved across eukaryotes.	88
Figure 5.2. Expression patterns of <i>A. thaliana</i> AT4G21110 and <i>S. cerevisiae</i> Bud31p upon agroinfection.	91

Figure 5.3. cDNA sequence alignment of predicted two isoforms of <i>NbBUD31</i>	93
Figure 5.4. cDNA sequence comparison of predicted <i>N. benthamiana NbBUD31</i> and <i>A. thaliana AT4G21110</i>	94
Figure 5.5. Effect of VIGS on <i>N. benthamiana</i>	97
Figure 5.6. Silencing of <i>NbBUD31</i> did not affect tumor formation in AMT.....	100
Figure 5.7. Silencing of <i>NbBUD31</i> did not affect transient expression.....	103
Figure 5.8. Silencing of <i>NbBUD31</i> did not affect VirE2 translocation.	105
Figure 5.9. Localization of <i>N. benthamiana NbBUD31</i> with GFP reporter.....	107

LIST OF ABBREVIATION

μg	microgram(s)		acetic acid
μl	microliter(s)	FISH	fluorescent <i>in situ</i>
μm	micrometer(s)		hybridization
Amp	ampicillin	g	gram(s)
AMT	<i>Agrobacterium</i> -mediated transformation	GFP	green fluorescence protein
AR	androgen receptor	GUS	β-D-glucuronidase
AS	acetosyringone	h	hour(s)
ATP	adenosine triphosphate	HR	homologous recombination
BMV	brome mosaic virus	HUVEC	human umbilical vein endothelial cells
bp	base pair(s)	kb	kilobase(s)
BSA	bovine serum albumin	kDa	kilodalton(s)
Cef	cefotaxime	Km	kanamycin
CM	cocultivation medium	LB	Luria-Bertani medium
DAPI	4', 6-diamidino -2-phenylindole	LiAc	lithium acetate
DNase	deoxyribonuclease	M	mole(s)
DSBR	double-strand break repair	ml	milliliter(s)
dsDNA	double-stranded DNA	mM	millimole(s)
DTT	dithiothreitol	MS	Murashige & Skoog
EDTA	ethylenediaminetet	NHEJ	non-homologous end

	joining	SDS	sodium dodecyl sulfate
NLS	nuclear localization signal	snRNA	small nuclear RNA
nm	nanometer(s)	ss	single-strand
NTC	NineTeen Complex	SSA	single-strand annealing
OD	optical density	T4SS	type IV secretion system
ORF	open reading frame	TAP	tandem affinity purification
PAGE	polyacrylamide gel electrophoresis	T-DNA	transferred DNA
PBS	phosphate buffered saline	TDR	telomerase deletion response
PCR	polymerase chain reaction	TdT	terminal deoxynucleotidyl- transferase
PEG	polyethylene glycol	Ti	tumor-inducing
RFP	red fluorescent protein	VIGS	virus induced gene silencing
RNase	ribonuclease	<i>vir</i>	virulence
RNP	ribonucleoprotein	WT	wild type
rpm	revolutions per min	YKO	yeast knock-out
RT-PCR	reverse transcription polymerase chain reaction	yTHC	Tet-promoters Hughes collection
SD	synthetic dropout		

Chapter 1 Introduction

Agrobacterium tumefaciens is a natural plant pathogen which causes tumors in plants by transferring a single stranded T-DNA molecule from the bacterium into host cell nucleus. Naturally, *A. tumefaciens* can only transfer DNA into most dicotyledonous plants and some of monocotyledonous plants. Under laboratory conditions, *A. tumefaciens* can also be induced to transfer T-DNA into a wide range of other eukaryotic species, such as yeast (Bundock, den Dulk-Ras et al. 1995), fungi (de Groot, Bundock et al. 1998) and mammalian cells (Relic, Andjelkovic et al. 1998; Kunik, Tzfira et al. 2001). With the unique capability of genome manipulation for various species, *A. tumefaciens* has become an important tool as “genetic engineer” for transgenic applications in biotechnology.

For a long period of time, *Agrobacterium*-mediated transformation (AMT) was the only known case of inter-kingdom DNA transfer in nature. Its DNA transfer process has been widely studied in a wide range of hosts. The molecular basis of its DNA transfer process and its complicated transfer mechanism has also been revealed. However, there are still huge gaps in understanding the communication between different organisms and investigation of the molecular mechanism of AMT will greatly help to address the gap.

Although many pathogenic factors involved in the AMT have been characterized, only few host genes and factors involved in AMT process have been identified, and much remains unclear. To better understand the sophisticated molecular mechanism of AMT, there is an urgent need to identify host factors involved in AMT. *Saccharomyces cerevisiae* (*S. cerevisiae*) is an ideal model for such a study for its simplicity, small genome size and available genome data. Besides, there are many commercial gene libraries which can facilitate the research. Therefore, *S. cerevisiae* has been chosen as a

model to study the role of host genes and factors involved in AMT and the underlying molecular mechanism of AMT.

This chapter aims to give an overview of *Agrobacterium tumefaciens*, known mechanisms of *Agrobacterium*-mediated transformation and the important factors involved in the transformation.

1.1. *Agrobacterium tumefaciens*: phytopathogen in genetic applications

A. tumefaciens is a gram-negative soil borne bacteria which belongs to bacterium kingdom, proteobacteria phylum, alpha proteobacteria class, rhizobiales order and rhizobiaceae family. It has rod shape with rounded ends, and is about 0.6 μm in diameter and 1.5-3.0 μm in length. Crown gall disease was firstly reported in 1853 and *Agrobacterium vitis* was discovered as the first strain that caused crown gall in grape (Galloway 1902; Smith and Townsend 1907). Over a few decades, *Agrobacterium* has been identified as the natural plant crown-gall disease pathogen of a wide plant species (140 species of dicotyledonous plants) (Van Larebeke, Engler et al. 1974).

Although *A. tumefaciens* is harmful to plants due to the genetic disturbance, it has been historically used to study genetic manipulation for the same reason. White and Braun demonstrated that persistent tumor-inducing phenotype can be caused by transient exposure to *A. tumefaciens*, and therefore they proposed an *Agrobacterium*-derived tumor-inducing principle (TIP) (Braun and Mandle 1948). It was later found by Vanlareb et al. that a large “tumor inducing plasmid” (Ti plasmid) was responsible for the crown galls formation (Van Larebeke, Engler et al. 1974). Moreover, the discovery of transferred DNA (T-DNA) in late 1970s, a tumor-inducing (Ti) plasmid fragment transferred from *A. tumefaciens* to plant cells, has allowed further T-DNA modification and Ti plasmid applications (Chilton, Drummond et al. 1977; Depicker, Van Montagu et al. 1978). For example, Zambryski et al. constructed

DNA of interest to the Ti plasmid vector and introduced it into target plant cells, thus creating first transgenic plant (Zambryski, Joos et al. 1983). Subsequently, more important crops, such as rice (Chan, Lee et al. 1992; Chan, Chang et al. 1993; Hiei, Ohta et al. 1994; Toki 1997) and wheat (Cheng, Fry et al. 1997), were transgenically modified to be antibiotic or herbicide resistance. The successful utilization of *A. tumefaciens* as a gene vector to create transgenic plants had made it a powerful tool for plant improvement and their transgenic varieties are growing worldwide (Valentine 2003). Moreover, the whole genome sequence of one nopaline-type strain *A. tumefaciens* C58 has been completed (Gelvin 2009).

1.2. *Agrobacterium*-mediated gene transfer and molecular basis

For a long period of time, as the only known species capable of inter-kingdom gene transfer, *Agrobacterium tumefaciens* had served as an important tool for research in biotechnology in the past several decades. The unique ability of transferring parts of its own DNA to the host plant genome has been rarely observed in naturally occurring horizontal gene transfer, thus make it the basis of its use for transgenesis (Gelvin 2003; Tzfira and Citovsky 2006).

Agrobacterium-mediated gene transfer is a sophisticated process and involves complicated molecular systems. Understanding the molecular basis of *Agrobacterium*-mediated gene transfer behind the process is of great importance in utilizing this technology to its greatest extent. It was found that a specialized plasmid, the tumor-inducing (Ti) plasmid, is required for the transgenesis. Ti plasmid contains two regions that are essential for DNA transfer to the host cell. The first region is the transferred DNA (T-DNA) itself (Gelvin 2003; Tzfira and Citovsky 2006). It was reported that T-DNA contains around 15 genes that are expressed in the transformed plant cells and lead to the crown-gall disease (Escobar and Dandekar 2003). The

second region contains the virulence (*vir*) genes which encode most of the bacterial proteins required for virulence (Zupan and Zambryski 1995).

There are four crucial steps in the transferring of DNA between *Agrobacterium* and host cells: 1) Detection of chemical signal: phenolics, sugars or acetosyringone are released by wounded plant cells and recognized by the *Agrobacterium* VirA/VirG two-component system; 2) Cell-cell contact and host attachment of *Agrobacterium*: a series of virulence (*vir*) genes on the tumor inducing (Ti) plasmid are continuously induced by the activation of VirA/VirG system and thus producing virulence proteins and one piece of transferred DNA (T-DNA) of the Ti plasmid; 3) T-complex formation and entry into host plant cell: after attaching to host cells, the single stranded linear T-DNA and the VirD2 form a T-complex and T-DNA transfer through type IV secretion system. *A. tumefaciens* cells attached to host cells then inject the T-complex to host cells through a VirD4/VirB type IV secretion system (T4SS); 4) Nuclear targeting and DNA integration: the injected T-complex targets to host cell nucleus and is integrated into host genome (Gelvin 2009).

1.2.1. Detection of chemical signal

The infection process starts from the recognition of signals of plant cells by *A. tumefaciens* via its cell surface sensors and the response to these signals by optimizing the activity of its virulence system. The main and first discovered plant signal is the phenolic compound acetosyringone (AS) (Stachel, An et al. 1985) which was recognized by bacteria via VirA/VirG two-component system (Stachel, Timmerman et al. 1986). Other chemical signals, such as sugars and amino acids, were later discovered (Loake, Ashby et al. 1988).

The detection of such signals will trigger *vir* gene induction in *A. tumefaciens*. From metabolites screening studies for plant cells, it was found that some plant

phenolic compounds and phenolic assemblies, such as hydroxy-acetosyringone and glycoside derivatives, are strong *vir* gene inducers (Stachel, An et al. 1985; Bolton, Nester et al. 1986). On the other hand, when plant phenolic compounds are present at very low concentration or are absent, some monosaccharides, such as glucose, arabinose, galactose, xylose and fructose, may play crucial roles in *vir* gene induction. Later, it was proved that the regulation pathway for *vir* gene induction by phenolics is different from the pathway induced by sugars, which is mediated by a chromosomal gene encoded protein ChvE (Cangelosi, Ankenbauer et al. 1990).

In addition, some chemicals emitted by some plant species were found to be inhibitors of the *Agrobacterium* virulence. This may explain the importance of inter-specific variability in resistance to *Agrobacterium*.

1.2.2. Cell-cell contact and host attachment of *Agrobacterium*

A close cell-cell contact between the *Agrobacterium* and the host cells is required for T-DNA transfer. An *agrobacterium* mutant with decreased ability to attach to plant cells has shown reduced virulence (Matthysse 1987). Candidate receptors from both the host plant and bacterial cell surface were identified to be involved in the attachment process.

Numerous bacterial candidate receptors have been studied. For example, extracellular components of the type IV secretion system (T4SS), specifically adhesin VirB2 and VirB5 were considered as good candidates for interacting with a potential plant receptor. However, it is still unknown whether these VirB proteins are involved in the early steps of cell-cell recognition. Furthermore, the available data suggests that the entire *vir* region is not essential for bacterial attachment. In another subset of the *Agrobacterium* genes, the *att* region has initially been suspected to mediate attachment (Matthysse and McMahan 1998). However, later studies showed that the *att* genes are

not required for virulence (Nair, Liu et al. 2003). Finally, only three bacterial factors, including chromosome-located *chvA*, *chvB*, and *exoC* genes which are involved in synthesis of exocellular oligosaccharides, have played unequivocal roles in both attachment and virulence (Cangelosi, Martinetti et al. 1989; de Iannino and Ugalde 1989). Then the host factors that might recognize and bind these exocellular oligosaccharides of *Agrobacterium* were studied.

Agrobacterium's ability to infect fungal and animal cells suggests that a host-specific receptor is not absolutely required for virulence. A genetic screening for *Arabidopsis* resistant to *Agrobacterium* (*rat*) mutants led to the identification of several plant lines which mutate in genes encoding extracellular proteins that are potentially involved in bacterial attachment. For example, the *rat4* mutant is deficient in a homolog of cellulose synthase; CSLA9, raising a possibility that modifications of the plant cell surface by CSLA9 could affect bacterial attachment (Zhu 2003).

Furthermore, the attachment of *Agrobacterium* to host cell is consolidated by forming a biofilm where bacteria is embedded at the plant cell surface. Biofilm formation appears essential for the virulence of most plant-associated bacteria including *Agrobacterium* (Tomlinson, Ramey-Hartung et al. 2010). However, *Agrobacterium* mutants with disrupted synthesis ability of cellulose and impaired attachment to plant cells, has shown only slightly diminished tumorigenicity (Matthysse 1983). Thus, unlike cyclic glucans (de Iannino and Ugalde 1989), cellulose fibrils are not absolutely required for *Agrobacterium* virulence. Although at the initial attachment stage, there are no known plant factors that interact with bacterial exocellular glucans. These glucans might play roles during the attachment consolidation stage by dictating the structural and chemical properties of the host cell surface and thus affecting the formation of biofilm.

1.2.3. T-complex formation and entry into host plant cell

The attachment of *A. tumefaciens* to host cells occurs prior to or concurrently with the *vir* gene induction process. Following the *vir* gene induction, a series of downstream events occurs. A linear single-stranded (ss) DNA fragment, the T-DNA or T-strand is produced by the cleavage of VirD2/VirD1 on the bottom strand (the coding strand) of T-region (Albright, Yanofsky et al. 1987). In addition to VirD2/VirD1, two other *vir* proteins, VirC1 and VirC2 were suggested to be involved in the T-DNA processing (Toro, Datta et al. 1989). After processing and association with VirD2, the T-strand is naked and susceptible to nuclease degradation. To prevent nucleolytic degradation, the ss T-strand is coated with VirE2 to form the T-complex which is composed of the T-strand DNA containing the 5'-associated VirD2 and coated VirE2 along its length (Gietl, Koukolikova-Nicola et al. 1987; Zupan and Zambryski 1995).

After proper processing and packaging, *agrobacterium* T-DNA and protein are translocated into the host cell. The translocation is mediated by the bacterial T4SS which composes of the eleven proteins encoded by the *virB* operon and the *virD4* gene. *Agrobacterium* T4SS is particularly well studied with its structure and the functions of its protein components well understood (Christie 2004). Moreover, the sequence of contacts of the T-DNA transport substrate with different subunits of T4SS has also been revealed (Cascales and Christie 2004).

Similar to protein translocation by type III secretion systems (Thanassi, Bliska et al. 2012), macromolecules translocated by T4SS could be injected directly from the bacterial to the host cytoplasm through the T-pilus acting as a hollow needle (Kado 2000). Alternatively, the T-pilus may mechanically perforate the host cell wall and plasma membrane, thus allowing the entry of the transported molecules through a T4SS transport conduit (Llosa, Gomis-Ruth et al. 2002). The fact that these two possible modes of macromolecule translocation do not postulate a plant-specific receptor is

consistent with the *Agrobacterium*'s ability to transfer macromolecules to a wide variety of eukaryotic cells, including non-plant hosts (Lacroix, Tzfira et al. 2006).

A radically different mechanism invoked for the entry of T-DNA into the host cell relies upon the formation of protein channels in lipidic membrane which composes of the *Agrobacterium*VirE2 protein (Dumas, Duckely et al. 2001). Such channels may allow the passage of macromolecules through host membrane. In addition, the very efficient and cooperative binding of VirE2 (Citovsky, Wong et al. 1989) to the T-strand in the host cell cytoplasm may actively pull the T-DNA molecule out of the T4SS and/or VirE2 channels without requiring external energy sources (Grange, Duckely et al. 2008).

1.2.4. Nuclear target and DNA integration

Soon after their entry in the host cell cytoplasm, the VirD2-T-strand complex and VirE2 form the mature T-complex in the form of VirD2-ssT-strand-VirE2 which later has to be transported to host cell nucleus and integrated into host genome (Citovsky, Zupan et al. 1992). Therefore, T-DNA targeting to the nucleus and its passage through the nuclear pore represent important steps of the genetic transformation process. The T-DNA nuclear import is mediated by bacterial effector proteins, VirD2 and VirE2, associated with the T-DNA and several host proteins that interact with these effectors. This interaction network is summarized in Figure 1.1 (Lacroix and Citovsky 2013).

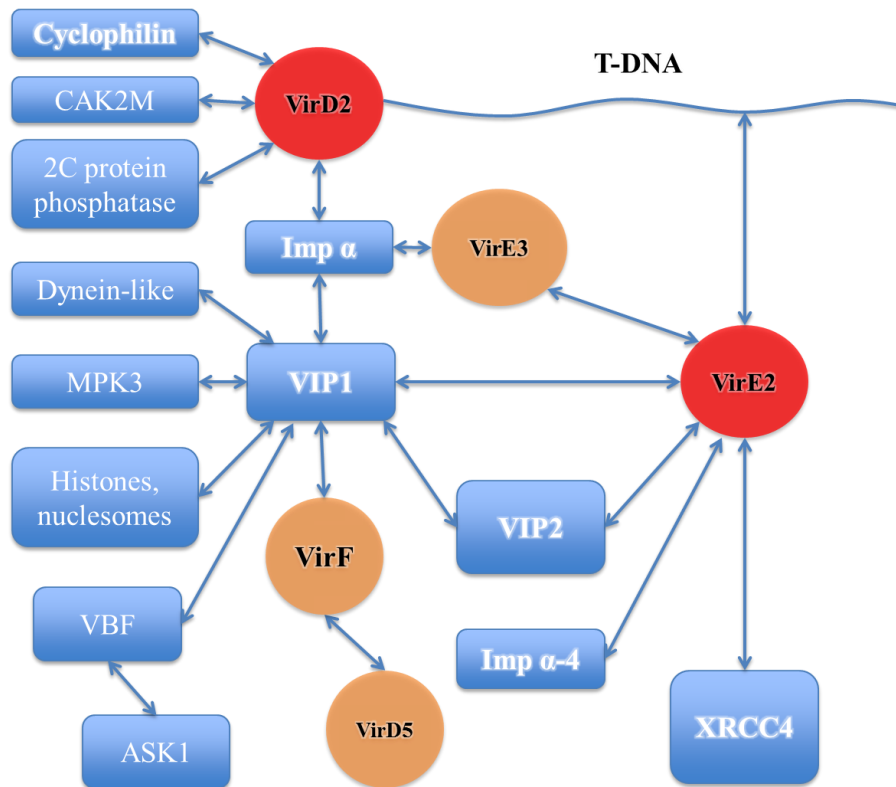


Figure 1.1 Network of interactions between translocated *Agrobacterium* effectors and host cell proteins.

VirD2 interacts with the plant importin α , a component of the cellular nuclear import machinery. There are two nuclear localization signals (NLSs) found within VirD2, a monopartite amino terminal NLS and a bipartite carboxyl terminal NLS (Herrera-Estrella, Van Montagu et al. 1990; Howard, Zupan et al. 1992; Tinland, Koukolikova-Nicola et al. 1992) with only the latter is found to be essential for the VirD2 nuclear import (Howard, Zupan et al. 1992; Ziemienowicz 2001). In addition, two other plant proteins interacting with VirD2 might modulate its nuclear localization: an *Arabidopsis* cyclophilin that may further assist VirD2 nuclear import (Deng, Chen et al. 1998) and a tomato type 2C serine/threonine protein phosphatase which is thought to dephosphorylate VirD2 and thereby inhibits its nuclear import, although the role of

VirD2 phosphorylation in the nuclear import has not been directly demonstrated (Tao, Rao et al. 2004).

VirE2 nuclear import is more complex and does not interact efficiently with importin α (Citovsky, Kapelnikov et al. 2004). Rather, it relies on VirE2 interacting protein 1 (VIP1). VIP1 binds directly to both VirE2 and importin α and acts as a molecular adapter between VirE2 and the host nuclear import machinery (Citovsky, Kapelnikov et al. 2004). Thus, both VirD2 and VirE2 are imported into the host cell nucleus via the importin α -dependent pathway, VirD2 – directly, and VirE2 – largely by piggybacking on VIP1. Interestingly, VirE3, another *Agrobacterium* virulence protein translocated into the plant cell, partially mimics the VIP1 function. VirE3 can interact with both VirE2 and importin α and facilitates the nuclear import of VirE2 (Lacroix, Vaidya et al. 2005). VirE3 is not absolutely essential for plant genetic transformation by *Agrobacterium*, but might compensate for the lack of VIP1-like protein in some plant species, consistent with its proposed role as a host range factor (Hirooka and Kado 1986).

After its entry into nucleus, T-DNA needs to be integrated into the host genome. Generally, studies of T-DNA integration in plant, in yeast and in vitro have demonstrated that integration is largely dependent on the host DNA repair machinery. However, later studies have shown that besides DNA repair machinery, host proteins that are mainly involved in chromatin structure or remodeling are important for T-DNA integration as well.

In general, *Agrobacterium* might “choose” different cellular pathways to achieve successful infection, which relies on bacterial or plant factors according to the host species and/or physiological conditions.

1.3. Host factors involved in *Agrobacterium*-mediated gene transfer

Besides plant species, *A. tumefaciens* can infect a broad range of host species, including yeast, fungi and mammalian cells under laboratory condition. Moreover, the current list of host species that can be genetically modified by *A. tumefaciens* is growing every day (Gelvin 2003). The host range determination or recognition is a complex process and involves many factors including bacterial factors and host factors. To date, a variety of host proteins involved in the AMT process have been identified through different approaches, including forward genetic screening, protein two-hybrid interaction assay, transcriptional profiling and reverse genetic experiments. In this section, the host factors related to the *Agrobacterium*-mediated transformation will be reviewed.

1.3.1. Host factors involved in the cell attachment and virulence factors transfer

In addition to bacterial proteins, some host factors are crucial for the *Agrobacterium*-plant cell attachment. Previous work has indicated some plant factors including vitronectin-like protein (Wagner and Matthyse 1992), a plant surface proteinaceous substance (Neff and Binns 1985; Neff, Binns et al. 1987) and a rhicadhesin-binding protein (Swart, Logman et al. 1994), played important roles in bacterial attachment and *Agrobacterium*-mediated transformation. In addition, several *Arabidopsis* ecotypes, for example B1-1, Peterhof and UE-1, showed weak binding ability to *Agrobacterium* cells at the early stage of the binding (Nam, Matthyse et al. 1997). It was revealed that some mutants, such as *rat1* and *rat3*, with resistance to *Agrobacterium* transformation, could not bind *A. tumefaciens* on the cut root surface (Nam, Mysore et al. 1999). *Arabidopsis* arabinogalactan protein, *AtAGP17*, which is deficient in *rat1* and localized to plant cell walls or secreted into the apoplast, was confirmed to be important for transformation (Gaspar, Nam et al. 2004). Moreover,

rat4 mutant encoding the cellulose synthase-like protein CsA-09 and *rat10* mutant encoding a plant cell wall β -expansin were reported to have reduced *Agrobacterium*-mediated transformation efficiency (Ziemienowicz, Tinland et al. 2000; Zhu, Nam et al. 2003).

After the successful attachment to host cells, the *Agrobacteria* T4SS connects *Agrobacterium* cell to host cells and the T4SS itself serves as a transport channel to facilitate the transport of T-DNA and the relevant *vir* protein. The T-pilus which comprises of two virulence proteins (VirB2 and VirB5) may bring the bacterial and host membranes together for T-DNA and *vir* protein transport or may be a conduit for transport (Backert, Fronzes et al. 2008). VirB2, the major component of T-pilus, formed the body structure (Lai and Kado 1998; Eisenbrandt, Kalkum et al. 1999). The VirB5 is a minor component located to the pilus tip (Aly and Baron 2007). As the T-pilus components, VirB2 and VirB5 are potential targets for host surface receptors.

1.3.2. Host factors involved in nuclear targeting

After entering into plant cytoplasm, the T-complex must transfer through the cytoplasm and target to the nucleus. Both VirD2 and VirE2 proteins contain nuclear localization signal (NLS) sequences which are critical for T-complex nuclear targeting. Deletion of the VirD2 C-terminal bipartite NLS could not completely block the transformation process (Shurvinton, Hodges et al. 1992). This may be complemented by the VirE2 which coats the entire ssT-strand. The two VirE2 bipartite NLS sequences probably help the nuclear targeting of the T-complex even in the absence of VirD2 NLS (Gelvin 1998). In addition, many host proteins may interact with the T-complex to form super-T-complexes, which facilitates the T-complex nuclear targeting.

The importin α protein AtKAP α is the first identified plant protein to be involved in the T-complex nuclear targeting (Ballas and Citovsky 1997). In addition to importin

α protein family, importin β -like transportins may also be involved in the T-DNA transfer process (Zhu, Nam et al. 2003).

Besides importin protein families, VIP1 and VIP2, two VirE2 interacting proteins, were identified in a yeast two hybrid screening for VirE2 binding host proteins (Tzfira, Vaidya et al. 2001). VIP1 specifically binds to VirE2 but not to VirD2. VirD2 is a phosphoprotein and the phosphorylation of the T-complexes may play a role in the nuclear targeting. It was shown that VirD2 binds to a cyclin-dependent kinase-activating kinase, CAK2Ms (Bako, Umeda et al. 2003). It was also observed that a type 2C serine/threonine protein phosphatase (PP2C) deficient *Arabidopsis* mutant is susceptible to *Agrobacterium*-mediated transformation (Tao, Rao et al. 2004).

1.3.3. Host factors involved in chromatin targeting and T-DNA integration

Once inside the host nucleus, the T-DNA will be recruited to the host chromatin and integrate into the host genome. The T-DNA integration into plant genome is through non-homologous end-joining (NHEJ) process (Offringa, De Groot et al. 1990). Mutagenesis analysis revealed that in yeast model the NHEJ effector proteins Yku70, Rad50, Mre11, Xrs2, Lig4 and Sir4 are crucial for the integration of the T-DNA into yeast genome (van Attikum and Hooykaas 2003). Other than NHEJ proteins, Rad 51 and Rad52 are essential for T-DNA integration by homologous recombination (HR) (van Attikum, Bundock et al. 2001). Moreover, DNA-packaging proteins, such as histone proteins, may also be involved in the T-DNA integration process. It was found that *Arabidopsis* histone H2A plays a major role in T-DNA integration process in somatic cells by directing the T-complex to the integration sites (Loyter, Rosenbluh et al. 2005).

In addition to their role in T-DNA nuclear targeting, VIP1 and VIP2 proteins are

also important for T-DNA integration. Molecular and genetic data suggested that T-DNA integration process was blocked in *vip2* mutants (Anand, Krichevsky et al. 2007). Because of the importance of histone proteins in T-DNA integration process, the alteration of histone transcription profile indicates that VIP2 is crucial for regulating the expression of important genes in *Agrobacterium* T-DNA integration.

1.4. Objectives of this study

Agrobacterium tumefaciens is a natural plant pathogen which causes tumors in plants by transferring a single stranded T-DNA molecule from the bacteria into host cell nucleus. The molecular mechanism of *Agrobacterium*-mediated transformation has been studied for many years. Although many pathogenic factors involved in the AMT have been well characterized, and some host factors have been identified, many aspects of host factors and genes involved in AMT remain unclear (Gelvin 2010). *Saccharomyces cerevisiae* is an ideal model to study the *Agrobacterium*-mediated transformation for its small genome size, available genome data and available various gene libraries. Previous genome-wide screening study has identified more than 200 candidate genes which play potential roles in AMT (Tu 2010).

This study mainly focuses on the investigation of new host factors involved in AMT and their underlying molecular mechanism by using *Saccharomyces cerevisiae* as a model organism. A variety of approaches were employed to study the molecular mechanism of how host factors regulate the AMT process, including molecular genetics, biochemistry and bio-imaging. Various aspects of this process, such as T-DNA delivery, virulence protein translocation, T-DNA trafficking and T-DNA integration, will be studied. Moreover, this study adopted *Nicotiana benthamiana* as plant model to study the role of plant homolog of genes involved in *Agrobacterium*-mediated gene transfer.

Chapter 2. Materials and Methods

2.1. Stains, plasmids, primers and cultures

In this study, the collection of *S. cerevisiae* haploid deletion strains in BY4741 (*MATa his3Δ0 leu2Δ0 met15Δ0 ura3Δ0*) (Brachmann, Davies et al. 1998) were obtained from Open Biosystems. *S. cerevisiae* were grown in liquid yeast extract peptone dextrose (YPD) medium, or in synthetic defined (SD) minimal medium with appropriate amino acid dropout (DO) supplements at 30 °C. Yeast strains were stored in YPD or SD medium with 20% glycerol at -80 °C.

A. tumefaciens was cultured in mannitol glutamate / Luria (MG/L) (Garfinkel and Nester 1980), Luria-Bertani (LB) or induction medium (IBPO₄) at 28 °C (Cangelosi, Best et al. 1991) and *E. coli* was cultured in LB medium at 37 °C with appropriate antibiotics (Sambrook, Russell et al. 2001). Bacterial strains were stored in LB or MG/L with 20% glycerol at -80 °C.

Yeast and bacterial strains used in this study are listed in Table 2.1.

Plasmids used in this study are listed in Table 2.2.

Media and solutions used in this study are listed in Table 2.3. 100µg/ml Ampicillin (Amp), 50µg/ml Kanamycin (Km) and 100µg/ml cefotaxime (Cef) were supplemented when necessary.

Primers used in this study are listed in Table 2.4.

Table 2.1. Bacterial and yeast stains used in this study

Stains	Characteristics	Source
<i>Saccharomyces cerevisiae</i>		
BY4741	<i>MATa his3Δ1 leu2Δ0 met15Δ0 ura3Δ0</i>	Open
		Biosystem
<i>cor1Δ</i>	<i>MATa his3Δ1 leu2Δ0 met15Δ0 ura3Δ0</i>	Open
	<i>cor1::KanMX4</i>	Biosystem
<i>ade8Δ</i>	<i>MATa his3Δ1 leu2Δ0 met15Δ0 ura3Δ0</i>	Open
	<i>ade8Δ::kanMX4</i>	Biosystem
<i>are2Δ</i>	<i>MATa his3Δ1 leu2Δ0 met15Δ0 ura3Δ0</i>	Open
	<i>are2Δ::kanMX4</i>	Biosystem
<i>atp1Δ</i>	<i>MATa his3Δ1 leu2Δ0 met15Δ0 ura3Δ0</i>	Open
	<i>atp1Δ::kanMX4</i>	Biosystem
<i>bud13Δ</i>	<i>MATa his3Δ1 leu2Δ0 met15Δ0 ura3Δ0</i>	Open
	<i>bud13Δ::kanMX4</i>	Biosystem
<i>bud31Δ</i>	<i>MATa his3Δ1 leu2Δ0 met15Δ0 ura3Δ0</i>	Open
	<i>bud31Δ::kanMX4</i>	Biosystem
<i>cdc40Δ</i>	<i>MATa his3Δ1 leu2Δ0 met15Δ0 ura3Δ0</i>	Open
	<i>cdc40Δ::kanMX4</i>	Biosystem

<i>cef1Δ</i>	MATa <i>his3Δ1 leu2Δ0 met15Δ0 ura3Δ0</i>	Open
	<i>cef1Δ::kanMX4</i>	Biosystem
<i>clf1Δ</i>	MATa <i>his3Δ1 leu2Δ0 met15Δ0 ura3Δ0</i>	Open
	<i>clf1Δ::kanMX4</i>	Biosystem
<hr/>		
<i>cwc15Δ</i>	MATa <i>his3Δ1 leu2Δ0 met15Δ0 ura3Δ0</i>	Open
	<i>cwc15Δ::kanMX4</i>	Biosystem
<i>cwc21Δ</i>	MATa <i>his3Δ1 leu2Δ0 met15Δ0 ura3Δ0</i>	Open
	<i>cwc21Δ::kanMX4</i>	Biosystem
<i>cwc27Δ</i>	MATa <i>his3Δ1 leu2Δ0 met15Δ0 ura3Δ0</i>	Open
	<i>cwc27Δ::kanMX4</i>	Biosystem
<i>did4Δ</i>	MATa <i>his3Δ1 leu2Δ0 met15Δ0 ura3Δ0</i>	Open
	<i>did4Δ::kanMX4</i>	Biosystem
<i>ecm2Δ</i>	MATa <i>his3Δ1 leu2Δ0 met15Δ0 ura3Δ0</i>	Open
	<i>ecm2Δ::kanMX4</i>	Biosystem
<i>gbp2Δ</i>	MATa <i>his3Δ1 leu2Δ0 met15Δ0 ura3Δ0</i>	Open
	<i>gbp2Δ::kanMX4</i>	Biosystem
<i>hek2Δ</i>	MATa <i>his3Δ1 leu2Δ0 met15Δ0 ura3Δ0</i>	Open
	<i>hek2Δ::kanMX4</i>	Biosystem
<i>hrb1Δ</i>	MATa <i>his3Δ1 leu2Δ0 met15Δ0 ura3Δ0</i>	Open
	<i>hrb1Δ::kanMX4</i>	Biosystem

<i>isy1Δ</i>	MATa <i>his3Δ1 leu2Δ0 met15Δ0 ura3Δ0</i>	Open
	<i>isy1Δ::kanMX4</i>	Biosystem
<i>iwr1Δ</i>	MATa <i>his3Δ1 leu2Δ0 met15Δ0 ura3Δ0</i>	Open
	<i>iwr1Δ::kanMX4</i>	Biosystem
<i>mam33Δ</i>	MATa <i>his3Δ1 leu2Δ0 met15Δ0 ura3Δ0</i>	Open
	<i>mam33Δ::kanMX4</i>	Biosystem
<i>mdh1Δ</i>	MATa <i>his3Δ1 leu2Δ0 met15Δ0 ura3Δ0</i>	Open
	<i>mdh1Δ::kanMX4</i>	Biosystem
<hr/>		
<i>mfr1Δ</i>	MATa <i>his3Δ1 leu2Δ0 met15Δ0 ura3Δ0</i>	Open
	<i>mfr1Δ::kanMX4</i>	Biosystem
<i>mms2Δ</i>	MATa <i>his3Δ1 leu2Δ0 met15Δ0 ura3Δ0</i>	Open
	<i>mms2Δ::kanMX4</i>	Biosystem
<i>mrpl17Δ</i>	MATa <i>his3Δ1 leu2Δ0 met15Δ0 ura3Δ0</i>	Open
	<i>mrpl17Δ::kanMX4</i>	Biosystem
<i>mrpl3Δ</i>	MATa <i>his3Δ1 leu2Δ0 met15Δ0 ura3Δ0</i>	Open
	<i>mrpl3Δ::kanMX4</i>	Biosystem
<i>nmd2Δ</i>	MATa <i>his3Δ1 leu2Δ0 met15Δ0 ura3Δ0</i>	Open
	<i>nmd2Δ::kanMX4</i>	Biosystem
<i>ntc20Δ</i>	MATa <i>his3Δ1 leu2Δ0 met15Δ0 ura3Δ0</i>	Open
	<i>ntc20Δ::kanMX4</i>	Biosystem

<i>prp19Δ</i>	MATa <i>his3Δ1 leu2Δ0 met15Δ0 ura3Δ0</i>	Open
	<i>prp19Δ::kanMX4</i>	Biosystem
<i>rpl2bΔ</i>	MATa <i>his3Δ1 leu2Δ0 met15Δ0 ura3Δ0</i>	Open
	<i>rpl2bΔ::kanMX4</i>	Biosystem
<i>rps16aΔ</i>	MATa <i>his3Δ1 leu2Δ0 met15Δ0 ura3Δ0</i>	Open
	<i>rps16aΔ::kanMX4</i>	Biosystem
<i>rps19bΔ</i>	MATa <i>his3Δ1 leu2Δ0 met15Δ0 ura3Δ0</i>	Open
	<i>rps19bΔ::kanMX4</i>	Biosystem
<i>rps4bΔ</i>	MATa <i>his3Δ1 leu2Δ0 met15Δ0 ura3Δ0</i>	Open
	<i>rps4bΔ::kanMX4</i>	Biosystem
<i>snt309Δ</i>	MATa <i>his3Δ1 leu2Δ0 met15Δ0 ura3Δ0</i>	Open
	<i>snt309Δ::kanMX4</i>	Biosystem
<hr/>		
<i>syf2Δ</i>	MATa <i>his3Δ1 leu2Δ0 met15Δ0 ura3Δ0</i>	Open
	<i>syf2Δ::kanMX4</i>	Biosystem
<i>tex1Δ</i>	MATa <i>his3Δ1 leu2Δ0 met15Δ0 ura3Δ0</i>	Open
	<i>tex1Δ::kanMX4</i>	Biosystem
<i>tho2Δ</i>	MATa <i>his3Δ1 leu2Δ0 met15Δ0 ura3Δ0</i>	Open
	<i>tho2Δ::kanMX4</i>	Biosystem
<i>thp2Δ</i>	MATa <i>his3Δ1 leu2Δ0 met15Δ0 ura3Δ0</i>	Open
		Biosystem

	<i>thp2Δ::kanMX4</i>	
<i>urn1Δ</i>	MATa <i>his3Δ1 leu2Δ0 met15Δ0 ura3Δ0</i>	Open
	<i>urn1Δ::kanMX4</i>	Biosystem
<i>ypr098cΔ</i>	MATa <i>his3Δ1 leu2Δ0 met15Δ0 ura3Δ0</i>	Open
	<i>ypr098cΔ::kanMX4</i>	Biosystem
<i>rpl35bΔ</i>	MATa <i>his3Δ1 leu2Δ0 met15Δ0 ura3Δ0</i>	Open
	<i>rpl35bΔ::kanMX4</i>	Biosystem
<i>rps10aΔ</i>	MATa <i>his3Δ1 leu2Δ0 met15Δ0 ura3Δ0</i>	Open
	<i>rps10aΔ::kanMX4</i>	Biosystem
<i>rps4bΔ</i>	MATa <i>his3Δ1 leu2Δ0 met15Δ0 ura3Δ0</i>	Open
	<i>rps4bΔ::kanMX4</i>	Biosystem
<i>rpl21bΔ</i>	MATa <i>his3Δ1 leu2Δ0 met15Δ0 ura3Δ0</i>	Open
	<i>rpl21bΔ::kanMX4</i>	Biosystem
R1158	MATa <i>his3-1 leu2-0 met15-0 URA3::</i>	Open
	<i>CMV-tTA</i>	Biosystem
<i>prp19</i>	<i>pPRP19::kanR-tet07-TATA URA3::CMV-tTA</i>	Open
	MATa <i>his3-1 leu2-0 met15-0</i>	Biosystem
<i>cef1</i>	<i>pCEF1::kanR-tet07-TATA URA3::CMV-tTA</i>	Open
	MATa <i>his3-1 leu2-0 met15-0</i>	Biosystem
<i>clf1</i>	<i>pCLF1::kanR-tet07-TATA URA3::CMV-tTA</i>	Open

Escherichia coli

DH5 α	<i>endA1 hsdR17 supE44 thi-1 recA1 gyrA96</i>	Bethesda
	<i>relA1 (argF-lacZYA) U169 ϕ80dlacZ ΔM15</i>	Research Laboratory

Agrobacterium tumefaciens

EHA105	Wild-type, containing pTiBo542, disarmed	(Hood, Gelvin et al. 1993)
EHA105 <i>virE2::GFP11</i>	EHA105 derivative, <i>virE2</i> fused with GFP11 small fragment at +162	Lab collection
A348	Wild-type chromosomal background of strain C58 and contains pTiA6	(Sciaky, Montoya et al. 1978)

Table 2.2. Plasmids used in this study

Plasmids	Relevant characteristic(s)	Source or reference
pHT101	Binary vector pCB301 derivative, ligated at Sall site with pACT2, in which the <i>GAL4AD</i> gene is replaced by EGFP reporter gene at HindIII site; Km ^R , Amp ^R , 2 μ origin, <i>LEU2</i>	Lab collection
pHT101-2μ ⁻	pHT101 derivative, 2 μ origin of pHT101 destroyed by double digestion of SnaBI and NruI	Lab collection
pHT105	Yeast expression vector; 2 μ replicon; <i>ADHI</i> promoter, <i>ADHI</i> terminator; <i>URA3</i> , Amp ^R	Lab collection
pHT105-BUD31	pHT105 derivative, expressing yeast <i>BUD31</i> gene, <i>URA3</i> , Amp ^R	This study
pHT105-SNT309	pHT105 derivative, expressing yeast <i>SNT309</i> gene, <i>URA3</i> , Amp ^R	This study
pHT105-SYF2	pHT105 derivative, expressing yeast <i>SYF2</i> gene, <i>URA3</i> , Amp ^R	This study
pHT105-YCR064 C	pHT105 derivative, expressing yeast putative ORF YCR064C, <i>URA3</i> , Amp ^R	This study
pHT105-GFP	pHT105 derivative, expressing <i>EGFP</i> reporter gene, <i>URA3</i> , Amp ^R	Lab collection

pHT105-BUD31-GFP	pHT105 derivative, expressing BUD31-GFP fusion protein, <i>URA3</i> , Amp ^R	This study
pYES2	Yeast expression vector, 2μ origin, <i>GAL1</i> promoter, <i>CYCI</i> terminator, <i>URA3</i> , Amp ^R	Invitrogen
pYES2-GFP-virD2	pYES2 derivative, expressing GFP-VirD2 upon galactose induction	Lab collection
pQH303	Binary vector for yeast, <i>URA3</i> flanked by homologous arms cloned from <i>LYS2</i>	Lab collection
pQH304	Binary vector for yeast, <i>URA3</i> , 2μ origin	Lab collection
pQH121	Derivative from pBI121, with <i>GUS</i> substituted by a multiple cloning site	Lab collection
pQH121-GFP	pQH121 derivative, expressing <i>GFP</i>	This study
pQH121-NbBUD31-GFP	pQH121 derivative, expressing NbBUD31-GFP fusion protein	This study
pQH121-GFP-NbBUD31	pQH121 derivative, expressing GFP-NbBUD31 fusion protein	This study
pQH308a	Binary vector for plants, <i>nptIII</i> , Kan ^R , <i>Pmas::GFP1-10</i> , <i>35S::DsRed</i>	Lab collection

Table 2.3. Media and solutions used in this study

Media	Preparation (1 L)*	Reference
LB	Tryptone, 10 g; yeast extract, 5 g; NaCl, 10 g; pH 7.5	(Sambrook, Russell et al. 2001)
MG/L	LB, 500 ml; mannitol, 10 g; g sodium glutamate, 2.32; KH ₂ PO ₄ , 0.5 g; NaCl, 0.2 g; MgSO ₄ . 7H ₂ O, 0.2 g; biotin, 2 µg; pH 7.0.	(Cangelosi, Best et al. 1991)
IBPO ₄	20 × AB salts, 50 ml; 20 × AB buffer, 1 ml; 1 M KH ₂ PO ₄ (pH 5.0), 8 ml; glucose, 18 g in 941 ml RO H ₂ O (autoclaved separately before mixing together).	(Piers, Heath et al. 1996)
20 × AB salts	NH ₄ Cl, 20 g; MgSO ₄ . 7H ₂ O, 6 g; KCl, 3 g; CaCl ₂ , 0.2 g; FeSO ₄ . 7H ₂ O, 50 mg.	(Cangelosi, Best et al. 1991)
20 × AB buffer	K ₂ HPO ₄ , 60 g; NaH ₂ PO ₄ , 23 g; pH 7.0.	(Cangelosi, Best et al. 1991)
0.5 M MES	MES, 97.6 g; pH 5.5.	(Cangelosi, Best et al.)

		1991)
YPD	Difco peptone, 20 g; yeast extract, 10 g; glucose, 20 g	Clontech user manual
SD (broth)	Minimal SD base, 26.7 g; appropriate drop-out supplement	Clontech user manual
<hr/>		
Cocultivation medium (CM)	IBPO ₄ ; histidine, 20 mg; leucine 60 mg; methionine 20 mg; uracil 20 mg.	(Piers, Heath et al. 1996)
1/2 x Murashige & Skoog (MS)	Murashige and Skoog basal medium lacking phytohormones, 2.2g; Sucrose, 10g; MES, 0.5g; pH5.8 (0.8% phyto agar for solid media)	(Murashige and Skoog 1962)

*For solid media, 1.5% agar was added

Table 2.4. Primers used in this study

Primers	Sequences
Primers used in molecular cloning and regular PCR	
BUD31-KpnI-F	5' GGGGTACCATGCCGCGCATAAAGACCAGAAGAT 3'
BUD31-KpnI-R	5' GGGGTACCTTAGTCTGTGCTTGCACATCCACGG 3'
SNT309-KpnI-F	5' GGGGTACCATGGACGGCCTTAGCTTTGTTGATA 3'
SNT309-KpnI-R	5' GGGGTACCTTATAACCTCTTTCTGTATATTTCC 3'
SYF2-KpnI-F	5' GGGGTACCATGGATTTTTACAAATTAGACGAGA 3'
SYF2-KpnI-R	5' GGGGTACCTTATTCTGATCCTCCTTTTGATTCCCTG 3'
YCR064C-KpnI-F	5' GGGGTACCATGTATCTAGAGCGCTGGTGGTGGA 3'
YCR064C-KpnI-R	5' GGGGTACCTACAAGACTTAGCACATTTACAACC 3'
pHT106-BUD31-KpnI-R	5' GGGGTACCCCGTCTGTGCTTGCACATCCACGGC 3'
NbBUD31F-KpnI-VIGS	5' GGGGTACCTGGGAGCTGATTGAGCCTAC 3'
NbBUD31R-KpnI-VIGS	5' GGGGTACCTTGCATCTGCATAACCTTGTT 3'
G-gk-BamHI-R	5' CGGGATCCTTACTTGTACAGCTCGTCCATGCCG 3'
G-gk-KpnI-F	5' GGGGTACCATGGTGAGCAAGGGCGAGGA 3'

NbBUD31- XbaI -F	5' GCTCTAGAATGCCTAGGGTCAAGACAAATCG 3'
NbBUD31 -KpnI -F	5' GGGGTACCATGCCTAGGGTCAAGACAAAT 3'
NbBUD31-Eco53kI- R	5' CGAGCTCTTAGTCCCCACTTGCACAGCCTT GA 3'
<hr/>	
NbBUD31- KpnI-link-R	5' GGG GTACCCCCGGGCTGCAGGAAT TCGATAT CTCGGTCCCCACTTGCACAGCCT TGACAT 3'
NbBUD31-BamHI-link-F	5' CGGGATCCCGAGATATCGAATTCCTGCAGCCC GGGATGCCTAGGGTCAAGACAAATCGTA 3'
pHT105-F1	5' TTCCTCGTCATTGTTCTCGT3'
pHT105-R1	5' GCACAGATGCGTAAGGAGAAAA3'
pQH121-F	5' CGTAAGGGATGACGCACAA 3'
pQH121-R	5' AGTTGGGTAACGCCAGGGTTT 3'

Primers used in real time PCR

ACT1-RT-F	5'GATGGACCACTTTCGTCGTA 3'
ACT1-RT-R	5'TCCATCTTCCATGAAGGTCA 3'
BUD31F-RT	5' AATGAGCAGCTCTGGGAGA 3'
BUD31R-RT	5' CCATTTGGCAATTAGCAAT 3'
UBQ10-F	5' GGCCTTGTATAATCCCTGATGAATAAG 3'

UBQ10-R	5' AAAGAGATAACAGGAACGGAAACATAGT 3'
AT4G21110-mRNA-F	5' CCAGAAGGATGGGAGTGGATCGAGC 3'
AT4G21110-mRNA-R	5' CCTTGACAGCCGCAGTGAACGCAT 3'
PMP3-F	5' ATGGATTCTGCCAAGATCATTAAC 3'
PMP3-R	5' TTAATCTTGTAGGACAATGTACAAGG 3'
VirE2-F	5' CATAGAGGAAATGAGCGGCAGTC 3'
VirE2-R	5' AACTTCCGTTCCGGTAGGGCT 3'
<hr/>	
URA3-F	5' TCCTGTTGCTGCCAAGCTAT 3'
URA3-R	5' AATGTCTGCCCATCTGCTA 3'
NbEF1-RT-F	5'GATTGGTGGTATTGGAAGTGC 3'
NbEF1-RT-R	5'AGCTTCGTGGTGCATCTC 3'
NbBUD31-RT-F	5' TGAGCGTCTCTGCTGCTT 3'
NbBUD31-RT-R	5' CCACTTGCACAGCCTTGA 3'

2.2. DNA manipulations

2.2.1. General DNA manipulation techniques

Polymerase chain reaction (PCR), DNA gel electrophoresis and purification, DNA sequencing, DNA digestion, ligation, plasmid DNA preparation, competent cell preparation and bacterial cells transformation were carried out following standard protocols as described (Sambrook, Russell et al. 2001).

2.2.2. Genomic DNA preparation

In this study, *A. tumefaciens* genomic DNA was prepared as described with a few modifications (Charles and Nester 1993). Briefly, *A. tumefaciens* was grown overnight in 5ml MG/L. Bacterial cells were harvested by centrifugation, washed once with TES (10 mM Tris-HCl, 25 mM EDTA, 150 mM NaCl, pH 8.0), and then resuspended in TE buffer (10 mM Tris-HCl, 25 mM EDTA, pH 8.0). Cells were lysed by adding 75 μ l of NaCl (5 M), 62.5 μ l of proteinase K (5 mg/ml) and 62.5 μ l of SDS (10%), and incubated at 68 °C for 30 minutes. After centrifugation, the supernatant was transferred to a new tube and subsequently extracted once with equal volume of base layer of phenol-chloroform solution (Phenol/ Chloroform/ Isoamyl alcohol 25:24:1). The tube was mixed by vortex and spun down by centrifugation. The aqueous phase was then transferred into a new tube. Genomic DNA was precipitated with 2 volumes of absolute ethanol supplemented at 4 °C for 1 hour. After spinning down by centrifugation, the DNA pellet was washed twice with 70% ethanol and vacuum dried. Genomic DNA was dissolved in distilled water and stored at 4 °C.

Yeast genomic DNA used in this work was prepared as described with some modifications. Yeast was grown overnight in 5 ml YPD or SD medium. Cells were washed once with PBS and re-suspended in 450 μ l TES (10 mM Tris-HCl, 25mM

EDTA, 150mM NaCl, pH 8.0). 50 µl of 10 × lyticase was added into cell suspension and incubated at 37 °C with RNase for 1 hour. The mixture was incubated at 95 °C for 10 minutes to lyse the cell. After centrifugation, the upper phase was transferred to a new tube to carry out DNA extraction as *A. tumefaciens* genomic DNA (Looke, Kristjuhan et al. 2011).

2.2.3. Transformation of *A. tumefaciens* by electroporation

Plasmids were introduced into *A. tumefaciens* by electroporation (Cangelosi, Best et al. 1991). *A. tumefaciens* was grown in MG/L medium until early log phase ($OD_{600} = 1.0$). About 10^9 cells were centrifuged at 4 °C and washed twice with cold water and once with cold glycerol (15%). The cell pellet was resuspended in 50 µl of cold glycerol (15%) and incubated on ice for 2 minutes.

The cell suspension together with plasmid DNA was transferred to a pre-chilled 0.2 cm electroporation cuvette (BioRad). The Gene Pulser II Electroporation System (Bio-Rad) was used for electroporation (Capacitance 25 µF, Voltage 2.5 kV, Pulse controller set to 400 Ω, 8-9s). 1 ml of MG/L broth was added to the electroporation cuvette immediately after electroporation. The cell suspension was transferred into a 14 ml culture tube for 1 hour recovery at 28 °C. The electroporated cells were collected and plated on MG/L agar plate with appropriate antibiotics for selection.

2.2.4. Lithium acetate transformation of yeast

Lithium acetate transformation of yeast was performed as described with some modifications (Gietz, Schiestl et al. 1995). Yeast was grown in liquid YPD or SD medium overnight and subcultured into fresh medium for 3 to 4 hours incubation until $OD_{600} = 1.0$. Then yeast cells were washed sequentially with double distilled H₂O (ddH₂O) and with 100 mM lithium acetate. The cells were resuspended in

transformation mixture (80 μ l of H₂O, 5 μ l of carrier DNA, 36 μ l of 1 M lithium acetate, 240 μ l of 50% PEG, 1 μ l of 200ng/ μ l plasmid DNA) and mixed by vortex. The mixture was then heat shocked at 42 °C for 30 minutes.

The cells were pelleted by centrifugation and resuspended in 1 ml of ddH₂O. Appropriate amount of cells were spread onto SD agar plates with amino acid drop out supplement and incubated at 30 °C for selection. 10⁵ times dilution can be made and the diluted cells were spread onto SD agar recovery plates with full amino acids to calculate transformation efficiency (when necessary) .

2.2.5. Real-time PCR

Real-time PCR was used in this study to amplify and quantify targeted DNA molecule (Heid, Stevens et al. 1996).

KAPA SYBR fast universal qPCR kit and Bio-Rad CFX384 Touch™ Real-Time PCR Detection System were used to perform real-time PCR. (94 °C 10 s – 55 °C 30 s) \times 40 cycles were used followed by melting curving checking. The 2^{- $\Delta\Delta$ CT} method was employed for data analysis.

2.3. RNA manipulations

2.3.1. Total RNA extraction from yeast cells

TRIzol-based method was used in yeast total RNA extraction (Hummon, Lim et al. 2007). Yeast cells were centrifuged and re-suspended in 450 μ l TES supplemented with 50 μ l 10 \times lyticase. The mixture was incubated at 37 °C for 30 minutes. The cells were harvested by centrifuging at 4 °C. 0.8 ml of TRIzol reagent was added to cell pellet and re-suspended. After incubation at room temperature for 5 minutes, 0.16 ml of chloroform was added to the mixture and mixed by shaking tube vigorously for 15

seconds. The mixture was incubated at room temperature for 3 minutes, and then centrifuged at 4 °C, 12000 g for 15 minutes. The colorless upper aqueous phase was transferred to a new 1.5 ml tube, followed by adding equal volume of isopropanol. The samples were incubated at room temperature for 10 minutes and centrifuge at 4 °C, 12000g for 10 minutes. The RNA precipitate was washed once with 75% ethanol and dissolved in double distilled water.

2.3.2. Total RNA extraction from *A. thaliana* and *N. benthamiana*

TRIZol-based method was used in total RNA extraction of *A. thaliana* cells and *N. benthamiana* as described for yeast (Hummon, Lim et al. 2007). 50 to 100 mg of plant leaf tissue was frozen in liquid nitrogen and grinded into powder by using pre-sterilized blue pestle to generate homogenize tissue samples. These samples were resuspended in 0.8 ml of TRIZol reagent, and followed by same procedure as described for yeast RNA extraction.

2.3.3. Reverse transcription polymerase chain reaction (RT-PCR)

After total RNA extraction, iScript cDNA Synthesis Kit (Bio-Rad) was used to perform reverse transcription PCR (RT-PCR) for cDNA synthesis.

2.4. Protein analysis

2.4.1. Total proteins extraction from yeast cells

A rapid protein extraction method was performed to extract total proteins from small amount of yeast cells (Kushnirov 2000). About 10^8 of yeast cells were harvested by centrifugation and resuspended in 100 μ l of ddH₂O. Equal volume of 0.2 mM NaOH was added to the cell suspension and incubated at room temperature for 5 minutes.

After centrifugation, the cell pellet was resuspended in an appropriate volume of SDS gel-loading buffer and boiled for another 5 minutes. The sample was pelleted again and the supernatant was used in Sodium Dodecyl Sulfate Polyacrylamide Gel Electrophoresis (SDS-PAGE).

2.4.2. SDS-PAGE gel electrophoresis and Coomassie blue staining

Total protein profile of yeast cells were analyzed according to their molecular weights by SDS-PAGE gel electrophoresis (Laemmli 1970). The buffers and solutions used in this study and gel preparation recipe are listed in Table 2.5. 40 μ l of protein sample was mixed with 10 μ l 1 M DTT solution and 50 μ l loading buffer followed by incubating at 95 $^{\circ}$ C for 5 minutes for preparing loading sample. The Mini-Protean III Electrophoresis Cell (Bio-Rad) was used in this study to perform SDS-PAGE gel electrophoresis 70 volts for 20 minutes and followed by 200 volts. The protein profile could be visualized by Coomassie blue staining after running SDS-PAGE. The SDS-PAGE gel was then placed in staining solution and left for staining on a slowly rotating flat rotator. The destaining solution was added to destain the gel after removing the staining solution (Sambrook, Russell et al. 2001).

Table 2.5. Buffers and solutions used in SDS-PAGE gel electrophoresis

Buffer/Gel	Components
10 × Tank buffer	0.25 M Tris, 2.5 M Glycine, 1% SDS
Stacking gel	1.4 ml of H ₂ O, 320 µl of 30% Acrylamide, 250 µl of 1 M Tris-HCl, pH 6.8, 20 µl of 10% SDS, 20 µl of 10% APS, 2 µl Temed
10% Running gel	1.9 ml of H ₂ O, 1.7 ml of 30% Acrylamide, 1.3 ml of 1.5 M Tris-HCl, pH 8.8, 50 µl of 10% SDS, 50 µl of 10% APS, 2 µl Temed
2 × Sample-loading buffer	100 mM Tris-HCl, 4% SDS, 20% glycerol, 0.002% bromophenol blue
DTT stock solution	1 M DTT
Staining buffer	0.5 g Coomassie Brilliant Blue R250 in 180 ml methanol : H ₂ O (1:1, V/V) and 20 ml glacial acetic acid
Destaining solution	Methanol : H ₂ O : glacial acetic acid (V/V) = 9:9:1

2.4.3. Immunofluorescence (IF)

Immunofluorescence experiment was performed as described with some modification (Sambrook, Russell et al. 2001).

Yeast cells were fixed with 4% paraformaldehyde for 1 hour. After removing cell wall by treatment with lyticase, the yeast cells were dropped onto coverslip and kept at 4 °C for 30 minutes. The coverslip was incubated with blocking solution (0.1% Triton100/PBS/1% BSA) for 1 hour. Rat anti- α tubulin antibody with a dilution ratio of 1:25 was added into blocking solution for 1 hour incubation. After washing with PBS three times for 5 minutes respectively, the coverslip was incubated with Goat anti Rat IgG antibody with a dilution ratio of 1:200 in blocking solution (light protected) for 1 hour. The coverslip was washed with PBS three times for 5 minutes, followed by Dapi staining and dehydrating with 100% ethanol. After that, mounting solution was added onto slide, and the coverslip was put on the slide with cells facing down. The sample was used for fluorescence imaging under microscopy.

2.5. *Agrobacterium*-mediated transformation (AMT) of yeast

Agrobacterium-mediated transformation of yeast was performed based on reported protocol with modifications (Bundock, den Dulk-Ras et al. 1995; Piers, Heath et al. 1996). Media, chemicals and solutions used in the AMT process are listed in Table 2.4.

A single colony of *Agrobacterium* strain was inoculated into MG/L liquid medium with appropriate antibiotics and grown overnight at 28 °C. The *Agrobacterium* culture was subculture into fresh MG/L medium with 50 times dilution and grown for additional 6-7 hours until $OD_{600} = 1.0$. *Agrobacterium* cells were then collected by centrifugation, washed once with $IBPO_4$ and resuspended in $IBPO_4$ with 200 μ M

acetosyringone for 16 - 18 hours induction at 28 °C. Table 2.6. Media and solutions used in this study ??? Meanwhile, a single colony of yeast strain was inoculated into YPD or SD medium and grown overnight at 30 °C. The overnight yeast culture was subcultured in YPD or SD medium with 20 times dilution and incubate for additional 3-4 hours until $OD_{600} = 0.35$.

1×10^8 *Agrobacterium* cells and 5×10^5 yeast cells were mixed and collected by centrifugation for cocultivation. After washed once with $IBPO_4$, the cells were resuspended in 100 μ l $IBPO_4$, and dropped onto a cocultivation medium (CM) plate. The cocultivation mixture was left in the laminar flow hood until the mixture is dried out on the plate. The CM plates were incubated at 20 °C for cocultivation for 24 hours in darkness. The cocultivated cells were washed off the plate with 1 ml of 0.9% NaCl and plated on SD selection plates with appropriate amino acid drop out supplement and cefotaxime, as well as SD plates with full amino acids for recovery. The plates were incubated at 30 °C for 3-4 days to count the colonies.

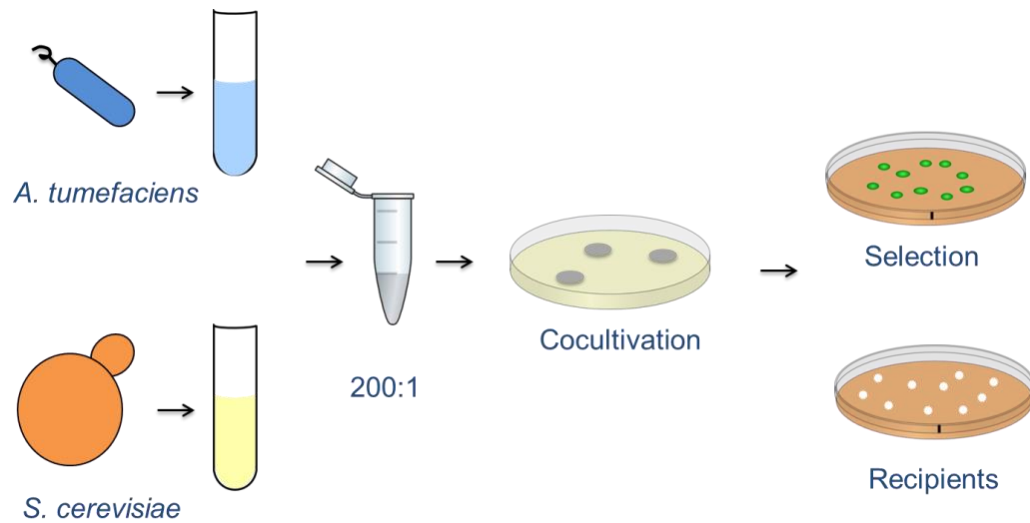


Figure 2.1. Standard protocol for *Agrobacterium*-mediated transformation of yeast.

Agrobacterium is grown in YPD or SD medium and induced in IBPO_4 with AS. After 16 hours of induction, *Agrobacterium* cells are mixed with yeast cells and dropped onto CM plate. CM plate is dried in a laminar flow hood, followed by cocultivation at 20 °C for 24 hours. Afterwards, cocultivated cells are washed off from the plate and spread on selection/recovery plates. The plates are incubated at 30 °C for 3 - 4 days until single colonies occur.

2.6. Quantitative real-time PCR detection of T-DNA

The cellular T-DNA level in AMT recipient cells was detected by using real-time PCR. First, cocultivated yeast cells were washed off from the CM plate. The mixture was sequentially subjected to repeated differential centrifugation, frozen-thawed treatment and lysozyme treatment. These treatments aimed to remove bacteria as much as possible. Total DNA was extracted from the yeast cells as described in Chapter 2.2.2. Real-time PCR was performed as described in Chapter 2.2.5.

Primers were designed to amplify DNA fragments of *URA3*, *virE2* and *PMP3*, which represent the abundance of T-DNA, agrobacteria DNA and yeast DNA, respectively. The primers used in this assay were listed in Table 2.4. The efficiency of three primer pairs were tested, and all three pairs of primer efficiency was close to 100% (data not shown). Therefore, the $2^{-\Delta\Delta CT}$ method was applied for data analysis.

URA3 represent T-DNA both from yeast and bacteria while *VirE2* gene can be detected only in *agrobacterium*. DNA extraction from induced *A. tumefaciens* was used to establish a standard curve showing correlation between Ct (*URA3^{agro}*) and Ct (*virE2*). This standard curve was used for converting Ct (*virE2*) (amount of agrobacteria DNA) into corresponding value of Ct (*URA3^{agro}*) (contaminant T-DNA). Normalizing Ct (*URA3*) and Ct (*URA3^{agro}*) with Ct (*PMP3*) obtained relative abundance of T-DNA and contaminant T-DNA. Therefore, contaminant proportion of T-DNA would be deducted from total T-DNA levels to obtain *Agrobacterium*-delivered T-DNA level inside host cells.

2.7. Visualization of *Agrobacterium*-delivered VirE2 by Split-GFP assay

In order to achieve real-time visualization of *Agrobacterium*-delivered VirE2 in *S.*

cerevisiae and *N. benthamiana* recipient cells, a split-GFP assay was performed in this study (Li, Yang et al. 2014). Briefly, the small GFP fragment (GFP11) was first inserted into VirE2 at a permissive site to create the VirE2-GFP11 fusion protein and expressed in *Agrobacterium* (EHA105*virE2::GFP11*). The large fragment (GFP1–10) was expressed in recipient cells. For yeast, EHA105*virE2::GFP11* was cocultivated with yeast cells as described in Chapter 2.2.5. For the natural host plant, EHA105*virE2::GFP11* was infiltrated into *N. benthamiana* Nb308A leaves using the protocol described in Chapter 2.2.10. The GFP fluorescence signals were visualized by microscopy observation after delivery of VirE2-GFP11 into the recipient cells.

2.8. Virus induced gene silencing (VIGS)

Virus induced gene silencing (VIGS) was performed to generate gene silencing *N. Benthamiana* (Liu, Schiff et al. 2002; Anand, Vaghchhipawala et al. 2007; Dong, Burch-Smith et al. 2007).

A ~220 bp sequence of *NbBUD31* was amplified by PCR from *N. benthamiana* cDNA. The PCR products were cloned into the VIGS vector pTRV2. The construct pTRV2-*NbBUD31* was confirmed by DNA sequencing.

pTRV1, pTRV2 and pTRV2-*NbBUD31* were introduced into *Agrobacterium* strain GV3101 by electroporation, respectively. Transformed bacteria were grown for 2 days on LB plates containing 50 µg/ml Kanamycin for selecting positive cells.

Agrobacterium strain GV3101 containing pTRV1, pTRV2 and pTRV2-*NbBUD31* plasmids were grown overnight at 28 °C in liquid LB medium. *Agrobacterium* cells were harvested by centrifugation and resuspended in infiltration buffer (10 mM MgCl₂, 10 mM MES, and 200 µM acetosyringone) to OD₆₀₀ = 0.8. *Agrobacterium* cultures containing TRV or TRV-derivative plasmids were mixed in 1:1 ratio and then incubated at room temperature for 3 hours.

Agrobacterium culture was infiltrated onto the abaxial side of lower leaf of 4-leaf stage *N. benthamiana* plants using a 1ml syringe. 2 or 3 leaves of each plant need to be injected.

Total RNA was extracted from upper leaves of gene silenced plants (TRV::*NbBUD31*), empty vector control plants (TRV::00) and untreated wide type plants (WT) with protocol described in Chapter 2.3.2.

Real-time PCR was performed with protocol described in Chapter 2.2.5 to detect the transcriptional level of *NbBUD31* gene in TRV::*NbBUD31*, TRV::00 and WT. To ensure the endogenous gene is tested, real-time PCR primers were design to anneal outside the region targeted for silencing.

2.9. Tumorigenesis

2.9.1. In planta tumor assay

Three weeks after VIGS, the in planta tumor assays were performed on the gene silenced plants (TRV::*NbBUD31*), control plant (TRV::00) and WT. The stem of the plant were punctured by using a needle. *Agrobacterium tumefaciens* A348 was inoculated onto stem wound by the same needle. The crown gall tumor was observed 4 weeks after *Agrobacterium* inoculation (Anand, Vaghchhipawala et al. 2007).

2.9.2. Leaf-disk tumorigenesis assay

Leaves from *NbBUD31* silenced plants (TRV::*NbBUD31*), control plants (TRV::00) and untreated plants (WT) were collected 3 weeks after VIGS infiltration, then washed twice with ddH₂O and then treated with 10% Clorox for 10 minutes. After washing for three times with sterile ddH₂O, the leaves were punched into disk by a cork borer (0.5 cm). *A. tumefaciens* strain A348 was grown in MG/L medium overnight and

subcultured with 1:50 dilution for additional 6-7 hours until $OD_{600} = 1.0$. The cells were collected by centrifugation and resuspended in sterile ddH₂O to a final concentration of $OD_{600} = 0.1$.

The leaf disks were incubated with *Agrobacterium* suspension for 15 min for sufficient attachment, followed by washing with sterile ddH₂O and placed on sterile filter paper to blot up and remove unattached bacteria. The leaf disks were transferred to solid MS medium to cocultivate with *Agrobacterium* at 20 °C for 2 days. 20 leaf disks for each plant were transferred to MS medium with 100 µg /ml Cef.

The plate was incubated at 20 °C in darkness for 4 weeks for tumor formation. The total biomass of the leaf was measured by weighing the fresh and dry weights. After weighing the fresh weight, the leaves were incubated at 37 °C for 5 days to weigh dry weights (Anand, Vaghchhipawala et al. 2007).

2.10. Agroinfiltration

Agrobacterium strain was grown overnight, and subcultured with 50 times dilution for additional 6-7 hours growing until $OD_{600} = 1.0$. The bacteria cells were pelleted by centrifuging, and then resuspended in infiltration buffer (10 mM MgCl₂, 10 mM MES, and 200 µM acetosyringone) to $OD_{600} = 1.0$. Cell suspension was then infiltrated into the abaxial side (lower side) of *N. benthamiana*/*A. thaliana* leaves using a 1 ml syringe without needle. The infiltrated plant was kept at 22 °C with a photoperiod of 16 h of light and 8 h of dark (Lee and Yang 2006).

2.11. Imaging techniques

2.11.1. Sample preparation for microscopy imaging

Yeast and bacterial cells were fixed and stained by DAPI (if necessary) before microscopy imaging. The cells were collected by centrifugation and washed with ddH₂O. The cells were then fixed with 4% paraformaldehyde for 1 hour at room temperature, followed by washing twice with water and resuspended in water. After the addition of 95% ethanol, the mixture was incubated for 2 min and pelleted. 10 µl DAPI (1: 20 in H₂O) was added and incubated at room temperature for 10 minutes. The cells were collected by centrifugation and resuspended in ddH₂O for microscopy observation.

N. benthamiana sample was cut from an agroinfiltrated leaf. The leaf tissue was placed on slide and sealed in 2% low melting agarose under a coverslip.

2.11.2. Fluorescent microscopy and confocal microscopy

In this study, Olympus Fluoview FV1000, Carl Zeiss Laser Scanning Microscope (LSM) 510 Meta and PerkinElmer UltraViewVox Spinning Disk were used to perform fluorescent microscopy and confocal microscopy for visualized observation.

Chapter 3. Involvement of Spliceosome Components in

***Agrobacterium*-yeast gene transfer**

During *Agrobacterium*-mediated gene transfer process, many bacterial factors involved in T-DNA transfer have been well studied in previous studies (Lacroix and Citovsky 2013). However, it still remains elusive how T-DNA complex travels inside the host cells and how host factors facilitate this process. In this study, *Saccharomyces cerevisiae* was used as a model to investigate the host roles in the AMT for its small genome size and easy-going manipulation approaches compared to plants.

A genome-wide transformation screening has been performed by using liquid transformation assay. This high-throughput screening has identified more than 200 candidate genes which may have effects on AMT process (Tu 2010). In this chapter, based on the global profiling results, a small scale screening was performed for further confirmation. Among these candidates, yeast mutant *bud31Δ* was found to show significantly decreased transformation efficiency and therefore it was selected for further study. *Agrobacterium*-mediated efficiency tests of genes related to *BUD31* showed that proteins from the NineTeen Complex (NTC), which associates with spliceosome during pre-mRNA splicing, may play a role in *Agrobacterium*-yeast transformation process.

3.1. Introduction of BUD31p and NineTeen Complex (NTC)

3.1.1. Literature review of *BUD31* gene

BUD31 (Systematic Name YCR063W) was first found as an open reading frame (ORF) located on right arm of chromosome III of *Saccharomyces cerevisiae*, the sequence of which is found to have 51% homology with the G10 gene product of

Xenopus laevis (Benit, Chanet et al. 1992). After the release of sequence of yeast chromosome III, ORFs were re-examined by computer methods. YCR063W ORF was predicted to encode a protein of 157 amino acids with a Zn finger region and have nucleic acid binding activity (Koonin, Bork et al. 1994). A human homologue of YCR063W, *edg-2*, was isolated from human umbilical vein endothelial cells (HUVEC). The structure of *edg-2* polypeptide suggests that it may be a nuclear regulator of transcription. Its sequence is highly conserved in evolution from yeast and *Caenorhabditis elegans* to human, suggesting that it may be an important regulator of general nuclear function (Hla, Jackson et al. 1995). The high identity between YCR063W, *edg-2* and *G10* showed that this gene is conserved among different species during evolution. In a genome-wide screening of homozygous diploid yeast deletion strains, which aim to identify non-essential genes participating in the bipolar budding pattern, knockout strain of YCR063W showed a random distribution of bud scars on the cell surface, therefore it was named as *BUD31* (Ni and Snyder 2001). YCR063W was also named as *Cwc14* because it was identified in a Cef1p sub-complex of spliceosome through tandem affinity purification (TAP) assay. Cwc14p could be coimmunoprecipitated with Cef1p (Ohi, Link et al. 2002). These results first implied an involvement of Bud31p in splicing process.

After *BUD31* was identified, detailed function of Bud31p was investigated by many research groups. First of all, the function of Bud31p involved in splicing has been reported in many papers (Gavin, Bosche et al. 2002; Masciadri, Areces et al. 2004; Wang, He et al. 2005; Saha, Banerjee et al. 2012; Saha, Khandelia et al. 2012; Saha, Khandelia et al. 2012).

Bud31p was identified as a member of NTC-associated complex in a Mass Spectrometry-based proteomic study (Gavin, Bosche et al. 2002). *BUD31*-null yeast strain was generated and showed a phenotype with abnormality in cytoskeleton

structure, actin distribution and bud formation. Bud31p was also found to interact with proteins involved in mRNA splicing. Accumulation of unspliced mRNA of two genes, *ACT1* and *PFY1* which are involved in cytoskeletal organization, were found in *BUD31*-null yeast which indicates that Bud31p may play a role in pre-mRNA splicing process (Masciadri, Areces et al. 2004). SF3b is a subcomplex of U2 small nuclear ribonucleoprotein (snRNP). Some proteins including Bud31p were purified with SF3b U2 subcomplex that associates with the pre-mRNA branch point region (Wang, He et al. 2005). Bud31p is a non-essential splicing factor required for viability of *S. cerevisiae* cells at growth temperatures > 34 °C. Like a number of other non-essential pre-mRNA splicing factors required for growth in specific conditions, the functions of Bud31p can be hypothesized to increase the efficiency of selected splicing steps. By using *in vitro* splicing assays, Bud31p was found to be required for efficient progression to the first catalytic step and for the second catalytic step of splicing at high temperatures. It was found in pre-catalytic B complex and B^{act} complex. It interact with U5 and U6 snRNPs, and associates with spliceosome containing pre-mRNA although it does not interact with pre-mRNA directly. It was also found that Bud31p affects the interaction of a ~25 kDa protein to the exonic 5' splice site in splicing reactions at elevated temperature. Therefore, the function of Bud31p is to stabilize pre-mRNA protein interactions that may facilitate efficient splicing (Saha, Khandelia et al. 2012). In addition, Bud31p is required for the splicing of some pre-mRNAs, not all of them. For example, *ARP2* and *SRC1* encode proteins required for budding. Wild type cells have a long and a short isoform of *SRC1* mRNA and protein, while *bud31Δ* cells entirely lack the shorter *SRC1* spliced mRNA isoform (Saha, Banerjee et al. 2012).

Like other splicing factors in *S. cerevisiae*, besides its function as a splicing factor, *BUD31* has also been reported to relate to other cellular processes such as cell cycle, ribosome biogenesis and DNA repair. For example, loss of the protective function of

telomeres had been hypothesized to cause a DNA damage response. The telomerase deletion response (TDR) occurs when telomeres can no longer be maintained by telomerase. In a genome-wide expression response to telomerase deletion assay in yeast, Bud31p was found to be up-regulated in TDR(Nautiyal 2002). Eukaryotic cells have two enzymatically distinct pathways for double-strand break repair (DSBR). One is the repair by homologous recombination which is known as single-strand annealing (SSA) and the other is the repair by non-homologue end joining (NHEJ). In a genome-wide screening, *BUD31* mutant was found to have enhanced NHEJ, deficient SSA and increased NHEJ/SSA ratio (Wilson 2002). By using a high-throughput method called selective ploidy ablation (SPA), a genome-wide screening was performed and the screening results indicate that *BUD31* was required for viability upon expression of top1-T722A. Top1-T722A is a mutant DNA topoisomerase I which could mimic the activity of the chemotherapy drug camptothecin (CPT) that leads to replication dependent DNA breaks and ultimately cell death if those breaks cannot be repaired (Reid, Gonzalez-Barrera et al. 2010). These results indicate an involvement of *BUD31* in DNA repair function.

In a systematic genome-wide screening for identification of yeast genes which affect replication of a positive-strand RNA virus Brome mosaic virus (BMV), Bud31p deletion mutant was found to have enhanced BMV-directed Rluc expression more than 1000 folds compared to wild type yeast(Kushner 2003). Bud31p mutant was also found to be sensitive to the drug in a screening of the *S. cerevisiae* homozygous diploid deletion library against a sublethal concentration of cisplatin (Liao, Hu et al. 2007). *BUD31* was found to be necessary for normal growth of yeast on oleic acid in a screening of the haploid yeast deletion collection to investigate the peroxisome and other processes in membrane function, as peroxisome is the sole site of β -oxidation in yeast and known to be required for optimal growth in the presence of fatty acid

(Lockshon, Surface et al. 2007). In a genome wide screening for genes conferring resistance to the simultaneous presence of different relevant stresses, Bud31p was found to be essential for maximal fermentation performance under industrial conditions. The expression of Bud31p could lead to the increase of both ethanol yield and fermentation rate (Pereira, Guimaraes et al. 2011).

BUD31 was also found to bind androgen receptor (AR) in human prostate cancer cells. ARs bind to peptides containing an FxxY motif cluster with Tyr in the +5 position. *BUD31* is found to contain the same peptide sequence. The *BUD31*-FxxFY peptide suppressed AR transactivation and AR-mediated cell growth effectively (Hsu, Liu et al. 2014).

In summary, *BUD31* gene has been reported as a splicing factor which could interact with spliceosome during splicing process and is required for the splicing of some of pre-mRNAs, including those encoding for proteins required for budding. *BUD31* also involves in other biological process where the exact function of Bud31p is still unclear. The additional functions for splicing factors can be ascribed to two reasons. One possibility is some factors could be directly involved in two different cellular processes. On the other hand, their role in splicing may affect gene expression required for other cellular pathways.

In addition, there is no report of the involvement of *BUD31* in *Agrobacterium*-mediated transformation.

3.1.2. Literature review of NineTeen Complex (NTC)

NineTeen Complex (NTC), also known as *Prp19* complex (Prp19C) which was named by its founding member *Prp19* (Tarn, Lee et al. 1993), is a protein complex involved in various cellular processes for cell homeostasis. NTC is also highly conserved as it is found in yeast as well as higher eukaryotes such as animals and plants

(Koncz, deJong et al. 2012). In *Saccharomyces cerevisiae*, only one NTC has been identified which consists of eight core proteins (*Prp19*, *Cef1*, *Syf1*, *Syf2*, *Syf3*, *Snt309*, *Isy1* and *Ntc20*) and up to 19 associated proteins, while at least three Prp19-like complexes (PRP19/CDC5L, Prp19-associated and XAB2) exist in human cells (Chanarat and Sträßer 2013). NTC is important in cell homeostasis as it has multiple cellular functions which are related to the regulation of mRNA splicing (Chan, Kao et al. 2003; Will and Lührmann 2011), DNA repair (Grey, Düsterhöft et al. 1996; Mahajan and Mitchell 2003), lipid droplet biogenesis (Si, Eui et al. 2007), guidance for programmed protein degradation (Ohi, Vander Kooi et al. 2003; Löscher, Fortschegger et al. 2005) and transcription elongation (Zhou and Hayward 2001; Kang, Lee et al. 2009).

The most studied cellular function of NTC is its regulatory role in mRNA splicing. In eukaryotes, most pre-mRNAs consist of introns and exons. To form matured mRNAs for further translation, pre-mRNA should firstly be subjected to a splicing process, i.e. the removal of introns and the re-ligation of exons. This mRNA splicing process is catalyzed by spliceosome, a huge ribonucleoprotein (RNP) complex which consists of five small nuclear RNPs (U1, U2, U4, U5 and U6 snRNPs) with one corresponding small nuclear RNA (snRNA) in each snRNP. These five snRNPs assemble dynamically with the pre-mRNA at different stages in the splicing process, forming different spliceosome complexes (A, B, B^{act}, B* and C complexes) and catalyze two transesterification steps (cleavage of the intron at 5' and cleavage of the intron and re-ligation of exons at 3'). As a regulator, NTC functions at multiple stages of the splicing process (Hogg, McGrail et al. 2010). The first stage of NTC function in the splicing process is during the activation of the spliceosome complex (transformation from B to B^{act} complex). In this stage, NTC and *Prp19* associated proteins join the spliceosome with the U4/U6.U5 tri-snRNP before and during the unwinding of U4

from U6. NTC and NTC-associated proteins have been identified as essential stabilizers for the interaction between U5/U6 snRNP and the spliceosome after the activation process as the depletion of NTC causes disability of U5 and U6 snRNA to associate with activated spliceosome (Fabrizio, Dannenberg et al. 2009). This NTC-mediated stabilization of U5 and U6 is most likely due to the promotion of NTC to the interaction of U5 and U6 with substrate pre-mRNAs (Chan, Kao et al. 2003; Chan and Cheng 2005). Despite the stabilizing effect of NTC to snRNPs, at least two NTC-associated proteins, *Yju2* and *Cwc25*, have been identified as essential elements to the catalytic activity of spliceosome for the first step transesterification (Liu, Chen et al. 2007; Chiu, Liu et al. 2009; Warkocki, Odenw älder et al. 2009). *Yju2*'s capability of stalling pre-catalytic spliceosome with splicing functionality indicates its essential role in spliceosome activation (Liu, Chen et al. 2007). Nevertheless, *Yju2* interacts with spliceosome in a distinct manner as it only associates with spliceosome upon activation and appears disassociated with spliceosome after activation (Liu, Chen et al. 2007). *Cwc25* also shows its essence to spliceosome activation although the complementation of *Cwc25* only restores marginal level of the splicing activity of the spliceosome which indicates the involvement of other potential co-factors (Chiu, Liu et al. 2009). Despite its function in the spliceosome activation and first transesterification reaction, NTC also plays a role in spliceosome biogenesis and recycling. For example, *Cwc23*, one of the NTC-associated proteins, interacts with *Ntr1* which is a key protein catalyzing spliceosome disassembly (Sahi, Lee et al. 2010). It was found that the *Cwc23* mutant displays accumulation of un-spliced pre-mRNA and lariat intron, indicating the disruption of spliceosome disassembly and subsequent recycling (Arenas and Abelson 1997; Sahi, Lee et al. 2010). On the other hand, deletion of other NTC proteins, such as *PRP19*, *NTC90*, *NTC77*, *NTC20* and *NTC30*, results in the accumulation of free U4 snRNP, which also indicates the hampering of spliceosome recycling (Chen, Kao et al.

2006).

Despite its main function in regulating mRNA splicing, NTC also involves in the DNA repair process to maintain the integrity of the genome. *Prp19*, the first discovered member of NTC was initially identified as a protein involved in the error-prone repair in yeast (Henriques, Vicente et al. 1989). Its analog in human, *hPRP19*, was found to be a component of nuclear matrix NMP200 which interacts with terminal deoxynucleotidyltransferase (TdT) and assists cell revival after DNA damage (Gotzmann, Gerner et al. 2000; Mahajan and Mitchell 2003). It was found that the loss of *hPRP19* expression resulted in the accumulation of double strand breaks (DSB), a common form of genomic DNA damage (Mahajan and Mitchell 2003). Despite *PRP 19*, other proteins in NTC were also found to relate to DNA repair. For example, *P29*, the analog of *SYF2* in human, interacts with DNA replication licensing factor MCM3 and the deletion of *P29* results in the increased sensitivity of the cell to UV irradiation and slow down of DNA synthesis (Chu, Yang et al. 2006).

Lipid droplets are cellular organelles with important functions such as storing energy for cell metabolism, providing building blocks for cell membrane and detoxification of excess intracellular lipids (Farese Jr and Walther 2009). NTC is found to play a role in lipid droplet biogenesis. *PRP19* was found to reduce the level of triacylglycerols and the structural proteins of lipid droplets (Si, Eui et al. 2007). Moreover, *PRP19* is essential for lipid droplet maturation and for fat storage in preadipocytes. As there are few reports linking NTC with lipid droplets biogenesis, the exact mechanism for NTC still needs further investigation.

Ubiquitin-proteasome system is crucial in programmed protein degradation (Wilkinson 2000). The proteins labeled with multiple ubiquitin molecules is subjected to 26S proteasome for degradation. *PRP19* protein, which has an N-terminal U-box/RING domain, has E3 ubiquitin ligase activity (Ohi, Vander Kooi et al. 2003). It

was found that mouse *PRP19* interacts with *mSUG1*, a subunit of regulatory part of the proteasome and the overexpression of *PRP19* promotes proteasome activity *in vivo* (Sihn, Cho et al. 2007). Moreover, *hPRP19* can interact with *PSMB4/Pr4/beta7* which is a component of 20S catalytic core of proteasome (L öscher, Fortschegger et al. 2005). This indicates *hPRP19* could involve in the process for the recruitment of ubiquitin-tagged protein to the proteasome. Although evidences have linked *PRP19* to the ubiquitin-proteasome system, the actual target for its E3 ligase-like domain is still unknown and should be further explored.

Last but not least, NTC also functions in the process of gene transcription and RNA export. In yeast, NTC interacts with RNA polymerase II (RNAPII) and TREX complex (Chanarat, Seizl et al. 2011). The TREX complex moves along the gene with the transcription machinery and functions in the simultaneous assembly of mRNA into mRNP during DNA transcription process (St äßer, Masuda et al. 2002; Meinel, Burkert-Kautzsch et al. 2013). It was found that the *syf1*-truncated NTC displayed a decreased interaction with RNAPII and diminished recruitment to the genes (Chanarat, Seizl et al. 2011). It in turn decreased the occupancy of TREX to the gene. These results indicate that recruited TREX can be stabilized by NTC. Nevertheless, the exact interaction mechanism between NTC and TREX is still unknown and opens opportunity for future works.

***SNT309* in NTC**

SNT309, also known as *NTC25* with its analog of *SPF27* in human cells, is one of the eight core proteins in NTC. *SNT309* was first identified to interact with *PRP19* and function in the pre-mRNA splicing (Chen, Jan et al. 1998). The co-mutation of *SNT309* and *PRP19* was found to be lethal to yeast cells and the mutation of *SNT309* alone destabilizes the NTC and makes the NTC nonfunctional in splicing process (Chen, Tsao et al. 1999). In addition, the *SNT309* and *PRP19* mutant displays accumulation of free

U4 snRNA and the down regulation of U6 snRNA, while the overexpression of U6 snRNA suppress the temperature sensitive defect of the mutant (Chen, Kao et al. 2006). These results indicate the role of *SNT309* in the recycling of snRNPs. *SNT309* is also believed to modulate the interaction of Prp19p with other components of NTC, such as Cef1p which is involved in intron removal from pre-mRNA in the splicing process (Chen, Tsao et al. 1999). Despite its role in splicing, *SNT309* itself is one of the co-activators of nuclear receptors and is directly recruited as promoters of protein-coding gene in human cells (Zhou and Hayward 2001).

***SYF2* in NTC**

SYF2, also known as *NTC31*, is also a core component of NTC. *SYF2* gene encodes a small protein (215 aa). It is identified as a splicing factor by interacting with a group of proteins including *SYF1*, *SYF3*, *CEF1*, *NTC20*, *ISY1* and *PRP22* (Ben-Yehuda, Dix et al. 2000). *SYF2* is also involved in DNA replication in mammalian cells (Chu, Yang et al. 2006).

3. 2. Yeast *BUD31* is involved in *Agrobacterium*-mediated

transformation

3.2.1. Yeast mutant *bud31Δ* shows decreased efficiency of

***Agrobacterium*-mediated transformation**

Based on genome-wide screening data (Tu 2010), several yeast mutants that may affect T-DNA transfer were selected to test their AMT efficiency as described in Chapter 2. Briefly, yeast strain BY4741, a leucine auxotrophic mutant, was used in this study, while the *Agrobacterium* harbors a plasmid pHT101 with the marker genes *LEU2* and *GFP*. The nutrition-marker gene *LEU2* allows for the selection of transformed yeast cells in the absence of leucine, and the fluorescence-marker gene

GFP can confirm these positive transformants. *Agrobacterium* was induced in IBPO₄ with acetosyringone (AS), and then cocultivated with yeast cell on cocultivation (CM) plates with appropriate amino acid at 20 °C for 24 hours. The cell mixture were collected and plated onto SD Leu⁻ agar plates and recovery plates. Transformation efficiency was calculated as the ratio of number of transformants to the number of recipients and compared to the wild type (WT). Among these mutants, a yeast mutant *bud31Δ* shows significantly decreased transformation efficiency compared with wild type strain BY4741, indicating it may play a role in the AMT process (Figure 3.1.A).

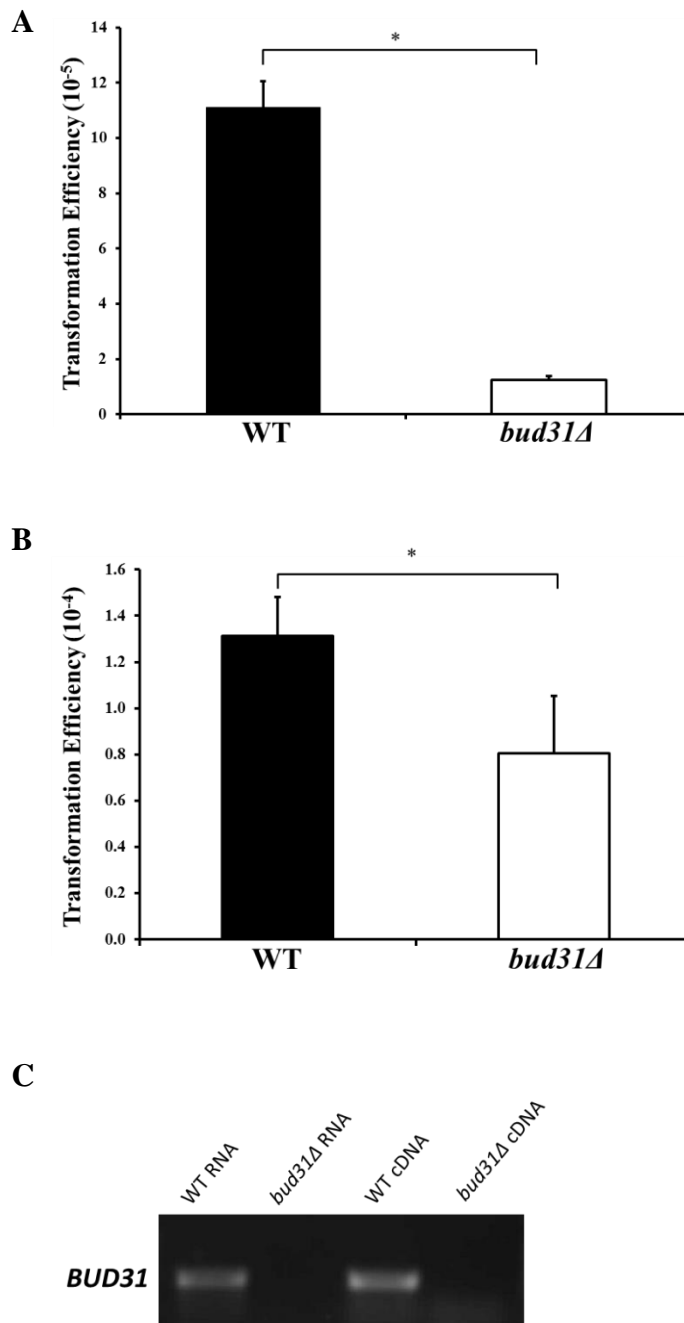


Figure 3.1. Yeast mutant *bud31Δ* showed decreased *Agrobacterium*-mediated transformation efficiency.

(A). AMT efficiency of yeast mutant *bud31Δ* and wild type strain BY4741, * $P < 0.05$. (B). LiAc transformation efficiency of *bud31Δ* and wild type strain BY4741, * $P < 0.05$. (C). Detection of transcriptional *BUD31* in *bud31Δ* and wild type strain BY4741.

3.3.2. The effect of yeast *BUD31* in *Agrobacterium*-mediated transformation is specific

In order to investigate the important role of *BUD31* in AMT, lithium acetate transformation and complementation experiment were performed.

After lithium acetate treatment of the cells, extracellular plasmid pHT101, the same plasmid used for AMT experiment, was transformed into yeast cell as described in Chapter 2. Transformation efficiency was calculated and showed in Figure 3.1.B. *Agrobacterium*-mediated transformation and LiAc transformation are two different pathways. LiAc method is a physicochemical approach shows the ability of the yeast cell to take up extracellular DNA and express it. Meanwhile, *Agrobacterium*-mediated transformation employs a type IV secretion system.

LiAc transformation efficiency of *bud31Δ* was lower than WT which indicates that *BUD31* may be involved in regulation of extracellular DNA uptake and expression. However, the fold changes of LiAc transformation efficiency was not as significant as that of AMT which suggested that the *Agrobacterium* factor was also needed. Therefore, Bud31p has specific effect on *Agrobacterium*-mediated transformation.

PCR results showed that transcripts of *BUD31* was not detected in total RNA and cDNA of *bud31Δ* (Figure 3.1.C), which confirmed the effect of *bud31Δ* on AMT and other experiments in this study, is caused by knockout of the *BUD31*.

According to chromosomal location map (Figure 3.2.A), there is a dubious open reading frame YCR064C partially overlaps with *BUD31*. Based on available experimental and comparative sequence data, YCR064C is unlikely to encode a functional protein (Fisk, Ball et al. 2006). Therefore, complementation experiment was performed to investigate if the decreased transformation efficiency of *bud31Δ* was caused by loss of *BUD31* function, or by loss of *YCR064C* function.

Genomic *BUD31* and *YCR064C* sequences were cloned into pHT105 vector and

expressed in wide type strain and mutant strain. When *bud31Δ* was complemented with genomic *BUD31* sequence, the decreased AMT efficiency was partially restored while the complementation with YCR064C showed no effect (Figure3.2.B). This result suggested that the loss of *BUD31* contributed to the AMT rather than *YCR064C*.

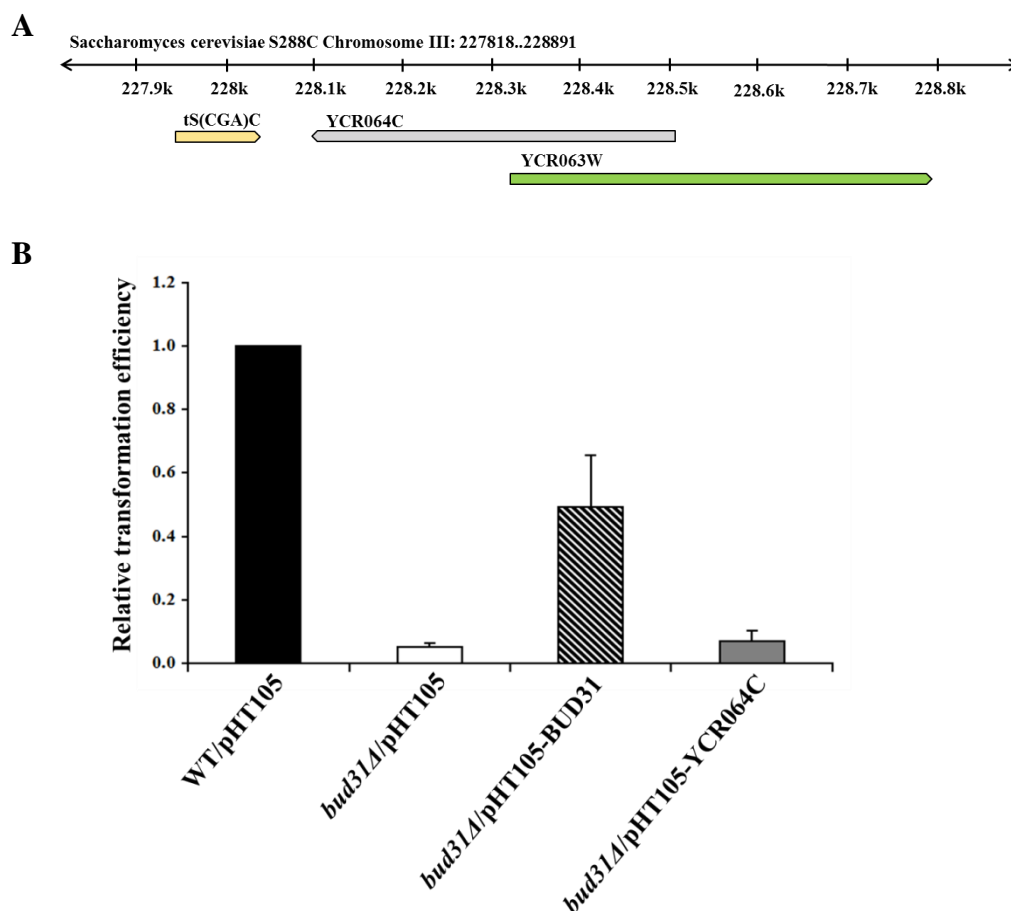


Figure 3.2. Complementation experiment confirmed the important role of yeast Bud31p in AMT process.

(A). Chromosomal location of *BUD31* and YCR064C. (B).Relative AMT efficiency of *bud31Δ* complemented with genomic *BUD31* and YCR064C sequence.

3.3. Yeast NineTeen Complex (NTC) is involved in *Agrobacterium*-mediated transformation

Bud31p is a splicing factor which involves in pre-mRNA splicing (Masciadri, Areces et al. 2004). It is found to associate with many other proteins, such as Cef1p (Ohi, Link et al. 2002) , SF3b U2 subcomplex (Wang, He et al. 2005) and Prp43p (Lebaron, Froment et al. 2005). In order to investigate the role of Bud31p in AMT, AMT efficiency of many genes related to Bud31p was tested. Among them, yeast NineTeen Complex (NTC) components showed to have effect on AMT process.

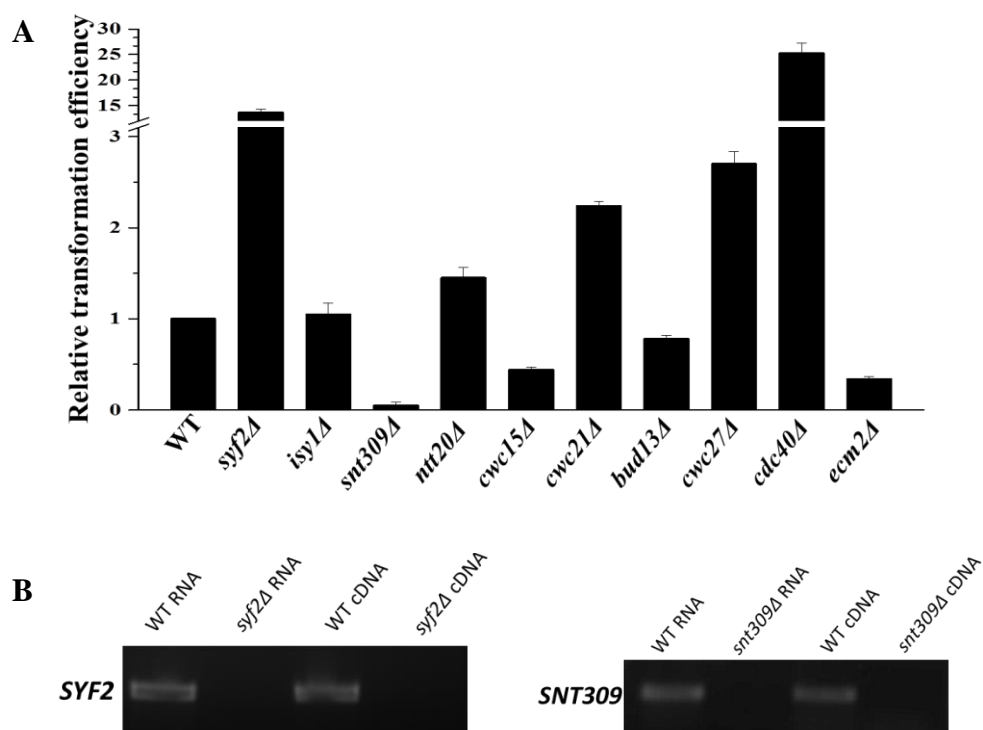
The NTC is named after PRP19, the first identified splicing factor in yeast (Cheng, Tarn et al. 1993). NTC has eight core proteins (Prp19p, Cef1p, Syf1p, Syf2p, Syf3p, Snt309p, Isy1p and Ntc20p) and many associated proteins (Wahl, Will et al. 2009; Hogg, McGrail et al. 2010). Bud31p is one of the proteins which have association with NTC.

AMT efficiency of four core protein mutants in yeast knock-out (YKO) collection (*syf2Δ*, *isy1Δ*, *snt309Δ*, *ntC20Δ*) and six NTC associated protein mutants (*cwc15Δ*, *cwc21Δ*, *bud13Δ*, *cwc27Δ*, *cdc40Δ*, *ecm2Δ*) was tested and showed in Figure 3.3.A. Interestingly, two of the NTC core proteins, Syf2p and Snt309p, have opposite effect on AMT efficiency. The knockout of Syf2p dramatically increased the transformation efficiency more than 20 times compared to wild type strain while the knockout of Snt309p reduced the transformation efficiency by 20 times. The knockout of another NTC related protein Cdc40p also showed enhanced AMT efficiency. Due to the extreme slow growth rate of *cdc40 Δ*, this mutant was not included in further study.

PCR results showed that transcripts of *SNT309* and *SYF2* were not detected in total RNA and cDNA of *snt309Δ* and *syf2Δ* (Figure 3.3.B). These results confirmed the effect of these two mutants in this study is caused by knockout of the *SNT309* and

SYF2.

LiAc transformation results showed deletion of *SNT309* caused decreased LiAc transformation efficiency, though the fold change was less than that in the AMT experiment. In addition, deletion of *SYF2* did not affect LiAc transformation efficiency (Figure 3.3.C). Complementation experiment was also performed and the results showed that expression of genomic sequence of *SNT309* in *snt309Δ* could complement the AMT deficiency in *snt309Δ*. Meanwhile, expression of *SYF2* in *syf2Δ* also partially recovered the enhanced transformation efficiency (Figure 3.3.D).



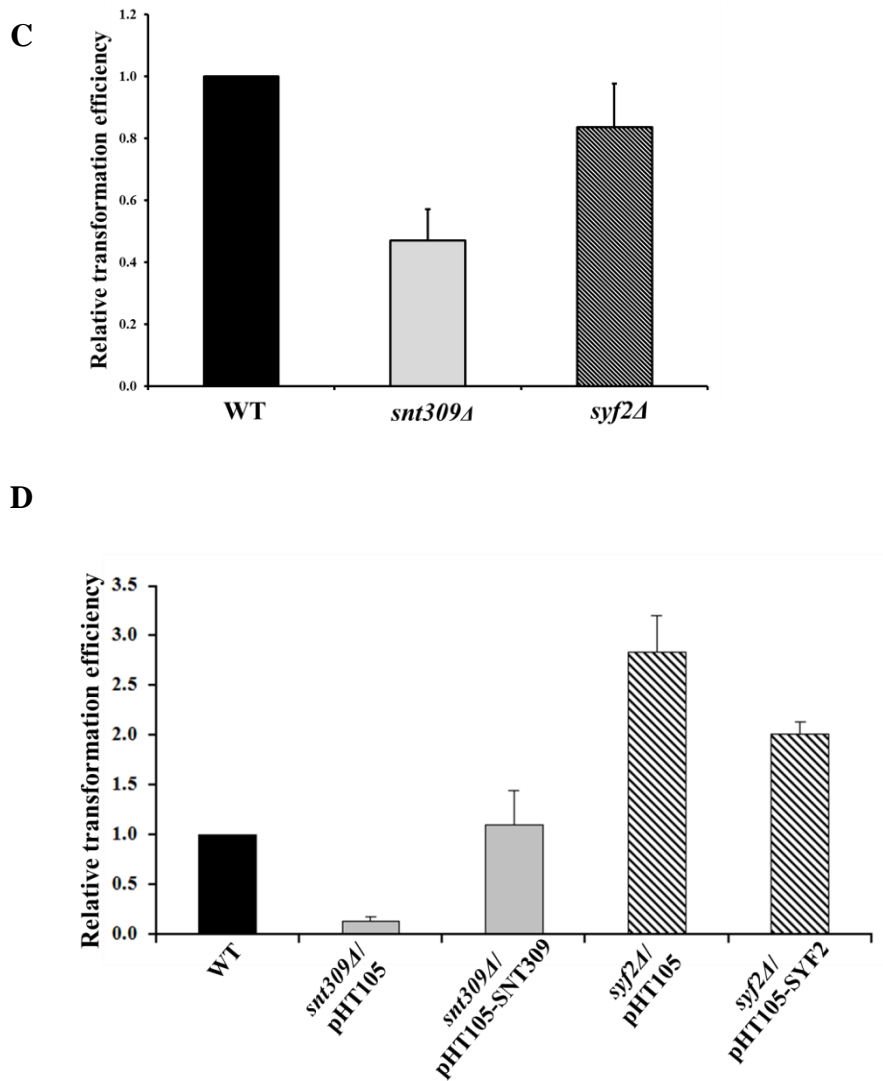


Figure 3.3. The involvement of Yeast NineTeen complex (NTC) components in *Agrobacterium*-mediated transformation.

(A).Relative AMT effecincy of yeast NineTeen complex mutant and wild type strain BY4741. (B).Detection of transcriptional *SNT309* and *SYF2* in *snt309Δ*, *syf2Δ* and wild type strain BY4741. (C). Relative LiAc transformation efficiency of *snt309Δ*, *syf2Δ* and wild type strain BY4741. (D). Relative AMT efficiency of *snt309Δ* and *syf2Δ* complemented with genomic *SNT309* and *SYF2* sequence.

Some essential genes deletion mutants are not included in yeast knock-out (YKO) collection (Winzeler, Shoemaker et al. 1999). Therefore, the Tet-promoters Hughes collection (yTHC) developed by Hughes Laboratory was used in which the expression of essential genes can be switched off by adding a chemical named doxycycline (Mnaimneh, Davierwala et al. 2004). The AMT protocol for yTHC library mutant was modified from AMT standard protocol. Yeast strain R1158 derived from BY4741 was used as wild type strain in the yTHC library AMT experiment. Doxycycline was added into yeast culture to a final concentration of 10 µg/ml and induced for 18 h before cocultivation. A standard AMT protocol was performed afterwards as described in Chapter 2.5.

Three NTC core components mutants (*PRP19*, *CEF1* and *CLF1*) and NTC associated factors mutants (*CWC2*, *PRP46*, *YJU2*, *CWC22*, *CWC24*, *CWC25*, *PRP22*, *SLU7*, and *SPP2*) were included in yTHC library. Figure 3.4 showed that *prp19* and *cef1* display decreased AMT efficiency after the addition of doxycycline compared to untreated cells, which suggested the suppression of Prp19p and Cef1p caused yeast resistant to *Agrobacterium* infection. Suppression of other essential NTC associated proteins did not affect AMT (data not show). This result verified the important role of NTC during AMT process.

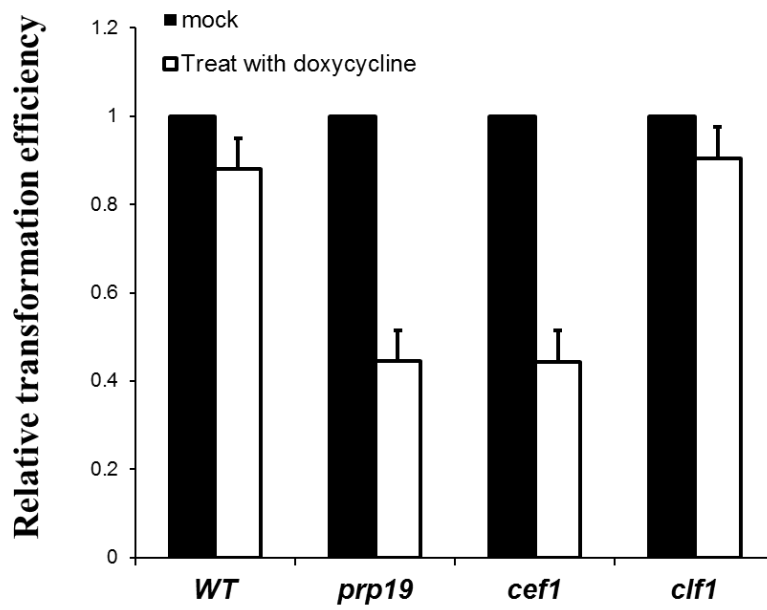


Figure 3.4. Switching off the expression of Prp19p and Cef1p caused decrease in AMT efficiency.

After treatment with doxycycline, AMT efficiency decreased as compared to the untreated cells.

3.4. Discussion

During *Agrobacterium*-mediated transformation, the process inside bacteria has been well studied. However, host factors which are involved in this process remain unclear. As natural host of *Agrobacterium*, plant species should be the first choice of model organism to study host factors involved in this process. However, their genome sizes are too big to achieve a genome wide screening. On the other hand, *Saccharomyces cerevisiae* is a good model to study the molecular mechanism of T-DNA trafficking pathway and the host factors involved in this process for its small genome size, easy manipulation approaches and available mutant library. Many studies have been carried out using *S. cerevisiae* to investigate the role of host factors during AMT process, and many host proteins have been found to be involved in AMT (reviewed in Chapter 1).

Based on a genome-wide transformation screening data (Tu 2010), a small scale screening was performed in this study to further confirm the role of some candidate genes in AMT by using a stranded solid AMT method described in Chapter 2. The AMT results showed that deletion of *BUD31* caused significantly decreased transformation efficiency. LiAc transformation efficiency of *bud31Δ* displayed similar trend as AMT. This indicates that *BUD31* may involve in the pathway shared by these two processes. However the LiAc transformation efficiency fold change is not as significant as AMT, suggesting Bud31p has specific effect on *Agrobacterium*-mediated transformation. According to chromosomal location map, there is a dubious open reading frame YCR064C partially overlaps with *BUD31*. Complementation experiment was performed to confirm that decreased transformation efficiency of *bud31Δ* was caused by loss of Bud31p function. Expression of genomic *BUD31* sequence in *bud31Δ* could partially restore the transformation deficiency in AMT

while expression of YCR064C has no effect. All the results above confirmed that Bud31p plays an important role in *Agrobacterium*-mediated transformation of yeast.

Agrobacterium-mediated efficiency tests of genes related to Bud31p showed the proteins from NineTeen Complex (NTC) which associates with spliceosome during pre-mRNA splicing may play a role in *Agrobacterium*-yeast transformation process.

NTC has eight core proteins and many associated proteins. AMT efficiency of four core proteins deletion mutant (*syf2Δ*, *isy1Δ*, *snt309Δ*, *ntC20Δ*) and six NTC associated protein deletion mutant (*cwc15Δ*, *cwc21Δ*, *bud13Δ*, *cwc27Δ*, *cdc40Δ*, *ecm2Δ*) was tested. Interestingly, knockout of Syf2p dramatically increased the transformation efficiency while a knockout of Snt309p reduced the transformation efficiency. Complementation experiment results showed that complementing *snt309Δ* and *syf2Δ* with *SNT309* and *SYF2*, respectively, will partially rescue the decreased and enhanced transformation efficiency in AMT. These results suggested an active role of NTC in *Agrobacterium*-mediated transformation.

Besides NTC, AMT efficiency of many other proteins related to Bud31p were tested. 30 genes having physical interaction with Bud31p were found in online database BioGRID3.1 (Stark, Breitkreutz et al. 2006). They were identified by affinity capture-MS, co-purification and yeast two-hybrid assay (<http://thebiogrid.org/31040>). 12 gene knockout mutants were found in YKO library. Besides *cwc21Δ* and *snt309Δ* which were already discussed before, relative AMT efficiency of 10 mutants was list in Table 3.1. Among them, a knockout of *ADE8* gene showed dramatically enhanced transformation efficiency about 100 times. The physical interaction between Ade8p and Bud31p was detected by yeast two-hybrid assay (Uetz, Giot et al. 2000). This result is consistent with findings from an early literature which reported that yeast strains containing deletions in some purine synthesis protein, such as *ADE4*, *ADE8*, *ADE1*, or *ADE5/7*, were all supersensitive to *A. tumefaciens* transformation (Roberts 2003).

Bud31p is a component of spliceosome. Knockout of Bud31p caused accumulation of unspliced mRNA of *ACT1* and *PFY1* in yeast cells (Masciadri, Areces et al. 2004). Genes with introns in *Saccharomyces cerevisiae* are the potential downstream genes whose expression may be affected by the deletion of Bud31p. Some of genes with introns were selected and the relative AMT efficiency is showed in Table 3.1. In this group, *IWR1* and several ribosomal proteins arouses our attention as *Iwr1Δ* showed dramatically increased transformation efficiency while the ribosomal proteins all display decreased transformation efficiency.

Previous study showed that NTC also functions in gene transcription and RNA export (reviewed in Chapter 3.1.2). In yeast, NTC interacts with RNA polymerase II (RNAPII) and TREX complex. The TREX complex contains following components: THO complex (*THO2*, *HPR1*, *MFR1*, and *THP2*), intranuclear mRNA export factors (*SUB2*, *YRA1*) and SR proteins (*GBP2*, *HRB1*, and *TEX1*). The AMT efficiency of several TREX complex knockout mutants was tested and listed in Table 3.1. The results showed that deletion of these genes did not affect AMT efficiency significantly (0.4 to 3 times fold change).

Lastly, *BUD31* was reported as a component of the SF3b (a subcomplex of the U2 snRNP) (Wang, He et al. 2005). SF3b subcomplex contains eight proteins: Rse1p, Hsh155p, Hsh49p, Cus1p, Rds3p Rcp10p, Ist3p and Bud31p. Most of them are essential genes. Yeast YKO collection does not include most SF3b subcomplex proteins mutant except *BUD31* and *IST3*. The function of essential genes on AMT is difficult to identify due to the lack of deletion mutant. Therefore the SF3b subcomplex was not included in this study.

Table 3.1. Comparison of the effects on AMT efficiency between other proteins and Bud31p

Gene name	Gene Description	AMT fold change
Physical interactors of Bud31p		
<i>mrpl3Δ</i>	Mitochondrial ribosomal protein of the large subunit	2.51
<i>ade8Δ</i>	Phosphoribosyl-glycinamidetransformylase	99.8
<i>rps4bΔ</i>	Protein component of the small (40S) ribosomal subunit	1.88
<i>mdh1Δ</i>	Mitochondrial malate dehydrogenase	1.15
<i>urn1Δ</i>	Pre-mRNA splicing factor associated with the U2-U5-U6 snRNPs	0.87
<i>hek2Δ</i>	RNA binding protein with similarity to hnRNP-K that localizes to the cytoplasm and to subtelomeric DNA	1.34
<i>mam33Δ</i>	Acidic protein of the mitochondrial matrix involved in oxidative phosphorylation	2.72
<i>mrpl17Δ</i>	Mitochondrial ribosomal protein of the large subunit	0.77
<i>atp1Δ</i>	Alpha subunit of the F1 sector of mitochondrial F1F0 ATP synthase, which is a large, evolutionarily conserved enzyme complex required for ATP synthesis	1.21
<i>rpl2bΔ</i>	Protein component of the large (60S) ribosomal	0.48

subunit

Genes with introns

are2Δ Acyl-CoA:sterolacyltransferase, isozyme of Are1p 0.76

iwr1Δ Protein involved in transcription from polymerase II promoters 29.8

did4Δ Class E Vps protein of the ESCRT-III complex 2.04

mms2Δ Ubiquitin-conjugating enzyme variant involved in error-free post replication repair 1.25

nmd2Δ Protein involved in the nonsense-mediated mRNA decay (NMD) pathway 0.74

rps16aΔ Protein component of the small (40S) ribosomal subunit 2.06

rps19bΔ Protein component of the small (40S) ribosomal subunit 0.58

ypr098cΔ Protein of unknown function, localized to the mitochondrial outer membrane 1.26

rpl35bΔ Ribosomal 60S subunit protein L35B 0.05

rps10aΔ Protein component of the small (40S) ribosomal subunit 0.30

rps4bΔ Protein component of the small (40S) ribosomal subunit; 0.13

rpl21bΔ Ribosomal 60S subunit protein L21B 0

TREX Complex

tho2Δ Subunit of the THO complex 0.57

<i>mft1Δ</i>	Subunit of the THO complex	0.61
<i>thp2Δ</i>	Subunit of the THO and TREX complexes	0.57
<i>gpb2Δ</i>	Poly(A+) RNA-binding protein	1.41
<i>hrb1Δ</i>	Poly(A+) RNA-binding protein	0.53
<i>tex1Δ</i>	Protein involved in mRNA export; component of the transcription export (TREX) complex	0.45

Chapter 4. Effects of *BUD31* and NTC genes in the *Agrobacterium*-yeast gene transfer

4.1. Characterization of Yeast Bud31p

4.1.1. Yeast Bud31p is a nuclear protein

Subcellular protein localization is tightly linked with function. To localize Bud31p inside yeast cells, an EGFP reporter was used to fuse with Bud31p at C-terminus to generate plasmid pHT105-BUD31-GFP. The plasmid pHT105-GFP expressing GFP was used as a control. The confocal images (taken by Carl Zeiss LSM 510 Meta) of BUD31-GFP fusion protein showed a nuclear localization inside both wild type cells and *BUD31* deletion mutant while GFP showed a diffusion expression pattern in cytoplasm (Figure 4.1), which suggested that Bud31p has nucleus localization.

4.1.2. Yeast mutant *bud31Δ* showed different microtubule structures

Immunofluorescence (IF) was performed as described in Chapter 2. Briefly, yeast cells were fixed, treated with lyticase and attached to coverslip. Rat anti- α tubulin antibody and Goat anti Rat IgG antibody were used as first and secondary antibody, respectively. The samples were mounted under fluorescent microscope for observation and the results were shown in Figure 4.2. The structures of microtubules were different in *bud31Δ* compared to WT.

BUD31 deletion mutant has been reported to show a phenotype with abnormality in cytoskeleton structure. Bud31p could affect mRNA splicing of genes involved in cytoskeletal organization and budding regulation: *ACT1*, *PFY1*, *ARP2* and *SRC1* (Masciadri, Areces et al. 2004; Saha, Banerjee et al. 2012). The different microtubules structure in *bud31Δ* could be one reason for its effect on AMT. The involvement of

microtubule related proteins in AMT was reported previously in some early reports (Tu 2010; Chen 2012).

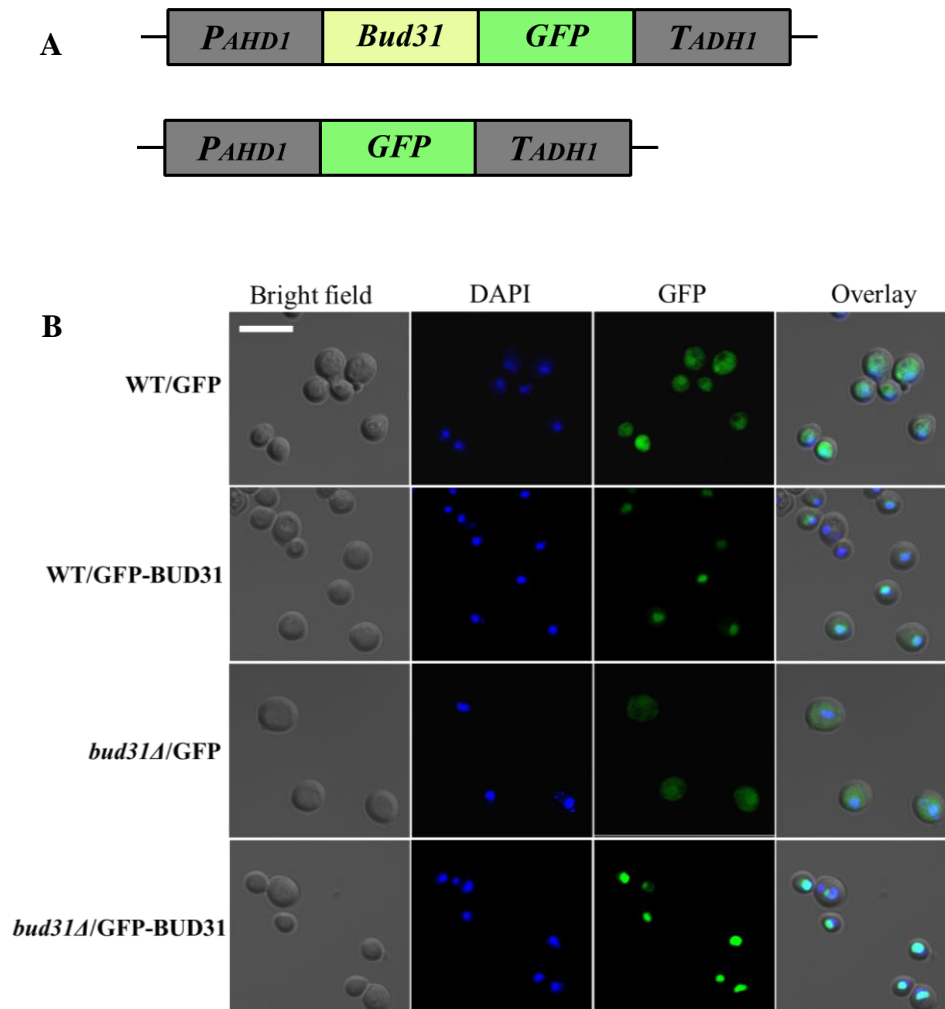


Figure 4. 1 Localization of yeast Bud31p with EGFP reporter.

(A). Plasmids used in the localization study, upper one represents pHT105-GFP-BUD31 which express GFP-BUD31 fusion protein and the lower one represents pHT105-GFP express GFP controlled by a *AHD1* promoter. (B). GFP-BUD31 fusion protein showed a nuclear localization, Scale bars, 10 μ m.

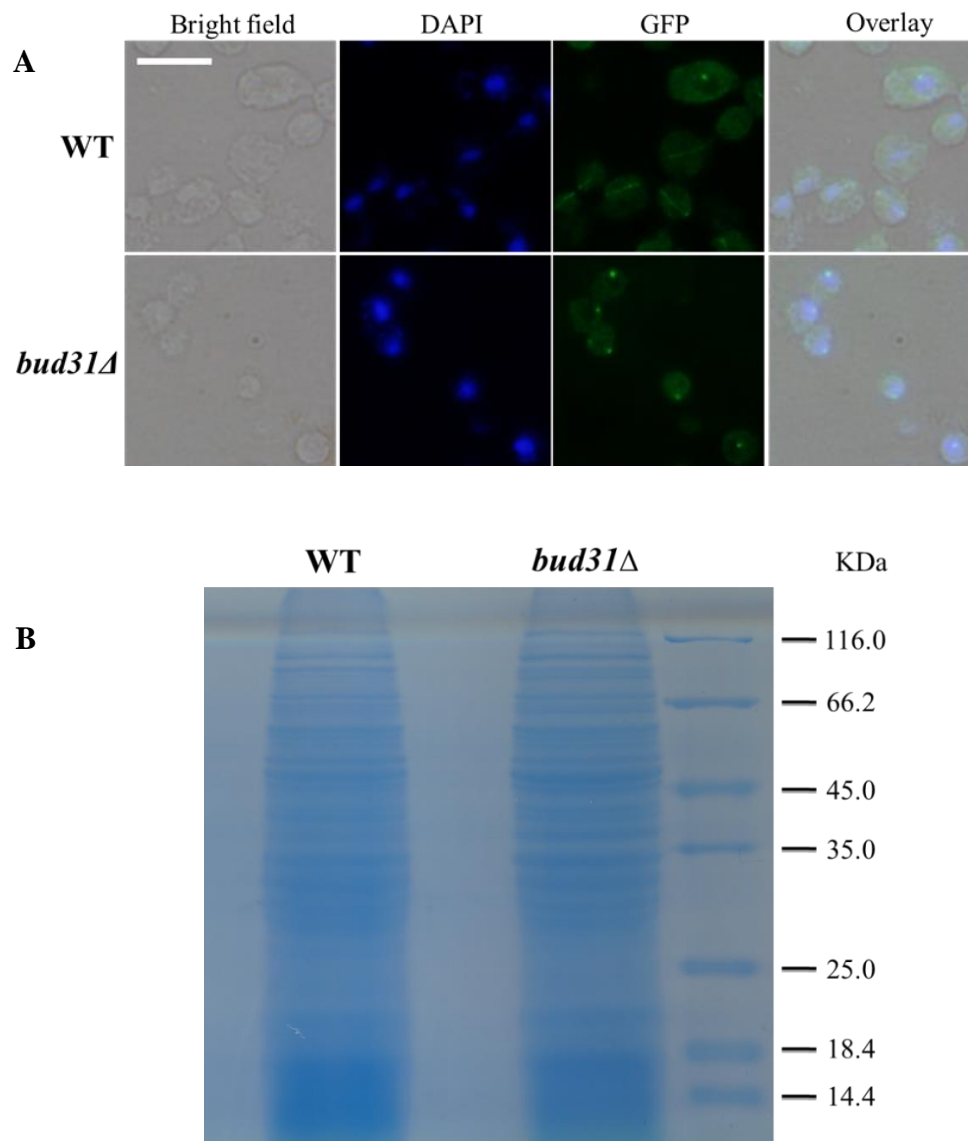


Figure 4.2 Characterization of Yeast Bud31p.

(A). Microtubules structure in *bud31Δ* and wide type strain. Scale bars, 10 μ m. (B). Total protein profile of *bud31Δ* and wide type strain.

4.1.3. Total protein profile of yeast mutant *bud31Δ* and WT

As Bud31p was reported to be involved in mRNA splicing, genes with introns are potential downstream genes of Bud31p. Total protein extraction, SDS-PAGE gel electrophoresis and Coomassie blue staining was performed as described in Chapter 2 to investigate whether protein expression profile of *bud31Δ* has a dramatic difference compared with WT. The results were showed in Figure 4.2.B. There is no obvious difference of protein bands between *bud31Δ* and WT.

4.2. Yeast mutant *bud31Δ* showed a decreased competency to receive *Agrobacterium*- delivered T-DNA

In order to investigate the reason of decreased AMT efficiency in *bud31Δ*, the *Agrobacterium* delivered T-DNA in receipt cells was detected and quantified as described in Chapter 2.6. To only examine the delivered T-DNA, *Agrobacterium* strain EHA105 (pHT101-2 μ) was used to perform AMT in this study. The pHT101-2 μ plasmid was pHT101 derivative without 2 μ origin. 2 μ origin contains an autonomous replication sequence together with related genes. Without 2 μ origin, the plasmid cannot self-maintain in recipient yeast cells by cyclization so that only *Agrobacterium* delivered T-DNA is detected in this experiment.

Cocultivated mixtures were washed off from the CM plate and employed repeated differential centrifugation to remove *Agrobacterium* cells as much as possible. After extracting total DNA, real-time PCR was performed to quantify the amount of T-DNA received in yeast cells. For real-time PCR, three pairs of primers were designed to detect Ti plasmid (VirE2-F and VirE2-R), T-DNA (URA3-F and URA3-R) and yeast genome (PMP3-F and PMP3-R), respectively. As *Agrobacterium* is attached to host cells through T4SS, repeated differential centrifugation, frozen-thawed and lysozyme

treatment cannot remove *Agrobacterium* cells in cocultivation mixture completely. Therefore, a pair of primers detecting Ti plasmid (VirE2-F and VirE2-R) was used in this experiment to deduct contaminant amount from total detected T-DNA.

Real-time PCR data was analyzed by $2^{-\Delta\Delta CT}$ method and the quantification results were showed in Figure 4.3. Clearly, *bud31Δ* showed three times decreased of T-DNA level compared to wild type yeast strain. In LiAc transformation or electroporation transformation, the amount of input DNA affects transformation efficiency significantly. Under the same experimental condition, DNA input amount and transformation efficiency showing a positively correlated pattern (Yang 2013). Taken together, T-DNA uptake process was affected in *bud31Δ*; a knockout of Bud31p caused 3-folds decreased competency to *Agrobacterium*-mediated delivery of T-DNA. The decreased transformation efficiency of *bud31Δ* could be ascribed to the reduced cellular T-DNA level in receipt cells.

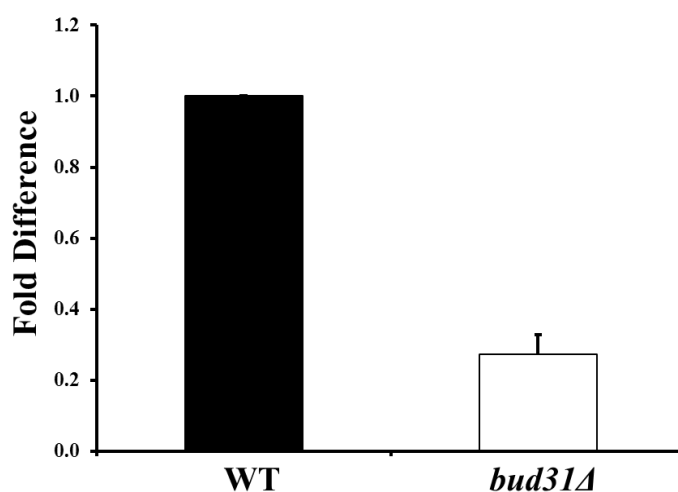


Figure 4.3. Real-time PCR analysis of T-DNA delivery.

Yeast mutant *bud31Δ* showed a decreased competency to receive *Agrobacterium*-delivered T-DNA compared to WT.

4.3. Yeast mutant *bud31Δ* showed a decreased competency to receive *Agrobacterium*-delivered VirE2

Besides T-DNA, *Agrobacterium* transfer a large amount of virulence proteins into host cells through Type IV secretion system. Virulence proteins translocation is a critical stage in AMT. As yeast mutant *bud31Δ* showed a decreased competency to receive *Agrobacterium*-delivered T-DNA, it became a question that whether the virulence protein translocation is also affected by the deletion of *BUD31*.

Among *Agrobacterium* delivered virulence proteins, VirE2 is the most abundant protein. Therefore, a Split-GFP detection assay was employed in this study to directly visualize VirE2 in yeast cells *in vivo* and investigate the virulence protein delivery in wild type yeast and mutant.

Briefly, GFP was divided into two non-fluorescent fragments including a small fragment (GFP11) and a large fragment (GFP1-10). GFP11 was inserted into a permissive site (Pro54) of VirE2. After delivery of GFP11 fused VirE2 into recipient cells such as yeast, GFP1-10 fragment would recognize and bind to *virE2::GFP11* to emit green fluorescent signal (Figure 4.4.A, B). Therefore, yeast cells with delivered VirE2 can be directly visualized and calculated.

The AMT experiments were following standard AMT protocol described in Chapter 2.5. pQH04-S1-10 was respectively introduced into yeast *bud31Δ*, *snt309Δ*, *syf2Δ* and wild type strain to express VirE2 S1-10 fragment in yeast. *Agrobacterium* EHA105*virE2::GFP11* was correspondingly cocultivated with yeast *bud31Δ*, *snt309Δ*, *syf2Δ* and wild type strain containing VirE2 S1-10 big fragment, respectively. Cocultivation mixture was washed off from CM plates after 24 hours and observed under a fluorescence microscope.

Although VirE2 is not required for *Agrobacterium*-yeast transformation, the

deletion of VirE2 will cause the decreased transformation efficiency (Rossi, Hohn et al. 1996). EHA105*virE2::GFP11* was proved to have full virulence compared with its wild type EHA105 (Li, Yang et al. 2014), thus the VirE2 function was not disrupted by VirE2-GFP11 fusion.

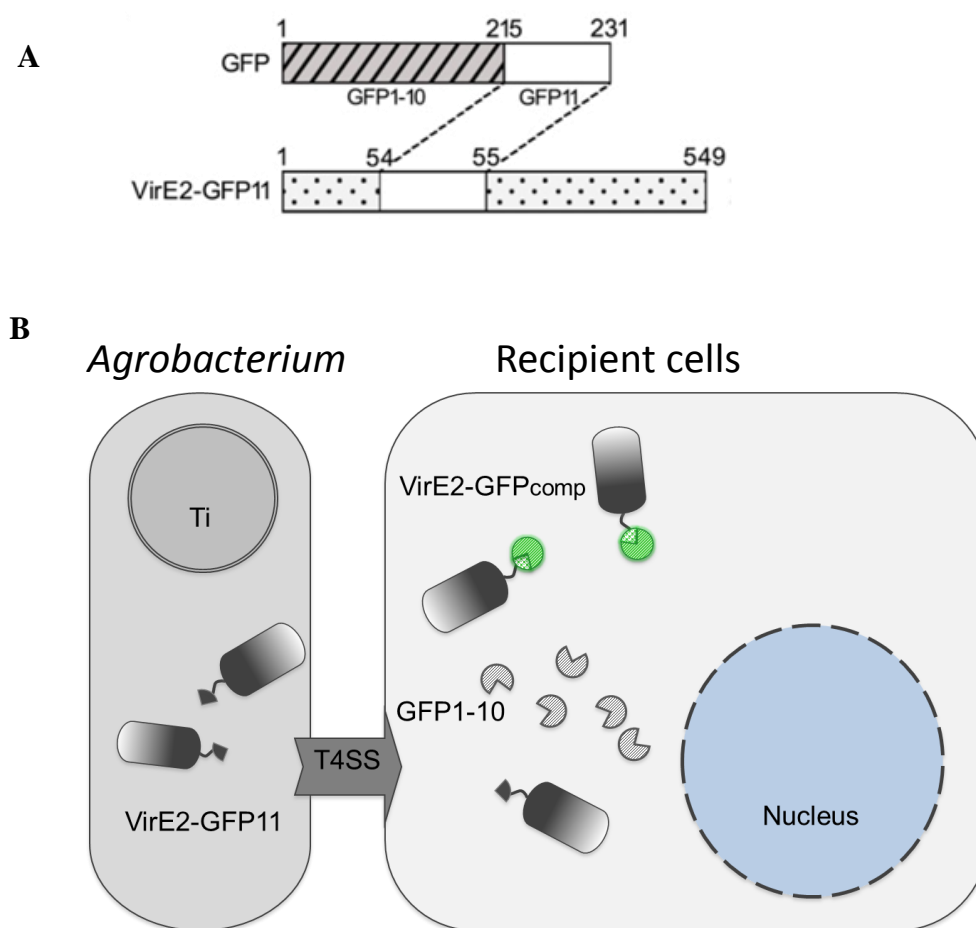


Figure 4.4. A split-GFP assay for visualization of VirE2 inside recipient cells.

(A). Construction of the VirE2-GFP11 fusion. The GFP11 was inserted into *virE2* at a permissive site Pro54; Cited from (Li, Yang et al. 2014). (B) Schematic diagram for the visualization of *Agrobacterium tumefaciens* VirE2 delivered into recipient cells.

Figure 4.5.A showed that cells with green spots which represent VirE2-GFP complex were reduced by deletion of *BUD31* and *SNT309*. On the other hand, deletion of *SYF2* increased the number of cells with GFP translocation signals. Yeast cells of three mutants with GFP signal in five random fields captured by fluorescence microscope were counted and compared with wild type. As shown in Figure 4.5.B, after 24 hours cocultivation, *bud31Δ* and *snt309Δ* showed two times decreased percentage of GFP positive cells while *syf2Δ* showed two times increased delivery of VirE2 compared with wild type. These results indicate that the VirE2 protein delivery process was affected in *bud31Δ*, *snt309Δ* and *syf2Δ*.

T4SS was employed in *Agrobacterium*-mediated transformation to deliver both T-DNA and virulence proteins. Due to the decreased competency of T-DNA and VirE2 delivery in *bud31Δ*, the deletion of Bud31p may affect the whole T4SS and other substrates. This could be the reason for decreased transformation efficiency in *bud31Δ*.

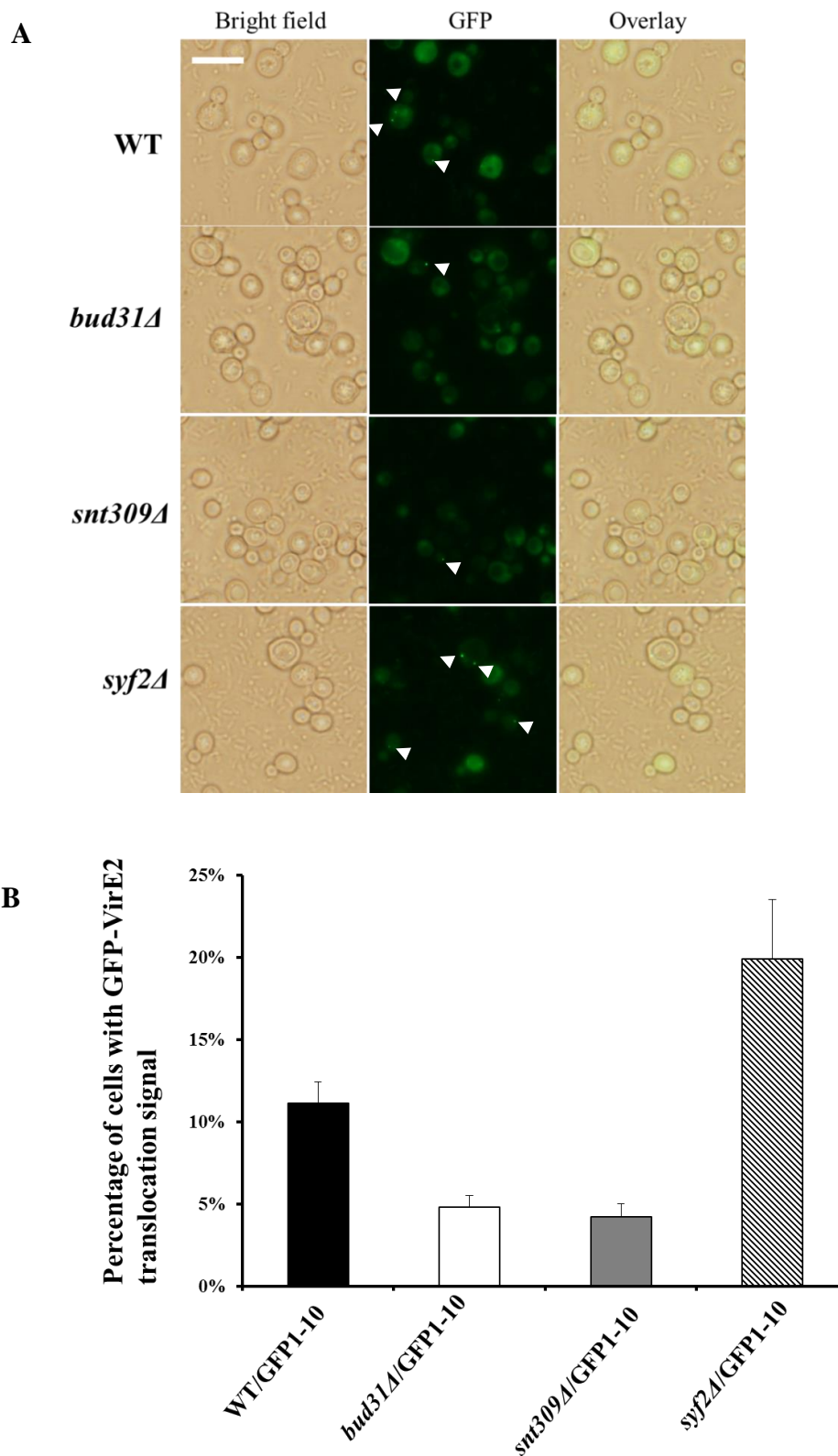


Figure 4.5. Yeast mutant *bud31Δ* showed a decreased competency to receive *Agrobacterium*-delivered VirE2.

(A). Cocultivation cells were harvested and observed under a fluorescence microscope, Scale bar, 10 μ m. (B). Percentages of cells with VirE2 delivery in three mutants and wild type strain.

4.4. VirD2 nuclear localization process was not affected in yeast mutant *bud31Δ*

VirD2 is required for T-complex formation and T-complex nucleus targeting during AMT process. Both of these steps are crucial for transformation which means AMT efficiency will change if these steps were affected. In order to investigate whether nucleus targeting of VirD2 could be affected in *bud31Δ*, a GFP-VirD2 expression and localization assay was performed.

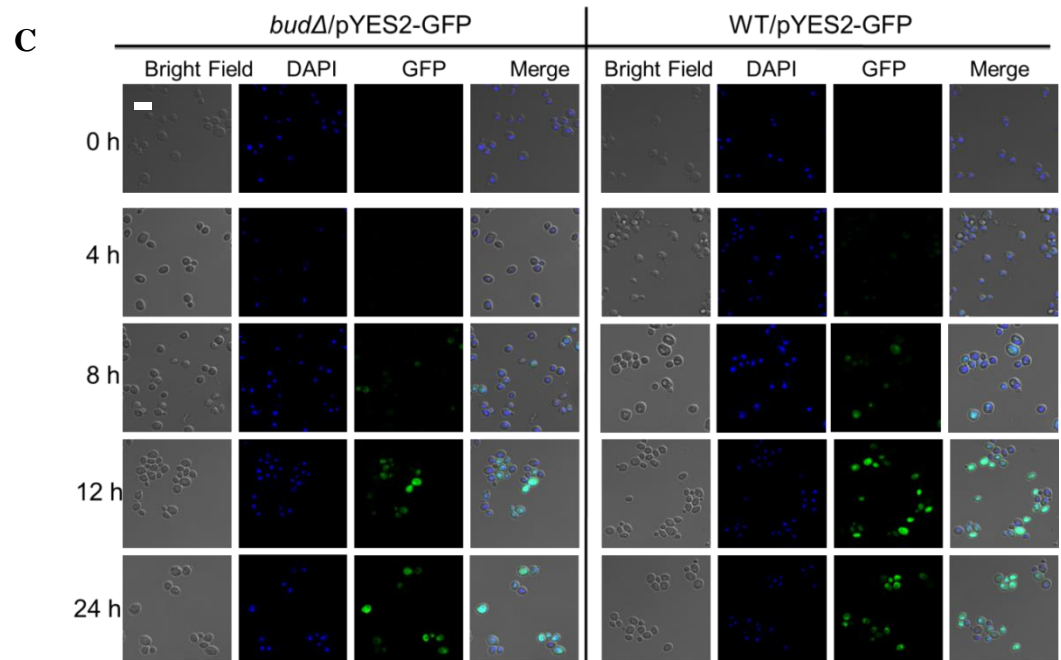
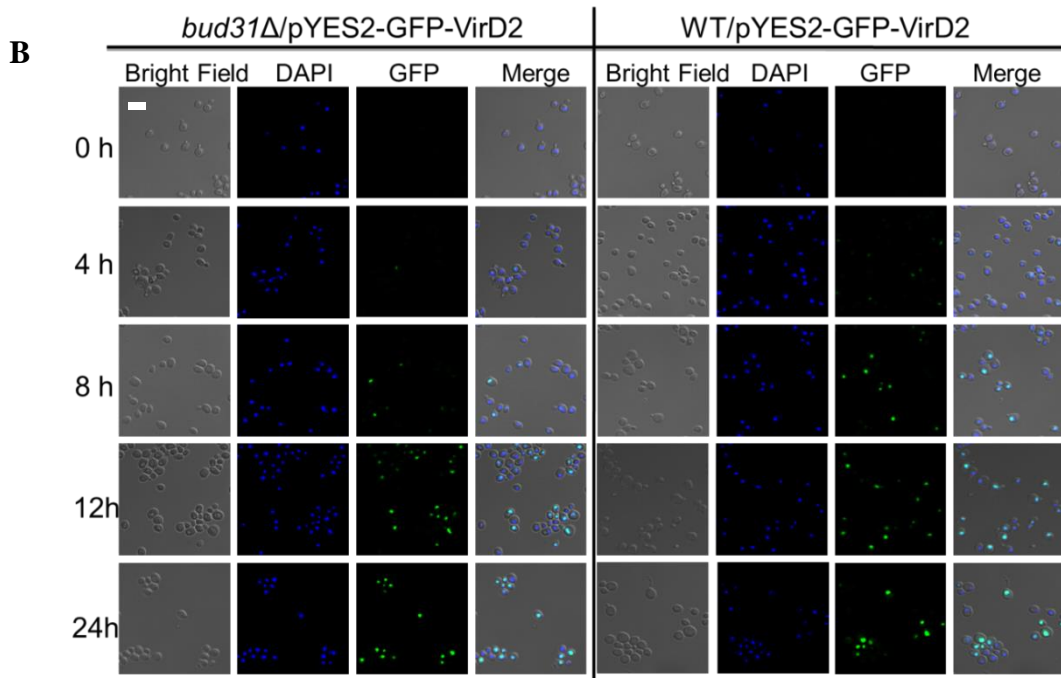
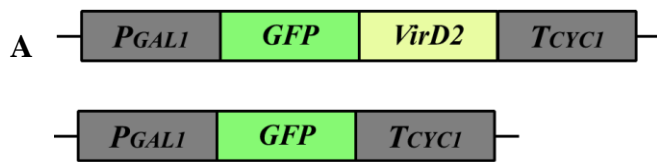
Yeast wild type strain and *bud31Δ* were transformed with pYES2-GFP-VirD2 and pYES2-GFP plasmid, respectively. The expression of GFP-VirD2 fusion protein or GFP protein was controlled by inducible promoter *Gall* (Figure 4.6.A). After induction, GFP-VirD2 was expressed in cytoplasm and localized into nucleus.

Yeast wild type strain and *bud31Δ* containing pYES2-GFP-VirD2/ pYES2-GFP were grown in SD Ura⁻ liquid medium overnight. The yeast cells were harvested and washed before subcultured in SD Gal Ura⁻ liquid medium. Yeast wild type and mutant cells were collected after galactose inducing at different time points. Then the cells were fixed with 4% paraformaldehyde and stained with DAPI. Afterwards, the cells were applied to fluorescence microscope for observation.

Figure 4.6.B showed the nuclear localization of GFP-VirD2 at different time points after galactose induction. Figure 4.6.D showed the corresponding quantitative data. Yeast cells with accumulated GFP signal in nucleus would be counted as positive. Both image results and quantitative data suggested that compared to WT, GFP expression was delayed in *bud31Δ* nucleus at early stage (4 hours post induction, 2.6% in mutant *versus* 15% in WT). This indicated that VirD2 may enter the nucleus slower in *bud31Δ* than in WT after induction of galactose.

However, GFP expression needs to be considered as a control. Figure 4.6.C and

Figure 4.6.E showed the GFP expression was delayed at the four and eight hour time points in *bud31Δ* as well (4 hours post induction, 6% in mutant *versus* 37% in WT). These results suggested that the lower GFP-VirD2 nucleus co-localization signal in *bud31Δ* may result from the delay of GFP gene expression and the VirD2 nucleus targeting process is not affected in yeast mutant *bud31Δ*.



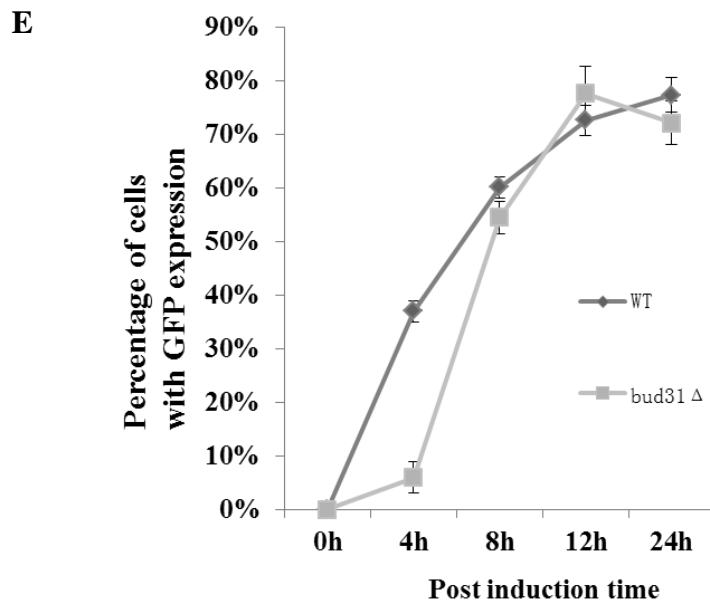
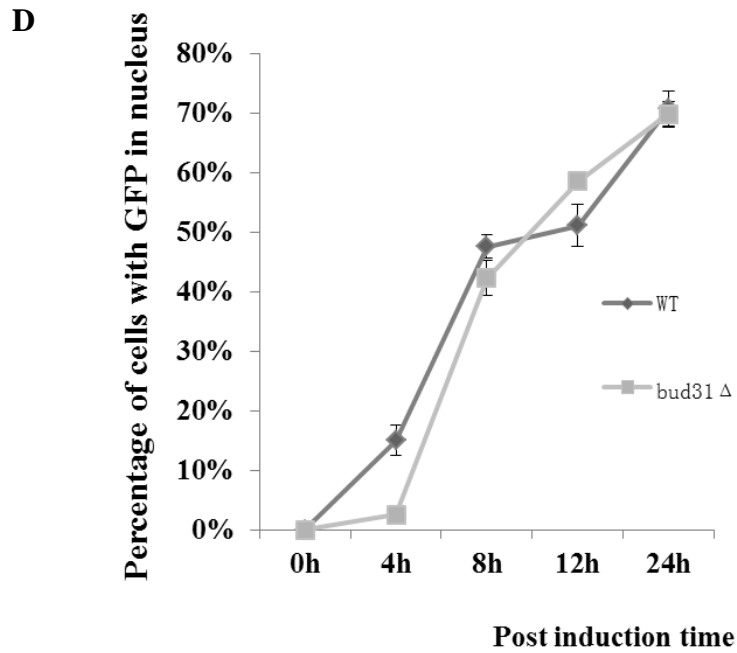


Figure 4.6. VirD2 nucleus targeting process is not affected in yeast mutant *bud31*Δ.

(A). Plasmids used in the VirD2 nucleus localization study, upper one represents pYES2-GFP-VirD2 and the lower one represents pYES2-GFP, respectively. (B). Nuclear localization of GFP-VirD2 in *bud31*Δ and WT; Scale bar, 10 μm. (C). GFP expression in *bud31*Δ and WT; Scale bar, 10 μm. (D) Percentage of cells with GFP in nucleus at different time points when expressing GFP-VirD2. (E). Percentage of GFP positive cells at different time points when expressing GFP.

4.5. Integration of T-DNA was not affected in yeast mutant *bud31Δ*

Three binary vectors based on mini binary vector pCB301 were designed to generate information on the fate of T-DNA in transformants' genome (Yang 2013). pQH302 generates a T-DNA containing a *URA3* marker, which can be randomly inserted into yeast genome through NHEJ only. pQH303 generates a T-DNA containing a *URA3* flanked by homologous arms cloned from *LYS2* locus, which can be targeted into *LYS2* locus through HR. pQH304 generates a T-DNA containing a 2 μ origin in addition of *URA3*, which is self-maintained in recipient yeast cells after cyclization (Figure 4.7.A).

Three *A. tumefaciens* strain EHA105 (pQH302), EHA105 (pQH303) and EHA105 (pQH304) were used to perform standard AMT protocol. Transformation efficiency results were shown in Figure 4.7.B.

In plant species, T-DNA was found to predominately integrate into plant genome via NHEJ. However, in yeast, the major event of T-DNA integration is through HR (Offringa, De Groot et al. 1990; Bundock, den Dulk-Ras et al. 1995; Bundock and Hooykaas 1996). Consistent with previous report, transformants of EHA105 (pQH302) had extremely low efficiency indicating the integration via NEHJ is hardly to detect in yeast.

By using pQH304, *bud31Δ* showed decreased AMT efficiency compared to WT, displaying similar effect as pHT101 (Figure 3.1). In this case, T-DNA fate was autonomous replication. However, by using pQH303, deletion of *BUD31* showed no effect compared with WT. These results suggested that deletion of *BUD31* did not affect T-DNA integrated into yeast genome through HR.

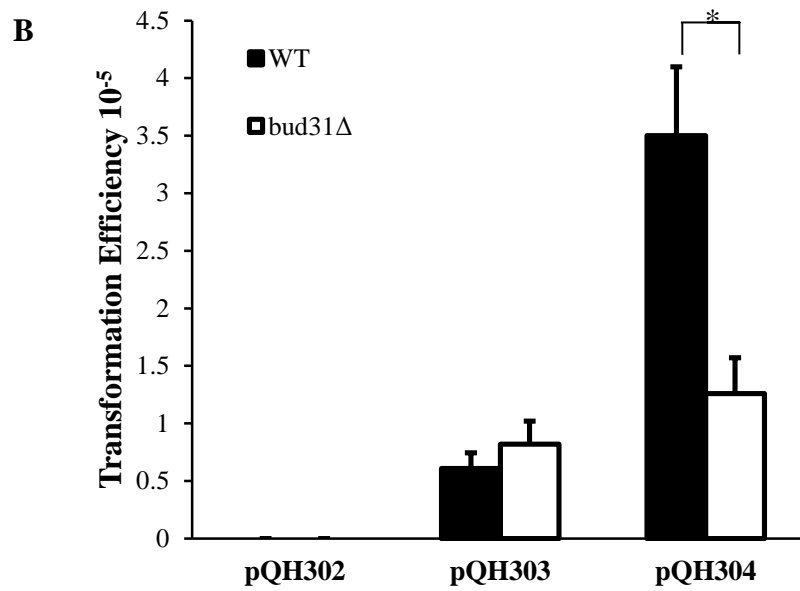
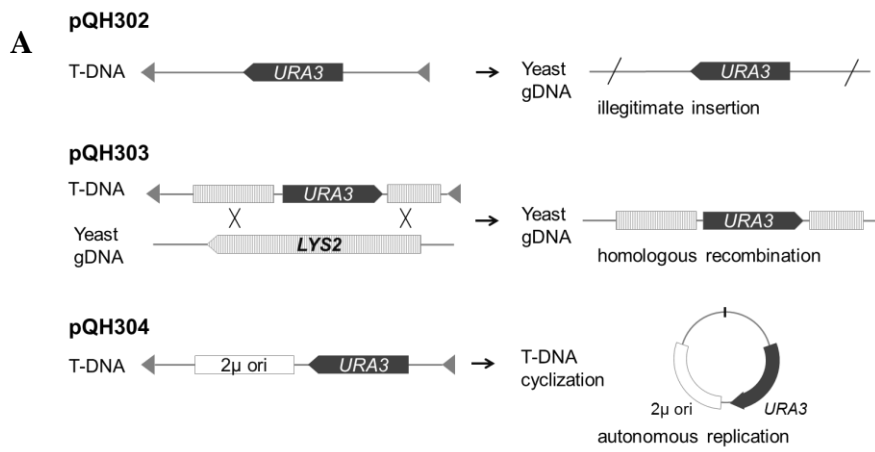


Figure 4.7. Integration of T-DNA was not affected in yeast mutant *bud31Δ*.

(A). Plasmids used in integration study are based on mini binary vector pCB301. pQH302 can be integrated into genome through NEHJ; pQH303 can be targeted into *LYS2* locus through HR; pQH304 is capable of self-maintaining in yeast after cyclization; cited from (Yang 2013). (B). AMT efficiency of yeast mutant *bud31Δ* and wild type strain BY4741 with *A. tumefaciens* strain EHA105 (pQH302), EHA105 (pQH303) and EHA105 (pQH304), * P < 0.05.

4.6. Discussion

Previous data showed a significantly decreased AMT efficiency of *bud31Δ*, suggesting an involvement of Bud31p in *Agrobacterium*-yeast gene transfer. The question is: what is the role of Bud31p in AMT process? How Bud31p regulate AMT process?

As reviewed in Chapter 1, host factors involved in AMT may affect following four steps in AMT process: cell attachment, virulence factors transfer, T-DNA trafficking and T-DNA integration.

For virulence factor transfer step, *bud31Δ* showed 3-fold decrease in competency to receive T-DNA and 2-fold decrease in competency to receive VirE2. The decreased AMT efficiency *bud31Δ* is probably caused by the decreased competency to receive T-DNA and VirE2 protein.

For T-DNA trafficking step, VirD2 nuclear localization was investigated in both wild type stain and *bud31Δ*. VirD2 can covalently bind to T-DNA and lead it travel through cytoplasm to nucleus. The time course results showed that at early stage, *bud31Δ* had less VirD2-GFP signal accumulated in nucleus. However, consider the GFP gene expression was also delayed in cytoplasm, the lower GFP-VirD2 nucleus localization signal in *bud31Δ* may be due to the delay of GFP gene expression. Therefore, I cannot conclude the VirD2 nuclear targeting process was affected by the deletion of Bud31p. T-DNA detection by fluorescent *in situ* hybridization (FISH) was also performed, but the percentage of cells having FISH signal was too low to provide meaningful results.

For T-DNA integration step, two major pathways for T-DNA integration are homologous recombination (HR) and non-homologous end joining (NHEJ). In yeast, HR was reported to be the predominant pathway for T-DNA integration. Deletion of

BUD31 neither affects T-DNA integrated into yeast genome through NEHJ nor through HR. In conclusion, integration of T-DNA was not affected in *bud31Δ*.

In this study, cell attachment step was not included.

A diagram to summarize the role of Bud31p on AMT was showed in Figure 4.8.

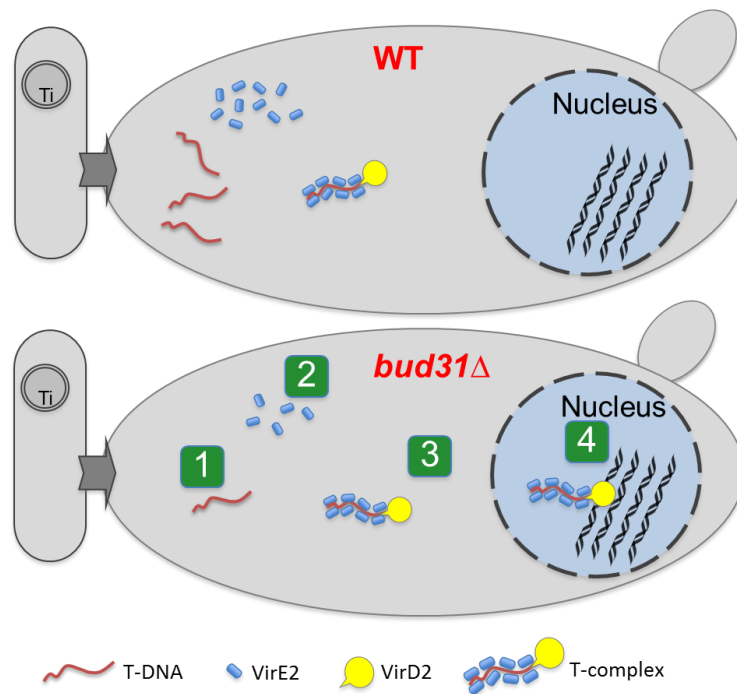


Figure 4.8. Summary of the role of yeast *BUD31* on AMT.

1. Decreased T-DNA delivery
2. Decreased VirE2 delivery
3. No effect on VirD2 nuclear targeting
4. No effect on T-DNA integration.

In Chapter 3, AMT efficiency tests of genes related to Bud31p suggested an involvement of NineTeen Complex (NTC) during AMT process. NTC has eight core proteins and many associated proteins. One interesting phenomenon is that deletion of NTC core proteins Syf2p and Snt309p had opposite effect on AMT. A knockout of Syf2p caused dramatically increased transformation efficiency, while a knockout of Snt309p showed decreased transformation efficiency. In addition, deletion of Bud31p, a NTC associated protein, showed similar effect as Snt309p.

As a splicing factor, Bud31p has been reported to involve in other cellular process such as cell division and DNA repair. There are two possibilities to explain additional functions of splicing factors. Firstly, the splicing factor could directly involve in another different cellular process besides splicing. On the other hand, it may have effects on gene expression required for other cellular pathway; therefore have indirect effects on this pathway.

In previous literature, in order to link *BUD31* function in cell division with splicing, splicing status of several budding function related genes was analyzed in *BUD31* deletion mutant. All these pre-mRNA were intron contained. Among them, splicing of *SRC1* and *ARP2* were restricted in *bud31Δ*. However, transcripts of other genes involved in budding function (*PFY1*, *YSC84* and *SAC6*) were not significantly altered. These results suggested that Bud31p promotes efficient splicing of only some pre-mRNAs, but not all of them (Saha, Banerjee et al. 2012).

Therefore, in this study, we propose an assumption to explain the opposite effects of NTC proteins on *Agrobacterium*-mediated transformation. There may be unknown protein(s) directly function in AMT, lack of which will cause disrupted AMT. Expression of this intron containing protein(s) is regulated by NTC proteins. Bud31p/Snt309p acts as enhancer. Deletion of them causes inefficient splicing of this protein(s), therefore lead to reduced AMT efficiency. In addition, Syf2p acts as

inhibitor, deletion of which causes overexpression of this protein(s), leading to enhanced AMT efficiency. Definitely, there is another possibility that this unknown protein(s) works as AMT inhibitor. Existing of Bud31p/Snt309p caused down expression of this protein(s) to facilitate AMT process.

Chapter 5. Effects of Bud31p plant homolog in *Agrobacterium*-mediated transformation

5.1. Bud31p is conserved across eukaryotes

Deletion of Bud31p showed a significant decreased AMT efficiency in yeast due to the reduced competency to receive T-DNA and virulence protein VirE2. It became interesting to know the role of Bud31p homolog in *Agrobacterium*-plant transformation.

Bud31p is a conserved protein across eukaryotes (Figure 5.1). *S. cerevisiae* Bud31p sequence was found to have 51% identity with the G10 gene product of *Xenopus laevis* (Benit, Chanet et al. 1992). Human and *Arabidopsis thaliana* homolog of Bud31p also shared 50% identity with yeast Bud31p (Hla, Jackson et al. 1995). The high identity between Bud31p homologs showed that this gene is conserved among different species during evolution.

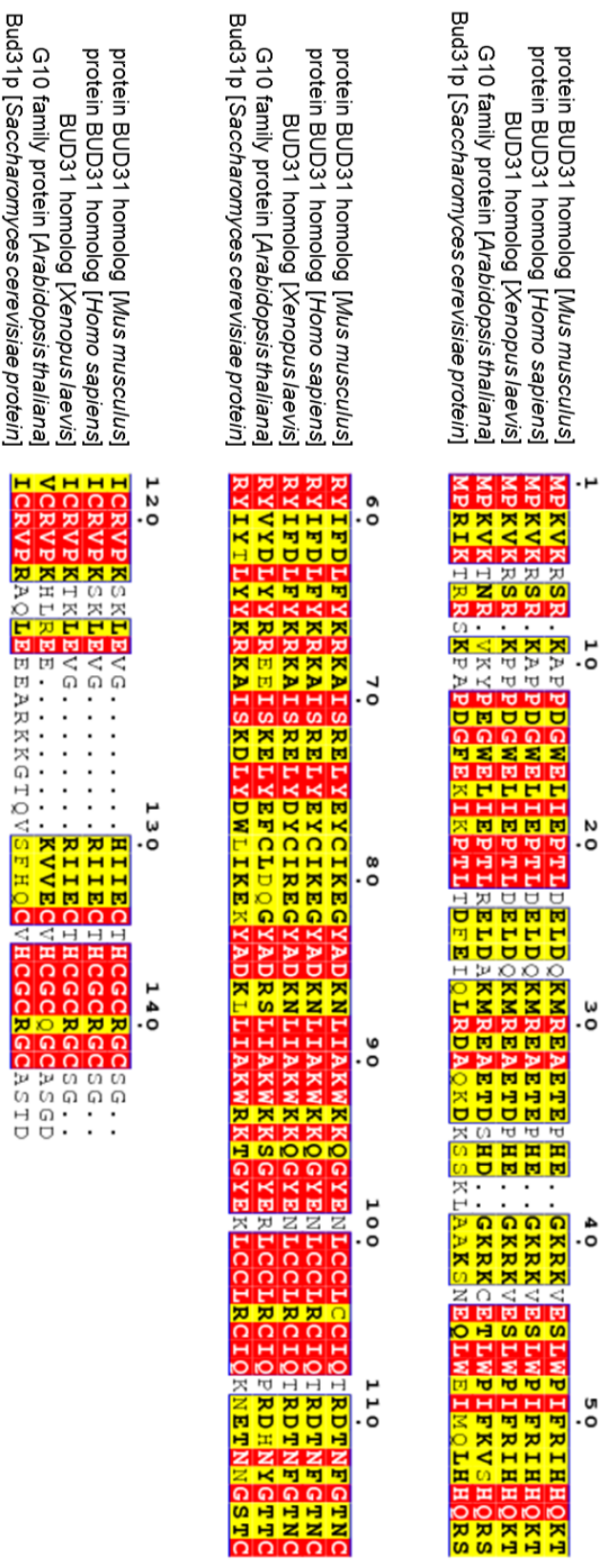


Figure 5.1 Bud31p is conserved across eukaryotes.

Amino acid sequence alignment was generated by Clustalw2 (<http://www.clustal.org/clustal2/>) and formatted by ESPript (<http://esprict.ibcp.fr/ESPript/ESPript/>); identical amino acids are shaded in red and conservative substitutions are shaded in yellow.

5.2. Bud31p Homolog of *Arabidopsis thaliana*

As natural host, plant is important aspect to study host factor regulated AMT process. Therefore, it is meaningful to investigate if Bud31p plant homolog has similar effect on AMT as in yeast. With a short life term and available genome sequence data, *Arabidopsis thaliana* is one of the most frequently-used model organisms in plant biology study. *AT4G21110*, the *A. thaliana* homolog of *S. cerevisiae BUD31*, shared 50% identity with yeast Bud31p. This locus is described as a G10 family protein with unknown function.

5.3.1. Expression pattern of *Arabidopsis AT4G21110* upon agroinfection

Plant cells employ variety of genes in response to environmental stresses, including biotic and abiotic stresses. In order to investigate whether Bud31p and its *Arabidopsis* homolog *AT4G21110* directly regulated by plant stress responses, expression pattern of Bud31p and its *Arabidopsis* homolog *AT4G21110* upon *agrobacterium* infection was employed.

For *Arabidopsis*, agroinfiltration was performed as described in Chapter 2.10. *Agrobacterium* strain EHA105 was grown overnight and subcultured until $OD_{600}=1.0$. The cells were harvest and resuspended in infiltration buffer to a final concentration of $OD_{600}=1.0$. The cell suspension was infiltrated to the lower side of *Arabidopsis* leaves (Col-0) by a syringe. Infiltrating the same plant with infiltration buffer was used as control. The *Arabidopsis* leaves were cut at 12, 24, 36 and 48 hours after infiltration. RNA extraction and real-time RT-PCR were performed as described in Chapter 2. The *Arabidopsis UBQ10* gene product was used as control.

For yeast, yeast strain BY4741 was cocultivated with *Agrobacterium* strain EHA105 as described in Chapter 2.5. *Agrobacterium* strain EHA105 was grown

overnight and induced in IBPO₄ with AS. BY4741 cells were grown overnight and subcultured until OD₆₀₀=0.35. The yeast cells and *Agrobacterium* cells were mixed at 1:200 and drop on CM plates. The cell mixture was washed off from CM plates 12 and 24 hours after cocultivation. RNA extraction and real-time RT-PCR were performed as described in Chapter 2. Yeast *ACT1* gene transcripts was used as control.

Primers used in this section were listed in Table 2.4. The results were showed in Figure 5.2. The expression of *Arabidopsis AT4G21110* did not have significant change at different time point after agroinfiltration (Figure 5.2.A). Transcription level of Bud31p was stable in yeast upon agroinfection as well (Figure 5.2.B). These results suggested that the expression of Bud31p and its homolog did not respond to agroinfection.

5.3.2. Genotyping of *AT4G21110* T-DNA insertion lines

In order to test AMT of loss-of-function mutants, T-DNA insertion lines were obtained from ABRC collection (<http://www.arabidopsis.org/>). After exaction of total RNA from *Arabidopsis* leaves as described in Chapter 2.3.2, RT-PCR was used to detect transcriptional product of Bud31p homolog in these lines. *AT4G21110* transcriptional product can be detected in all available lines including SALK_001179, SALK_035046, SALK_072062, SALK_108840, SALK_116000 and SAIL_202_H07 (data not shown). Therefore, none of these lines is *AT4G21110* knockout mutant.

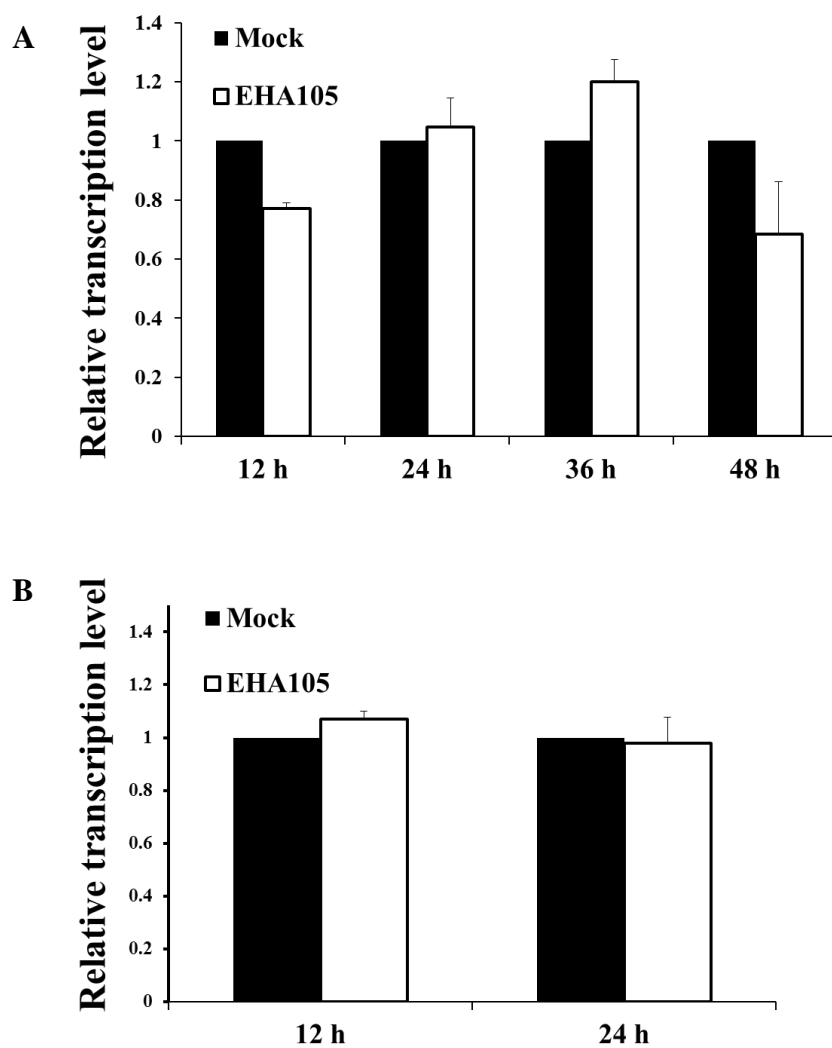


Figure 5.2. Expression patterns of *A. thaliana* AT4G21110 and *S. cerevisiae* Bud31p upon agroinfection.

(A). Expressions of *A. thaliana* AT4G21110 was not affected upon agroinfection; The *Arabidopsis* UBQ10 gene was used as reference gene. (B). An expression of *S. cerevisiae* Bud31p was not affected upon agroinfection; The yeast ACT1 gene was used as reference gene.

5.3. Bud31p Homolog of *Nicotiana benthamiana*

After performing genotyping for all available *A. thaliana* *AT4G21110* T-DNA insertion lines, none *AT4G21110* knockout mutant was found. Therefore, we turned to generate Bud31p homolog silencing plant by virus-induced gene silencing (VIGS) in *N. benthamiana*.

Although there is no completed available genome sequence data of *N. benthamiana*, a draft genome sequence can be used in this study to search Bud31p homolog (Knapp, Chase et al. 2004; Goodin, Zaitlin et al. 2008; Bombarely, Rosli et al. 2012).

There are two isoforms of *N. benthamiana* Bud31p Homolog found in draft genome sequence for *N. benthamiana* (cDNA sequence from http://solgenomics.net/organism/Nicotiana_benthamiana/genome). The upper isoform is same as what cloned from *N. benthamiana* cDNA. The lower one is unlikely to be translated (Figure 5.3). Therefore, the upper isoform was named *NbBUD31*. Alignment of the cDNA sequence of *NbBUD31* and *AT4G21110* showed 80% identity, indicating that Bud31p is a highly conserved gene in plant (Figure 5.4).

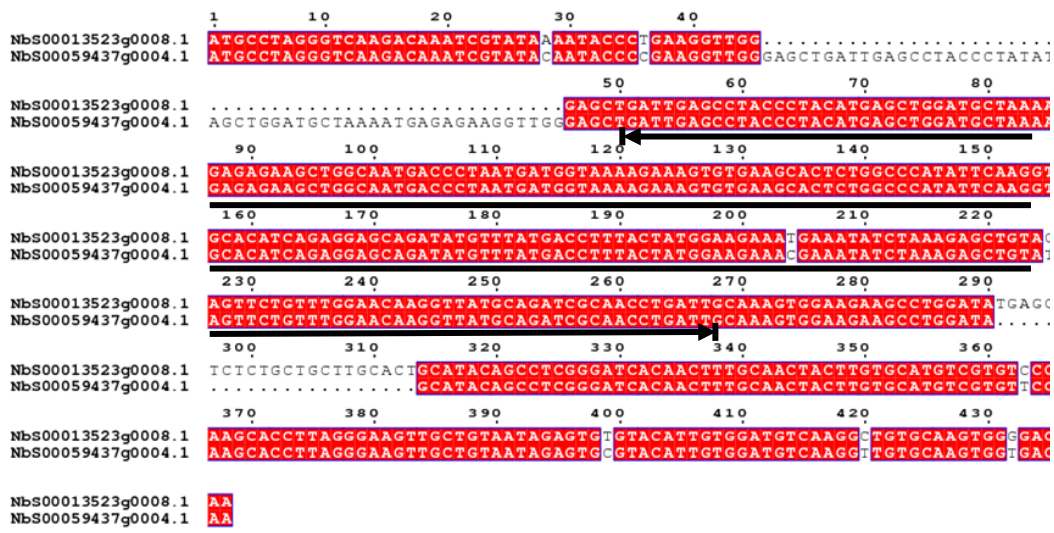


Figure 5.3. cDNA sequence alignment of predicted two isoforms of *NbBUD31*.

cDNA sequence alignment was generated by Clustalw2 (<http://www.clustal.org/clustal2/>) and formatted by ESPrpt (<http://esprpt.ibcp.fr/ESPrpt/ESPrpt/>); identical bases are shaded in red; VIGS target gene fragment are underlined.

```

1      10      20      30      40      50      60
AT4G21110 ATGCCAAAGGTAAACAAACGAGTCAAATACCAAGTACCCAGGAGATGGGAGTTGATCGAGCCT
NbBUD31   ATGCCTAAGGTCAAGACAAATCGTATAAAATACCCAGGAGTGGGAGCTGATCGAGCCT

70      80      90      100     110     120
AT4G21110 ACTCTTCGAGAGCTTGATGCCAAATGAGAGAAGCTGAGACTGATTCAATGATGTTAAAG
NbBUD31   ACCCTACATGAGCTTGATGCTAAATGAGAGAAGCTGCAACTGACCTAATGATGTTAAAG

130     140     150     160     170     180
AT4G21110 AGAAAGTGTGAAACITTAAGGCCATCTTCAAAGTTTCCATCAGAGGAGTCCGTATGTA
NbBUD31   AGAAAGTGTGAAACACTCTGGCCATATTCAAAGTTGACATCAGAGGAGCAGATATGTT

190     200     210     220     230     240
AT4G21110 TATGACCTTTATTAACGAAGGGAAGAAATATCTAAAGAGCTCTATGATTCTGCTTGGAC
NbBUD31   TATGACCTTTACTATGGAAGAAATGAAATATCTAAAGAGCTCTATGATTCTGCTTGGAA

250     260     270     280     290     300
AT4G21110 CAGGCCTATGCAGATCGCAACTGATTGCCAAATGGAAAGTCCGGATACGACCTTTA
NbBUD31   CAGGCTATGCAGATCGCAACTGATTGCCAAATGGAAAGTCCGGATATGACCTTTA

310     320     330     340     350     360
AT4G21110 TGCTGCTTGCCTGCATACAGCCAAAGAGACACAACATGGAACACATGTGATGCGT
NbBUD31   TGCTGCTTGCCTGCATACAGCCCTCGGATACAACATGGAACACATGTGATGCGT

370     380     390     400     410     420
AT4G21110 GTTCCCAAACACTTGCCTGAAGAGAAAAGTGGTCGAATGCGTTCACTGGCTGTCAAGGA
NbBUD31   GTTCCCAAACACTTAGGGAAGTTGCTGTAAATAGATGTTCACTGGATGTCAAGGC

430
AT4G21110 TCGCGAGTGGCGATTA
NbBUD31   TGTGCAAGTGGCGACTAA

```

Figure 5.4. cDNA sequence comparison of predicted *N. benthamiana* NbBUD31 and *A. thaliana* AT4G21110.

cDNA sequence alignment was generated by Clustalw2 (<http://www.clustal.org/clustal2/>) and formatted by ESPript (<http://esprict.ibcp.fr/ESPript/ESPript/>); identical bases are shaded in red.

5.4. Generation of *NbBUD31*-silencing plant by virus-induced gene silencing (VIGS)

Virus induced gene silencing (VIGS) was adopted in this study to generate *NbBUD31* silencing *N. Benthamiana*. VIGS mechanism is described as the fact that plant cell could specifically target against the viral genome to protect plant when plants were infected with unmodified viruses. Virus vectors carrying inserts from host genes can target against the corresponding mRNAs, therefore generating gene knock-down plant. VIGS has become a powerful method to study gene function in plants (Lu, Martin-Hernandez et al. 2003)

The TRV based VIGS approach was performed as described in Chapter 2.8. Briefly, overlapping part of two isoforms of *NbBUD31* (~220 bp, underlined region in Figure 5.3) was cloned into binary VIGS vector TRV2. pTRV1, pTRV2 and pTRV2-*NbBUD31* were introduced into *Agrobacterium* strain GV3101 by electroporation, respectively. *Agrobacterium* strain GV3101 containing pTRV1, pTRV2 and pTRV2-*NbBUD31* plasmids were grown overnight and suspended in infiltration buffer to a final concentration of OD₆₀₀=0.8. Bacteria culture containing pTRV1 was mixed with equal volume of bacteria culture containing pTRV2 or pTRV2-*NbBUD31*, respectively. *Agrobacterium* mixture was infiltrated onto the lower leaf of 4-leaf stage *N. benthamiana* plants (Anand, Vaghchhipawala et al. 2007).

After total RNA extraction from upper leaves of gene silenced plants (TRV::*NbBUD31*), empty vector control plants (TRV::00) and untreated plants (WT), real-time PCR was performed to detect the transcriptional level of *NbBUD31*. To ensure the endogenous gene is tested, real-time PCR primers were design to anneal outside the region targeted for silencing. *N. Benthamiana EF-1* gene was used as reference gene.

Figure 5.5.A showed the plants three weeks post VIGS. TRV::00 and TRV::*NbBUD31* displayed slower growth rate compared with WT, which may be caused by the virus infection. Comparing the *NbBUD31* transcriptional level in WT and TRV::00, it showed that virus infection would not change the transcriptional level of *NbBUD31* (Figure 5.5.B). For silenced plants (TRV::*NbBUD31*), transcriptional level of *NbBUD31* was suppressed by 100 times compared to TRV::00 and WT. Moreover, this gene silencing effect could last at least for four weeks (4-8 weeks post VIGS).

Taking together, transcriptional level of *NbBUD31* was suppressed in TRV::*NbBUD31*. The silencing plant by VIGS was adopted for further study.

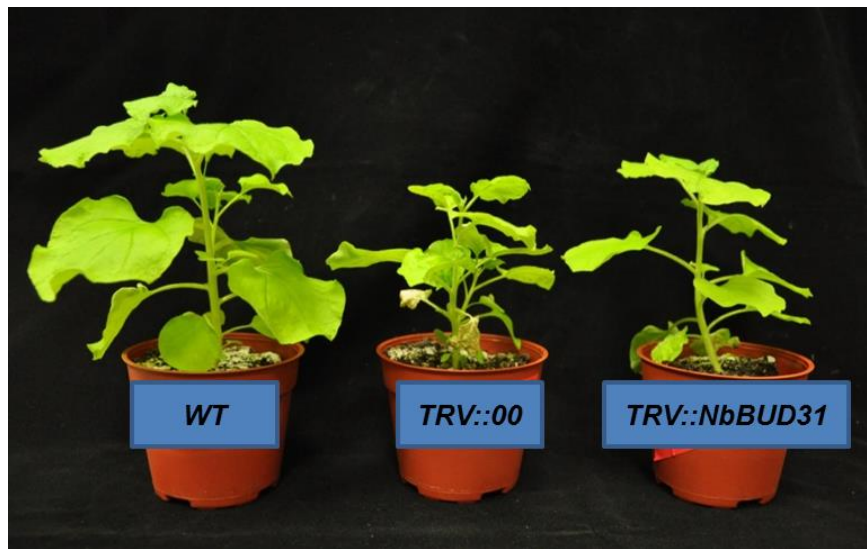
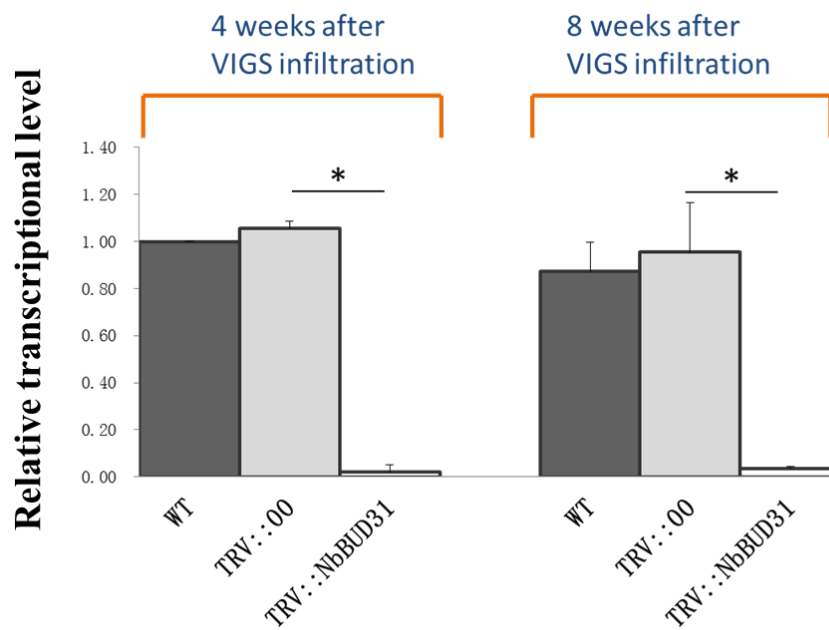
A**B**

Figure 5.5. Effect of VIGS on *N. benthamiana*.

(A). Untreated plant (WT), empty vector control plant (TRV::00) and gene silenced plant (TRV::NbBUD31) three weeks after VIGS infiltration. (B). Relative transcriptional level of *NbBUD31* in WT, TRV::00 and TRV::NbBUD31 plant at 4 weeks and 8 weeks post VIGS infiltration; Transcription of *NbBUD31* was suppressed in TRV::NbBUD31. * $P < 0.05$.

5.5. Silencing of *NbBUD31* did not affect tumor formation

After *NbBUD31* silenced plant was generated, the susceptibility of *NbBUD31* silenced plant to AMT was examined. Two tumorigenesis assays were performed as described in Chapter 2.9.

5.5.1. In planta tumorigenesis on silenced plants

Three weeks after VIGS, the stem of the plant was punctured by a needle. *A. tumefaciens* A348 was inoculated onto stem wound by the same needle. The crown gall tumor was observed four weeks and seven weeks post-agroinoculation. According to Figure 5.6.A, there is no significant difference in the size of tumors among WT, TRV::00 and TRV::*NbBUD31* at 4 weeks and 7 weeks after *Agrobacterium* A348 inoculation.

5.5.2. Leaf-disk tumorigenesis on silenced plants

For leaf-disk tumorigenesis assay, leaves from *NbBUD31* silenced plant (TRV::*NbBUD31*); control plants (TRV::00) and untreated plants (WT) were collected three weeks after VIGS infiltration. The leaves were punched into disks and cocultivated with *A. tumefaciens* strain A348 on MS medium. After two days, the leaf disks were transferred to MS medium with Cef to kill extra bacteria. The plate was incubated at 20 °C in darkness for four weeks for tumor formation. The total biomass of the leaf was measured by weighing the fresh and dry weights of leaf disks (Anand, Vaghchhipawala et al. 2007).

Leaf-disk tumorigenesis results showed that TRV::00 and TRV::*NbBUD31* formed mildly smaller tumors compared with WT. Due to the slow growth rate of TRV::00 and TRV::*NbBUD31*, it was reasonable that the tumor growth in TRV::00 and

TRV::*NbBUD31* was slightly lower than in WT. However, there was no obvious difference in tumor growth between TRV::00 and TRV::*NbBUD31* (Figure 5.6.B).

Figure 5.6.C and Figure 5.6.D showed the quantitative results of leaf-disk tumorigenesis. There was no statistically significant difference ($p > 0.1$, student's t-test) between TRV::00 and TRV::*NbBUD31*. These results were consistent with previous observation in Figure 5.6.B. In conclusion, in planta tumorigenesis and leaf-disk tumorigenesis experiment both showed silencing of *NbBUD31* did not affect tumor formation in AMT of *N. Benthamiana*.

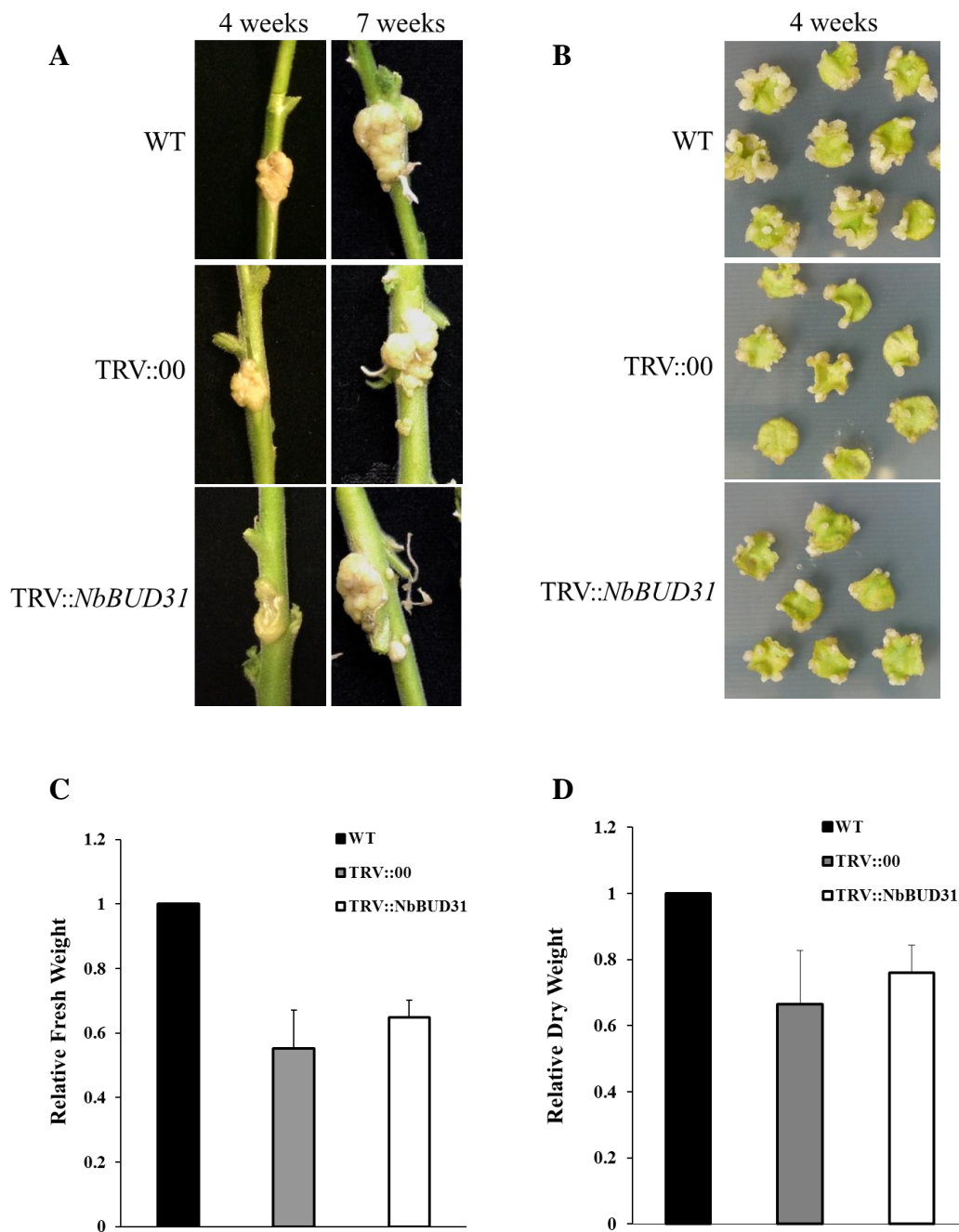


Figure 5.6. Silencing of *NbBUD31* did not affect tumor formation in AMT.

(A). In planta tumorigenesis on the silenced plants. Photo was taken four weeks and seven weeks after *A. tumefaciens* A348 infection, respectively. (B). Leaf-disk tumorigenesis on the silenced plants. Photo was taken four weeks after inoculation of *A. tumefaciens* A348. (C) and (D). Quantification of the relative biomass of leaf disks with tumors. The fresh (C) and dry (D) weights of the leaf disks with tumors were measured four weeks after inoculation of *A. tumefaciens* A348.

5.6. Silencing of *NbBUD31* did not affect transient expression and VirE2 translocation

5.6.1. Transient expression on silenced plants

A time course of transient expression in *N. benthamiana* was performed to investigate whether the silencing of *NbBUD31* affects transient expression efficiency of AMT. In this study, *A. tumefaciens* EHA105 (pQH308) was employed for transiently expressing DsRed driven by 35S promoter in *N. benthamiana* leaves (Yang 2013). *A. tumefaciens* EHA105 (pQH308) was inoculated in LB medium and grew overnight. The bacteria cells were collected, washed and resuspended in infiltration buffer to $OD_{600} = 1.0$. Cell suspension was infiltrated into lower side of *N. benthamiana* leaves by a syringe (WT, TRV::00 and TRV::*NbBUD31*, respectively).

At 12, 24, 36 and 48 hours post-infiltration, leaf epidermal cells were observed under confocal microscope and the results were showed in Figure 5.7. The fluorescence mean intensity of DsRed was automatically quantified by ImageJ.

Images and quantitative results both suggested that compared to WT, TRV::*NbBUD31* showed no significant difference in transient expression level, indicating that silencing of *NbBUD31* did not have effects on transient expression. TRV::00 showed decreased transient expression compared to WT and TRV::*NbBUD31*, which may be caused by the low growth rate of TRV::00 (Figure 5.7.C).

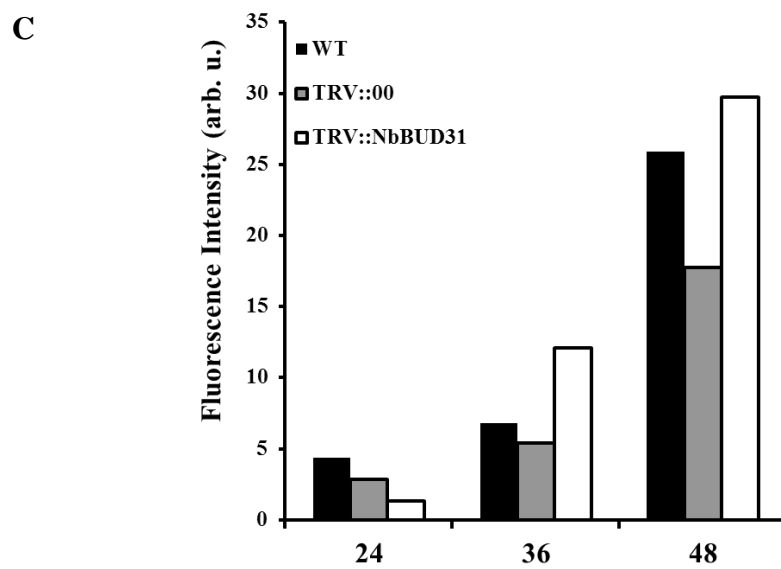
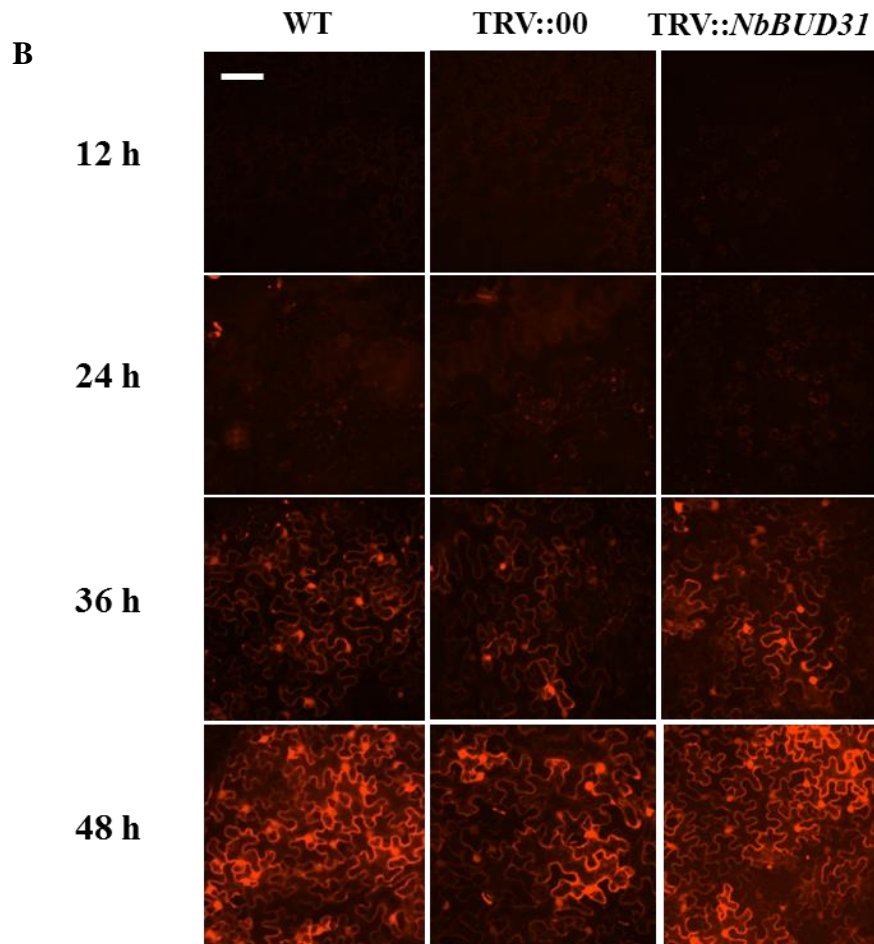
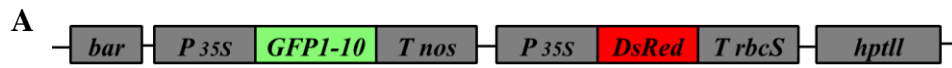


Figure 5.7. Silencing of *NbBUD31* did not affect transient expression.

(A). *A. tumefaciens* EHA105 (pQH308) was used in transient expression assay for transient expressing DsRed driven by 35S promoter. (B). Transient expression on silenced plant. Leaf epidermal cells were observed under confocal microscope 12, 24, 36 and 48 h post-infiltration, Scale bar, 50 μ m. (C). Quantification of transient expression on silenced plant. Fluorescence intensity of DsRed was quantified by ImageJ.

5.6.2. VirE2 translocation on silenced plants

During AMT process, alternative virulence protein translocation can affect transformation efficiency dramatically. In this section, time course experiment of VirE2 translocation in *N. benthamiana* was performed to study the effect of silencing of *NbBUD31* on VirE2 delivery during AMT process.

Agrobacterium EHA105*virE2::GFP11* cells were infiltrated into transgenic *N. benthamiana* (Nb308A) leaves expressing both GFP1-10 and DsRed. The leaves were observed under confocal microscope at 12, 24, 36 and 48 h post-agroinfiltration.

When VirE2-GFP11 was translocate into the plant cells, GFP1-10 fragment bound to VirE2-GFP11, then green fluorescence signals (VirE2-GFP complex) can be observed under a confocal microscope. The results were showed in Figure 5.8.B. GFP fluorescence intensity was quantified by ImageJ and the results were showed in Figure 5.8.C.

Both images and quantitative results suggested that the VirE2 delivery was not affected by silencing of *NbBUD31*.

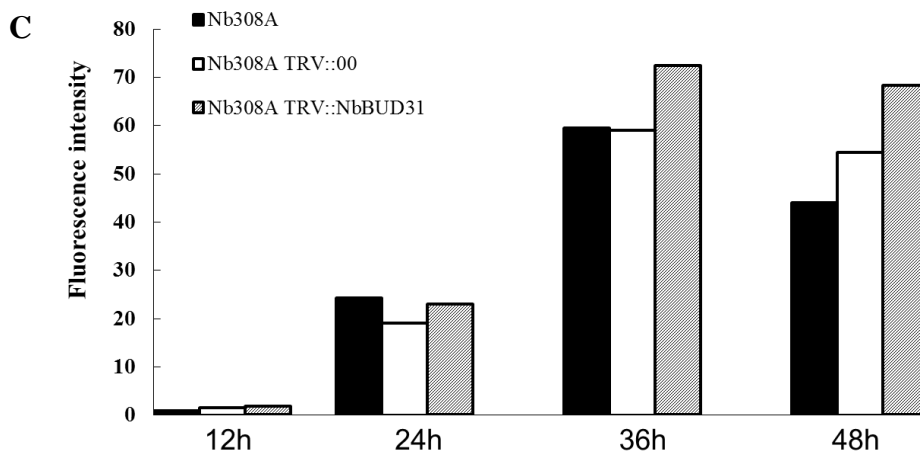
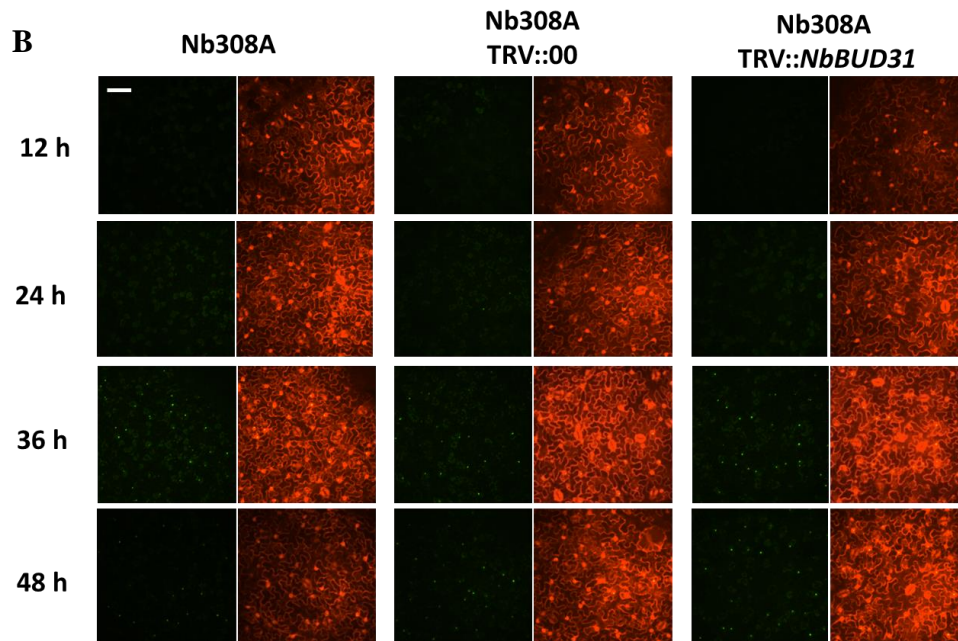
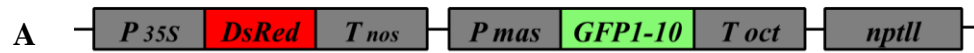


Figure 5.8. Silencing of *NbBUD31* did not affect *VirE2* translocation.

(A) Transgenic *N. benthamiana* (Nb308A) expressing both GFP1-10 and DsRed was used in *VirE2* translocation assay. (B) *VirE2* translocation on silenced plant. *A. tumefaciens* EHA105*virE2::GFP11* were infiltrated into transgenic *N. benthamiana* (Nb308A). Leaf epidermal cells were observed under confocal microscope 12, 24, 36 and 48 h post-infiltration; Scale bar, 50 μ m. (C) Quantification of *VirE2* translocation on silenced plant. The fluorescence mean intensity of GFP was quantified by ImageJ.

5.7. *NbBUD31* did not show specific sub-cellular localization in

***N. benthamiana*.**

As reported in Chapter 4.1.1, BUD31-GFP fusion protein showed nucleus localization in yeast cells. In order to locate *NbBUD31* inside *N. benthamiana* cells, *NbBUD31* was fused with GFP at C-terminus and N-terminus, and then cloned into binary vector pQH121, respectively. The plasmid pQH121-GFP expressing GFP was used as a control (Figure 5.9.A). *Agrobacterium* EHA105 (pQH121-GFP), EHA105 (pQH121-*NbBUD31*-GFP) and EHA105 (pQH121-GFP-*NbBUD31*) was grown overnight and infiltrated into transgenic *N. benthamiana* (Nb308A) leaves expressing both GFP1–10 and DsRed. DsRed expression is useful for visualization of cellular locations.

According to Figure 5.9.B, fusion protein GFP-*NbBUD31* and *NbBUD31*-GFP did not show altered localization and expression pattern compared to GFP protein. As *NbBUD31*-GFP showed lower GFP intensity compared with GFP and GFP-*NbBUD31*, fusing *NbBUD31* with GFP at C- terminus might affect GFP structure slightly.

In summary, *NbBUD31* did not show specific sub-cellular localization in *N. benthamiana*.

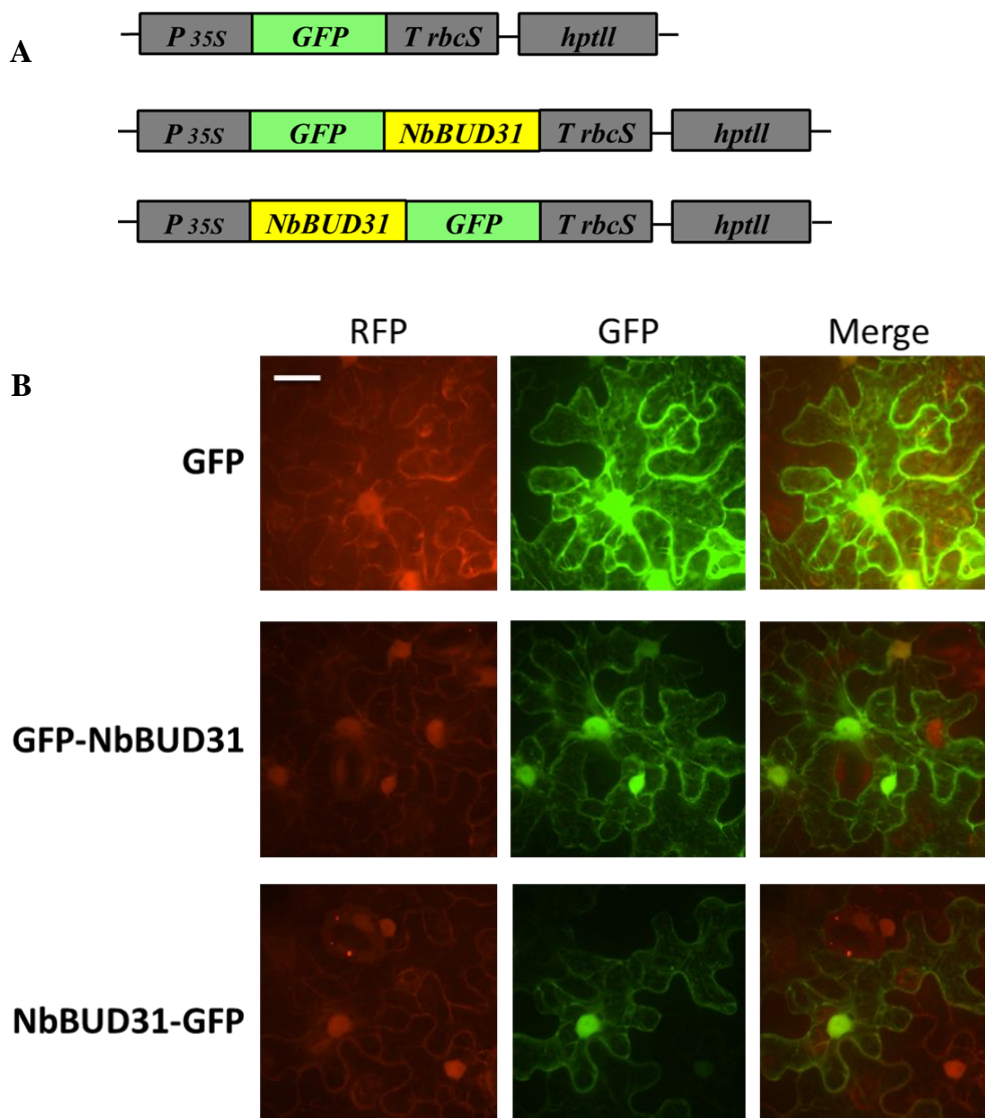


Figure 5.9. Localization of *N. benthamiana* NbBUD31 with GFP reporter.

(A). Plasmids used in localization study: upper one represents pHT121-GFP which only express GFP as a control; middle one and lower one represent pHT121-GFP-NbBD31 and pHT105- NbBD31-GFP in which GFP was fused with *NbBUD31* at C- terminus and N- terminus, respectively. (B). Localization of *N. benthamiana* *NbBUD31* with GFP reporter; Leaf epidermal cells were observed under confocal microscope 24 h post-infiltration; Scale bars, 20 μ m.

5.8. Discussion

Bud31p is a conserved protein across eukaryotes during evolution. *S. cerevisiae* Bud31p is found to have about 50% homology with G10 protein of *Xenopus laevis*, edg-2 of *Homo sapiens* and AT4G21110 of *Arabidopsis thaliana* (Benit, Chanet et al. 1992; Hla, Jackson et al. 1995). Investigating the effect of Bud31p homolog on AMT process in natural host plant could help to reveal the role of Bud31p in AMT.

Arabidopsis thaliana AT4G21110 is homologous to yeast *BUD31*. However, genotyping results showed none of available T-DNA insertion lines is AT4G21110 knockout mutant. *Nicotiana benthamiana* has *BUD31* homolog shared 80% identity with *Arabidopsis thaliana*. Therefore, virus-induced gene silencing (VIGS) was performed to generate *NbBUD31* silencing plant. Transcriptional level of *NbBUD31* was suppressed in silenced plant, and this silencing effect could last at least for four weeks.

In planta tumorigenesis and leaf-disk tumorigenesis results showed that silencing of *NbBUD31* did not affect tumor formation. Transient expression and VirE2 delivery was not affected on silenced plants as well. In addition, different from yeast Bud31p, *NbBUD31* did not show specific sub-cellular localization in *N. benthamiana*.

So the follow up question is: why are there different effects of *BUD31* and *NbBUD31* on AMT process in yeast and plant?

One possibility is that there is no completed available genome sequence data of *N. benthamiana*; only a draft genome sequence is available. Therefore, there may be redundant gene which has not been identified.

Secondly, the function of Bud31p may alter in *N. benthamiana* compared to yeast. *BUD31* was found to bind androgen receptor (AR) in human prostate cancer cell and suppress AR-mediated prostate cancer growth (Hsu, Liu et al. 2014). These results

indicated multi-function of Bud31p. Some of the functions may not be identified yet. In yeast system, Bud31p showed to locate in nucleus. However, different from yeast, *NbBUD31* did not show specific sub-cellular localization in *N. benthamiana* which indicating an altered localization and maybe altered function of *NbBUD31*.

Last but not least, T-DNA delivery and virulence protein translocation may not be limiting factors in natural host plant. In yeast system, deletion of Bud31p decreased 3-fold in competency to receive T-DNA and 2-fold to receive VirE2, with a 10-fold decrease in AMT efficiency. However, due to different transformation mechanism, T4SS is highly efficient to deliver virulence protein and T-DNA in plant. VirE2 delivery efficiency and transient transformation efficiency is 100% in *N. benthamiana* (Figure 5.7, Figure 5.8). Meanwhile, VirE2 delivery efficiency and transformation efficiency is 10% (Figure 4.5) and 0.1% (Figure 3.1) in *S. cerevisiae*. T-complex trafficking and T-DNA integration may be more critical in *Agrobacterium*-plant transformation. In yeast, *BUD31* showed no effect on T-DNA integration. Its homolog might not affect integration of T-DNA in plant as well.

Chapter 6. General conclusions and future prospects

6.1. General conclusions

For a long period of time, *Agrobacterium*-mediated transformation was the only known case of inter-kingdom DNA transfer in nature. Besides natural host plant, *Agrobacterium* can transfer a single-stranded DNA into many species including yeast under laboratory condition. Although the transformation process inside bacteria has been well studied, the process inside the host cells remains unclear. This study aims to use *Saccharomyces cerevisiae* as a model to study host factors involved in transformation process and investigate the role of these factors in AMT.

Based on genome wide screening data generated by Tu (Tu 2010), a small scale screening was performed. Among them, yeast NineTeen Complex (NTC) and its associated Bud31p were found to play important role in *Agrobacterium*-mediated transformation process. Deletion of yeast *BUD31* showed decreased *Agrobacterium*-mediated transformation efficiency. Interestingly, two NTC core proteins, Syf2p and Snt309p, had opposite effect on AMT. Deletion of *SYF2* dramatically increased the transformation efficiency, while deletion of *SNT309* reduced the transformation efficiency.

To investigate the role of Bud31p on *Agrobacterium*-yeast gene transfer, virulence factors delivery, VirD2 intracellular trafficking and T-DNA integration were analyzed in both yeast wild type stain and *bud31Δ*. Yeast mutant *bud31Δ* showed 3-fold decrease in competency to receive T-DNA and 2-fold decrease in competency to receive VirE2 during AMT process. The decreased AMT efficiency of *bud31Δ* probably attributes to the decreased competency to receive T-DNA and VirE2 protein. In addition, neither VirD2 nuclear targeting process nor T-DNA integration process showed to be affected in *bud31Δ*.

Sequence analysis showed Bud31p protein is highly conserved among many species. In order to reveal the role of Bud31p in AMT, the effect of Bud31p plant homolog on AMT was investigated. *NbBUD31* silencing *Nicotiana benthamiana* was generated by VIGS. Silencing of *NbBUD31* in *Nicotiana benthamiana* did not affect tumor formation, transient expression and VirE2 delivery during AMT process. The different effect of Bud31p and its plant homolog on AMT suggested a different pathway of AMT in nature host plant from yeast.

To the best of our knowledge, it is the first to report the involvement of yeast NineTeen Complex and its associated *BUD31* in AMT process and also the first to report that deletion of *BUD31* caused reduced competency to receive *Agrobacterium* delivered T-DNA and VirE2 protein. This finding helps in understanding the relationship between T-DNA/virulence protein delivery and *Agrobacterium*-mediated transformation efficiency.

6.2. Future prospects

Although the role of *BUD31* in *Agrobacterium*-mediated transformation was examined, the detail effects of other components of NTC involved in AMT were not studied carefully. The future study could investigate the detail function of other NTC proteins in AMT, e.g. *SNT309* and *SYF2*.

According to current results, the decreased AMT efficiency of *bud31Δ* probably ascribes to reduced competency to *Agrobacterium* delivery of T-DNA and virulence proteins. As a splicing factor, *BUD31* might directly involve in AMT process besides splicing; more likely, *BUD31* may have effects on gene expression required for AMT pathway. Genes with introns are potential downstream gene of *BUD31*. AMT efficiency of some of these mutants has been roughly tested. However, more effort is needed to identify downstream genes of *BUD31* and investigate their role on AMT

process.

Bibliography

- Albright, L. M., M. F. Yanofsky, et al. (1987). "Processing of the T-DNA of *Agrobacterium tumefaciens* generates border nicks and linear, single-stranded T-DNA." J Bacteriol **169**(3): 1046-1055.
- Aly, K. A. and C. Baron (2007). "The VirB5 protein localizes to the T-pilus tips in *Agrobacterium tumefaciens*." Microbiology **153**(Pt 11): 3766-3775.
- Anand, A., A. Krichevsky, et al. (2007). "Arabidopsis VIRE2 INTERACTING PROTEIN2 is required for *Agrobacterium* T-DNA integration in plants." Plant Cell **19**(5): 1695-1708.
- Anand, A., Z. Vaghchhipawala, et al. (2007). "Identification and characterization of plant genes involved in *Agrobacterium*-mediated plant transformation by virus-induced gene silencing." Mol Plant Microbe Interact **20**(1): 41-52.
- Arenas, J. E. and J. N. Abelson (1997). "Prp43: An RNA helicase-like factor involved in spliceosome disassembly." Proceedings of the National Academy of Sciences of the United States of America **94**(22): 11798-11802.
- Backert, S., R. Fronzes, et al. (2008). "VirB2 and VirB5 proteins: specialized adhesins in bacterial type-IV secretion systems?" Trends Microbiol **16**(9): 409-413.
- Bako, L., M. Umeda, et al. (2003). "The VirD2 pilot protein of *Agrobacterium*-transferred DNA interacts with the TATA box-binding protein and a nuclear protein kinase in plants." Proc Natl Acad Sci U S A **100**(17): 10108-10113.
- Ballas, N. and V. Citovsky (1997). "Nuclear localization signal binding protein from *Arabidopsis* mediates nuclear import of *Agrobacterium* VirD2 protein." Proc Natl Acad Sci U S A **94**(20): 10723-10728.

- Ben-Yehuda, S., I. Dix, et al. (2000). "Genetic and physical interactions between factors involved in both cell cycle progression and pre-mRNA splicing in *Saccharomyces cerevisiae*." Genetics **156**(4): 1503-1517.
- Benit, P., R. Chanet, et al. (1992). "Sequence of the sup61-RAD18 region on chromosome III of *Saccharomyces cerevisiae*." Yeast **8**(2): 147-153.
- Bolton, G. W., E. W. Nester, et al. (1986). "Plant phenolic compounds induce expression of the *Agrobacterium tumefaciens* loci needed for virulence." Science **232**(4753): 983-985.
- Bombarely, A., H. G. Rosli, et al. (2012). "A draft genome sequence of *Nicotiana benthamiana* to enhance molecular plant-microbe biology research." Mol Plant Microbe Interact **25**(12): 1523-1530.
- Brachmann, C. B., A. Davies, et al. (1998). "Designer deletion strains derived from *Saccharomyces cerevisiae* S288C: a useful set of strains and plasmids for PCR-mediated gene disruption and other applications." Yeast **14**(2): 115-132.
- Braun, A. C. and R. J. Mandle (1948). "Studies on the inactivation of the tumor-inducing principle in crown gall." Growth **12**(4): 255-269.
- Bundock, P., A. den Dulk-Ras, et al. (1995). "Trans-kingdom T-DNA transfer from *Agrobacterium tumefaciens* to *Saccharomyces cerevisiae*." EMBO J **14**(13): 3206-3214.
- Bundock, P. and P. J. J. Hooykaas (1996). "Integration of *Agrobacterium tumefaciens* T-DNA in the *Saccharomyces cerevisiae* genome by illegitimate recombination." Proceedings of the National Academy of Sciences of the United States of America **93**(26): 15272-15275.
- Cangelosi, G. A., R. G. Ankenbauer, et al. (1990). "Sugars induce the *Agrobacterium* virulence genes through a periplasmic binding protein and a transmembrane signal protein." Proceedings of the National Academy of Sciences **87**(17):

6708-6712.

Cangelosi, G. A., E. A. Best, et al. (1991). "Genetic analysis of *Agrobacterium*." Methods Enzymol **204**: 384-397.

Cangelosi, G. A., G. Martinetti, et al. (1989). "Role for [corrected] *Agrobacterium tumefaciens* ChvA protein in export of beta-1,2-glucan." J Bacteriol **171**(3): 1609-1615.

Cascales, E. and P. J. Christie (2004). "Definition of a bacterial type IV secretion pathway for a DNA substrate." Science **304**(5674): 1170-1173.

Chan, M.-T., T.-M. Lee, et al. (1992). "Transformation of indica rice (*Oryza sativa* L.) mediated by *Agrobacterium tumefaciens*." Plant and cell physiology **33**(5): 577-583.

Chan, M. T., H. H. Chang, et al. (1993). "Agrobacterium-mediated production of transgenic rice plants expressing a chimeric alpha-amylase promoter/beta-glucuronidase gene." Plant Mol Biol **22**(3): 491-506.

Chan, S. P. and S. C. Cheng (2005). "The Prp19-associated complex is required for specifying interactions of U5 and U6 with pre-mRNA during spliceosome activation." Journal of Biological Chemistry **280**(35): 31190-31199.

Chan, S. P., D. I. Kao, et al. (2003). "The Prp19p-associated complex in spliceosome activation." Science **302**(5643): 279-282.

Chanarat, S., M. Seizl, et al. (2011). "The prp19 complex is a novel transcription elongation factor required for TREX occupancy at transcribed genes." Genes and Development **25**(11): 1147-1158.

Chanarat, S. and K. Sträßler (2013). "Splicing and beyond: The many faces of the Prp19 complex." Biochimica et Biophysica Acta - Molecular Cell Research **1833**(10): 2126-2134.

Charles, T. C. and E. W. Nester (1993). "A chromosomally encoded two-component

- sensory transduction system is required for virulence of *Agrobacterium tumefaciens*." J Bacteriol **175**(20): 6614-6625.
- Chen, C. H., D. I. Kao, et al. (2006). "Functional links between the Prp19-associated complex, U4/U6 biogenesis, and spliceosome recycling." RNA **12**(5): 765-774.
- Chen, H. R., S. P. Jan, et al. (1998). "Snt309p, a component of the Prp19p-associated complex that interacts with Prp19p and associates with the spliceosome simultaneously with or immediately after dissociation of U4 in the same manner as Prp19p." Molecular and Cellular Biology **18**(4): 2196-2204.
- Chen, H. R., T. Y. Tsao, et al. (1999). "Snt309p modulates interactions of Prp19p with its associated components to stabilize the Prp19p-associated complex essential for pre-mRNA splicing." Proceedings of the National Academy of Sciences of the United States of America **96**(10): 5406-5411.
- Chen, Z. (2012). "Molecular analysis of the roles of yeast microtubule-associated genes in *Agrobacterium*-mediated transformation." National University of Singapore.
- Cheng, M., J. E. Fry, et al. (1997). "Genetic Transformation of Wheat Mediated by *Agrobacterium tumefaciens*." Plant Physiol **115**(3): 971-980.
- Cheng, S. C., W. Y. Tarn, et al. (1993). "PRP19: a novel spliceosomal component." Mol Cell Biol **13**(3): 1876-1882.
- Chilton, M. D., M. H. Drummond, et al. (1977). "Stable incorporation of plasmid DNA into higher plant cells: the molecular basis of crown gall tumorigenesis." Cell **11**(2): 263-271.
- Chiu, Y. F., Y. C. Liu, et al. (2009). "Cwc25 is a novel splicing factor required after Prp2 and Yju2 to facilitate the first catalytic reaction." Molecular and Cellular Biology **29**(21): 5671-5678.
- Christie, P. J. (2004). "Type IV secretion: the *Agrobacterium* VirB/D4 and related conjugation systems." Biochim Biophys Acta **1694**(1-3): 219-234.

- Chu, P. C., Y. C. Yang, et al. (2006). "Silencing of p29 affects DNA damage responses with UV irradiation." Cancer Research **66**(17): 8484-8491.
- Citovsky, V., A. Kapelnikov, et al. (2004). "Protein interactions involved in nuclear import of the Agrobacterium VirE2 protein in vivo and in vitro." J Biol Chem **279**(28): 29528-29533.
- Citovsky, V., M. L. Wong, et al. (1989). "Cooperative interaction of Agrobacterium VirE2 protein with single-stranded DNA: implications for the T-DNA transfer process." Proc Natl Acad Sci U S A **86**(4): 1193-1197.
- Citovsky, V., J. Zupan, et al. (1992). "Nuclear localization of Agrobacterium VirE2 protein in plant cells." Science **256**(5065): 1802-1805.
- de Groot, M. J., P. Bundock, et al. (1998). "Agrobacterium tumefaciens-mediated transformation of filamentous fungi." Nat Biotechnol **16**(9): 839-842.
- de Iannino, N. I. and R. A. Ugalde (1989). "Biochemical characterization of avirulent Agrobacterium tumefaciens chvA mutants: synthesis and excretion of beta-(1-2)glucan." J Bacteriol **171**(5): 2842-2849.
- Deng, W., L. Chen, et al. (1998). "Agrobacterium VirD2 protein interacts with plant host cyclophilins." Proceedings of the National Academy of Sciences **95**(12): 7040-7045.
- Depicker, A., M. Van Montagu, et al. (1978). "A DNA region, common to all Ti-plasmids, is essential for oncogenicity [proceedings]." Arch Int Physiol Biochim **86**(2): 422-424.
- Dong, Y., T. M. Burch-Smith, et al. (2007). "A ligation-independent cloning tobacco rattle virus vector for high-throughput virus-induced gene silencing identifies roles for NbMADS4-1 and -2 in floral development." Plant Physiol **145**(4): 1161-1170.
- Dumas, F., M. Duckely, et al. (2001). "An Agrobacterium VirE2 channel for

- transferred-DNA transport into plant cells." Proc Natl Acad Sci U S A **98**(2): 485-490.
- Eisenbrandt, R., M. Kalkum, et al. (1999). "Conjugative pili of IncP plasmids, and the Ti plasmid T pilus are composed of cyclic subunits." J Biol Chem **274**(32): 22548-22555.
- Escobar, M. A. and A. M. Dandekar (2003). "Agrobacterium tumefaciens as an agent of disease." Trends Plant Sci **8**(8): 380-386.
- Fabrizio, P., J. Dannenberg, et al. (2009). "The Evolutionarily Conserved Core Design of the Catalytic Activation Step of the Yeast Spliceosome." Molecular Cell **36**(4): 593-608.
- Farese Jr, R. V. and T. C. Walther (2009). "Lipid Droplets Finally Get a Little R-E-S-P-E-C-T." Cell **139**(5): 855-860.
- Fisk, D. G., C. A. Ball, et al. (2006). "Saccharomyces cerevisiae S288C genome annotation: a working hypothesis." Yeast **23**(12): 857-865.
- Galloway, B. T. (1902). "Applied Botany, Retrospective and Prospective." Science **16**(393): 49-59.
- Garfinkel, D. J. and E. W. Nester (1980). "Agrobacterium tumefaciens mutants affected in crown gall tumorigenesis and octopine catabolism." J Bacteriol **144**(2): 732-743.
- Gaspar, Y. M., J. Nam, et al. (2004). "Characterization of the Arabidopsis lysine-rich arabinogalactan-protein AtAGP17 mutant (rat1) that results in a decreased efficiency of Agrobacterium transformation." Plant Physiology **135**(4): 2162-2171.
- Gavin, A. C., M. Bosche, et al. (2002). "Functional organization of the yeast proteome by systematic analysis of protein complexes." Nature **415**(6868): 141-147.
- Gelvin, S. B. (1998). "Agrobacterium VirE2 proteins can form a complex with T

- strands in the plant cytoplasm." Journal of Bacteriology **180**(16): 4300-4302.
- Gelvin, S. B. (2003). "Agrobacterium-mediated plant transformation: the biology behind the "gene-jockeying" tool." Microbiol Mol Biol Rev **67**(1): 16-37, table of contents.
- Gelvin, S. B. (2009). "Agrobacterium in the genomics age." Plant Physiol **150**(4): 1665-1676.
- Gelvin, S. B. (2010). "Finding a way to the nucleus." Curr Opin Microbiol **13**(1): 53-58.
- Gietl, C., Z. Koukolikova-Nicola, et al. (1987). "Mobilization of T-DNA from Agrobacterium to plant cells involves a protein that binds single-stranded DNA." Proc Natl Acad Sci U S A **84**(24): 9006-9010.
- Gietz, R. D., R. H. Schiestl, et al. (1995). "Studies on the transformation of intact yeast cells by the LiAc/SS-DNA/PEG procedure." Yeast **11**(4): 355-360.
- Goodin, M. M., D. Zaitlin, et al. (2008). "Nicotiana benthamiana: its history and future as a model for plant-pathogen interactions." Molecular Plant-Microbe Interactions **21**(8): 1015-1026.
- Gotzmann, J., C. Gerner, et al. (2000). "hNMP 200: A novel human common nuclear matrix protein combining structural and regulatory functions." Experimental Cell Research **261**(1): 166-179.
- Grange, W., M. Duckely, et al. (2008). "VirE2: a unique ssDNA-compacting molecular machine." PLoS Biol **6**(2): e44.
- Grey, M., A. Düsterhöft, et al. (1996). "Allelism of PSO4 and PRP19 links pre-mRNA processing with recombination and error-prone DNA repair in *Saccharomyces cerevisiae*." Nucleic Acids Research **24**(20): 4009-4014.
- Heid, C. A., J. Stevens, et al. (1996). "Real time quantitative PCR." Genome Research **6**(10): 986-994.

- Henriques, J. A. P., E. J. Vicente, et al. (1989). "PSO4: A novel gene involved in error-prone repair in *Saccharomyces cerevisiae*." Mutation Research **218**(2): 111-124.
- Herrera-Estrella, A., M. Van Montagu, et al. (1990). "A bacterial peptide acting as a plant nuclear targeting signal: the amino-terminal portion of *Agrobacterium* VirD2 protein directs a beta-galactosidase fusion protein into tobacco nuclei." Proc Natl Acad Sci U S A **87**(24): 9534-9537.
- Hiei, Y., S. Ohta, et al. (1994). "Efficient transformation of rice (*Oryza sativa* L.) mediated by *Agrobacterium* and sequence analysis of the boundaries of the T-DNA." Plant J **6**(2): 271-282.
- Hirooka, T. and C. I. Kado (1986). "Location of the right boundary of the virulence region on *Agrobacterium tumefaciens* plasmid pTiC58 and a host-specifying gene next to the boundary." Journal of Bacteriology **168**(1): 237-243.
- Hla, T., A. Q. Jackson, et al. (1995). "Characterization of *edg-2*, a human homologue of the *Xenopus* maternal transcript G10 from endothelial cells." Biochim Biophys Acta **1260**(2): 227-229.
- Hogg, R., J. C. McGrail, et al. (2010). "The function of the NineTeen Complex (NTC) in regulating spliceosome conformations and fidelity during pre-mRNA splicing." Biochemical Society Transactions **38**(4): 1110-1115.
- Hogg, R., Joanne C. McGrail, et al. (2010). "The function of the NineTeen Complex (NTC) in regulating spliceosome conformations and fidelity during pre-mRNA splicing." Biochemical Society Transactions **38**(4): 1110.
- Hood, E. E., S. B. Gelvin, et al. (1993). "New *Agrobacterium* helper plasmids for gene transfer to plants." Transgenic Res **2**(4): 208-218.
- Howard, E. A., J. R. Zupan, et al. (1992). "The VirD2 protein of *A. tumefaciens* contains a C-terminal bipartite nuclear localization signal: implications for

- nuclear uptake of DNA in plant cells." Cell **68**(1): 109-118.
- Hsu, C. L., J. S. Liu, et al. (2014). "Identification of a new androgen receptor (AR) co-regulator BUD31 and related peptides to suppress wild-type and mutated AR-mediated prostate cancer growth via peptide screening and X-ray structure analysis." Mol Oncol.
- Hummon, A. B., S. R. Lim, et al. (2007). "Isolation and solubilization of proteins after TRIzol extraction of RNA and DNA from patient material following prolonged storage." BioTechniques **42**(4): 467-470, 472.
- Kado, C. I. (2000). "The role of the T-pilus in horizontal gene transfer and tumorigenesis." Curr Opin Microbiol **3**(6): 643-648.
- Kang, M. R., S. W. Lee, et al. (2009). "Reciprocal roles of SIRT1 and SKIP in the regulation of RAR activity: Implication in the retinoic acid-induced neuronal differentiation of P19 cells." Nucleic Acids Research **38**(3): 822-831.
- Knapp, S., M. W. Chase, et al. (2004). "Nomenclatural changes and a new sectional classification in *Nicotiana* (Solanaceae)." Taxon **53**(1): 73-82.
- Koncz, C., F. deJong, et al. (2012). "The spliceosome-activating complex: Molecular mechanisms underlying the function of a pleiotropic regulator." Frontiers in Plant Science **3**(JAN).
- Koonin, E. V., P. Bork, et al. (1994). "Yeast chromosome III: new gene functions." EMBO J **13**(3): 493-503.
- Kunik, T., T. Tzfira, et al. (2001). "Genetic transformation of HeLa cells by *Agrobacterium*." Proc Natl Acad Sci U S A **98**(4): 1871-1876.
- Kushner, D. B. (2003). "Systematic, genome-wide identification of host genes affecting replication of a positive-strand RNA virus." Proceedings of the National Academy of Sciences **100**(26): 15764-15769.
- Kushnirov, V. V. (2000). "Rapid and reliable protein extraction from yeast." Yeast **16**(9):

857-860.

Löschner, M., K. Fortschegger, et al. (2005). "Interaction of U-box E3 ligase SNEV with PSMB4, the $\beta 7$ subunit of the 20 S proteasome." Biochemical Journal **388**(2): 593-603.

Lacroix, B. and V. Citovsky (2013). "The roles of bacterial and host plant factors in Agrobacterium-mediated genetic transformation." Int J Dev Biol **57**(6-8): 467-481.

Lacroix, B., T. Tzfira, et al. (2006). "A case of promiscuity: Agrobacterium's endless hunt for new partners." Trends Genet **22**(1): 29-37.

Lacroix, B., M. Vaidya, et al. (2005). "The VirE3 protein of Agrobacterium mimics a host cell function required for plant genetic transformation." EMBO J **24**(2): 428-437.

Laemmli, U. K. (1970). "Cleavage of structural proteins during the assembly of the head of bacteriophage T4." Nature **227**(5259): 680-685.

Lai, E.-M. and C. I. Kado (1998). "Processed VirB2 is the major subunit of the promiscuous pilus of Agrobacterium tumefaciens." Journal of Bacteriology **180**(10): 2711-2717.

Lebaron, S., C. Froment, et al. (2005). "The Splicing ATPase Prp43p Is a Component of Multiple Preribosomal Particles." Molecular and Cellular Biology **25**(21): 9269-9282.

Lee, M. W. and Y. Yang (2006). "Transient expression assay by agroinfiltration of leaves." Methods Mol Biol **323**: 225-229.

Li, X., Q. Yang, et al. (2014). "Direct visualization of Agrobacterium-delivered VirE2 in recipient cells." Plant J **77**(3): 487-495.

Liao, C., B. Hu, et al. (2007). "Genomic screening in vivo reveals the role played by vacuolar H⁺ ATPase and cytosolic acidification in sensitivity to

- DNA-damaging agents such as cisplatin." Mol Pharmacol **71**(2): 416-425.
- Liu, Y. C., H. C. Chen, et al. (2007). "A novel splicing factor, Yju2, is associated with NTC and acts after Prp2 in promoting the first catalytic reaction of pre-mRNA splicing." Molecular and Cellular Biology **27**(15): 5403-5413.
- Liu, Y. L., M. Schiff, et al. (2002). "Tobacco Rar1, EDS1 and NPR1/NIM1 like genes are required for N-mediated resistance to tobacco mosaic virus." Plant Journal **30**(4): 415-429.
- Llosa, M., F. X. Gomis-Ruth, et al. (2002). "Bacterial conjugation: a two-step mechanism for DNA transport." Mol Microbiol **45**(1): 1-8.
- Loake, G. J., A. M. Ashby, et al. (1988). "Attraction of *Agrobacterium tumefaciens* C58C1 towards sugars involves a highly sensitive chemotaxis system." Journal of general microbiology **134**(6): 1427-1432.
- Lockshon, D., L. E. Surface, et al. (2007). "The sensitivity of yeast mutants to oleic acid implicates the peroxisome and other processes in membrane function." Genetics **175**(1): 77-91.
- Looke, M., K. Kristjuhan, et al. (2011). "Extraction of genomic DNA from yeasts for PCR-based applications." BioTechniques **50**(5): 325-328.
- Loyter, A., J. Rosenbluh, et al. (2005). "The plant VirE2 interacting protein 1. A molecular link between the *Agrobacterium* T-complex and the host cell chromatin?" Plant Physiology **138**(3): 1318-1321.
- Lu, R., A. M. Martin-Hernandez, et al. (2003). "Virus-induced gene silencing in plants." Methods **30**(4): 296-303.
- Mahajan, K. N. and B. S. Mitchell (2003). "Role of human Pso4 in mammalian DNA repair and association with terminal deoxynucleotidyl transferase." Proceedings of the National Academy of Sciences of the United States of America **100**(19): 10746-10751.

- Masciadri, B., L. B. Areces, et al. (2004). "Characterization of the BUD31 gene of *Saccharomyces cerevisiae*." Biochemical and Biophysical Research Communications **320**(4): 1342-1350.
- Matthysse, A. G. (1983). "Role of bacterial cellulose fibrils in *Agrobacterium tumefaciens* infection." J Bacteriol **154**(2): 906-915.
- Matthysse, A. G. (1987). "Characterization of nonattaching mutants of *Agrobacterium tumefaciens*." J Bacteriol **169**(1): 313-323.
- Matthysse, A. G. and S. McMahan (1998). "Root colonization by *Agrobacterium tumefaciens* is reduced in *cel*, *attB*, *attD*, and *attR* mutants." Appl Environ Microbiol **64**(7): 2341-2345.
- Meinel, D. M., C. Burkert-Kautzsch, et al. (2013). "Recruitment of TREX to the Transcription Machinery by Its Direct Binding to the Phospho-CTD of RNA Polymerase II." PLoS Genetics **9**(11).
- Mnaimneh, S., A. P. Davierwala, et al. (2004). "Exploration of Essential Gene Functions via Titratable Promoter Alleles." Cell **118**(1): 31-44.
- Murashige, T. and F. Skoog (1962). "A revised medium for rapid growth and bio assays with tobacco tissue cultures." Physiologia plantarum **15**(3): 473-497.
- Nair, G. R., Z. Liu, et al. (2003). "Reexamining the role of the accessory plasmid pAtC58 in the virulence of *Agrobacterium tumefaciens* strain C58." Plant Physiol **133**(3): 989-999.
- Nam, J., A. G. Matthysse, et al. (1997). "Differences in susceptibility of *Arabidopsis* ecotypes to crown gall disease may result from a deficiency in T-DNA integration." The Plant Cell Online **9**(3): 317-333.
- Nam, J., K. S. Mysore, et al. (1999). "Identification of T-DNA tagged *Arabidopsis* mutants that are resistant to transformation by *Agrobacterium*." Mol Gen Genet **261**(3): 429-438.

- Nautiyal, S. (2002). "The genome-wide expression response to telomerase deletion in *Saccharomyces cerevisiae*." Proceedings of the National Academy of Sciences **99**(14): 9316-9321.
- Neff, N. T. and A. N. Binns (1985). "Agrobacterium tumefaciens interaction with suspension-cultured tomato cells." Plant Physiology **77**(1): 35-42.
- Neff, N. T., A. N. Binns, et al. (1987). "Inhibitory Effects of a Pectin-Enriched Tomato Cell Wall Fraction on Agrobacterium tumefaciens Binding and Tumor Formation." Plant Physiol **83**(3): 525-528.
- Ni, L. and M. Snyder (2001). "A genomic study of the bipolar bud site selection pattern in *Saccharomyces cerevisiae*." Molecular Biology of the Cell **12**(7): 2147-2170.
- Offringa, R., M. De Groot, et al. (1990). "Extrachromosomal homologous recombination and gene targeting in plant cells after Agrobacterium mediated transformation." The EMBO Journal **9**(10): 3077.
- Ohi, M. D., A. J. Link, et al. (2002). "Proteomics Analysis Reveals Stable Multiprotein Complexes in Both Fission and Budding Yeasts Containing Myb-Related Cdc5p/Cef1p, Novel Pre-mRNA Splicing Factors, and snRNAs." Molecular and Cellular Biology **22**(7): 2011-2024.
- Ohi, M. D., C. W. Vander Kooi, et al. (2003). "Structural insights into the U-box, a domain associated with multi-ubiquitination." Nature Structural Biology **10**(4): 250-255.
- Pereira, F. B., P. M. Guimaraes, et al. (2011). "Identification of candidate genes for yeast engineering to improve bioethanol production in Very-High-Gravity and lignocellulosic biomass industrial fermentations." Biotechnol Biofuels **4**(1): 57.
- Piers, K. L., J. D. Heath, et al. (1996). "Agrobacterium tumefaciens-mediated transformation of yeast." Proceedings of the National Academy of Sciences **93**(4): 1613-1618.

- Piers, K. L., J. D. Heath, et al. (1996). "Agrobacterium tumefaciens-mediated transformation of yeast." Proceedings of the National Academy of Sciences of the United States of America **93**(4): 1613-1618.
- Reid, R. J. D., S. Gonzalez-Barrera, et al. (2010). "Selective ploidy ablation, a high-throughput plasmid transfer protocol, identifies new genes affecting topoisomerase I-induced DNA damage." Genome Research **21**(3): 477-486.
- Relic, B., M. Andjelkovic, et al. (1998). "Interaction of the DNA modifying proteins VirD1 and VirD2 of Agrobacterium tumefaciens: analysis by subcellular localization in mammalian cells." Proc Natl Acad Sci U S A **95**(16): 9105-9110.
- Roberts, R. L. (2003). "Purine synthesis and increased Agrobacterium tumefaciens transformation of yeast and plants." Proceedings of the National Academy of Sciences **100**(11): 6634-6639.
- Rossi, L., B. Hohn, et al. (1996). "Integration of complete transferred DNA units is dependent on the activity of virulence E2 protein of Agrobacterium tumefaciens." Proc Natl Acad Sci U S A **93**(1): 126-130.
- Saha, D., S. Banerjee, et al. (2012). "Context dependent splicing functions of Bud31/Ycr063w define its role in budding and cell cycle progression." Biochem Biophys Res Commun **424**(3): 579-585.
- Saha, D., P. Khandelia, et al. (2012). "S.cerevisiae NineTeen complex (NTC) associated factor Bud31/Ycr063w assembles on pre-catalytic spliceosomes and improves first and second step pre-mRNA splicing efficiency." J Biol Chem.
- Saha, D., P. Khandelia, et al. (2012). "Saccharomyces cerevisiae NineTeen Complex (NTC)-associated Factor Bud31/Ycr063w Assembles on Precatalytic Spliceosomes and Improves First and Second Step Pre-mRNA Splicing Efficiency." Journal of Biological Chemistry **287**(8): 5390-5399.
- Sahi, C., T. Lee, et al. (2010). "Cwc23, an essential J protein critical for pre-mRNA

- splicing with a dispensable J domain." Molecular and Cellular Biology **30**(1): 33-42.
- Sambrook, J., D. W. D. W. Russell, et al. (2001). Molecular cloning : a laboratory manual, Cold Spring Harbor Laboratory.
- Sciaky, D., A. L. Montoya, et al. (1978). "Fingerprints of Agrobacterium Ti plasmids." Plasmid **1**(2): 238-253.
- Shurvinton, C. E., L. Hodges, et al. (1992). "A nuclear localization signal and the C-terminal omega sequence in the Agrobacterium tumefaciens VirD2 endonuclease are important for tumor formation." Proc Natl Acad Sci U S A **89**(24): 11837-11841.
- Si, Y. C., S. S. Eui, et al. (2007). "Identification of mouse Prp19p as a lipid droplet-associated protein and its possible involvement in the biogenesis of lipid droplets." Journal of Biological Chemistry **282**(4): 2456-2465.
- Sihn, C. R., S. Y. Cho, et al. (2007). "Mouse homologue of yeast Prp19 interacts with mouse SUG1, the regulatory subunit of 26S proteasome." Biochemical and Biophysical Research Communications **356**(1): 175-180.
- Smith, E. F. and C. O. Townsend (1907). "A Plant-Tumor of Bacterial Origin." Science **25**(643): 671-673.
- Stäßer, K., S. Masuda, et al. (2002). "TREX is a conserved complex coupling transcription with messenger RNA export." Nature **417**(6886): 304-308.
- Stachel, S. E., G. An, et al. (1985). "A Tn3 lacZ transposon for the random generation of beta-galactosidase gene fusions: application to the analysis of gene expression in Agrobacterium." EMBO J **4**(4): 891-898.
- Stachel, S. E., B. Timmerman, et al. (1986). "Generation of Single-Stranded T-DNA Molecules during the Initial-Stages of T-DNA Transfer from Agrobacterium-Tumefaciens to Plant-Cells." Nature **322**(6081): 706-712.

- Stark, C., B. J. Breitkreutz, et al. (2006). "BioGRID: a general repository for interaction datasets." Nucleic Acids Res **34**(Database issue): D535-539.
- Swart, S., T. J. Logman, et al. (1994). "Purification and partial characterization of a glycoprotein from pea (*Pisum sativum*) with receptor activity for rhicadhesin, an attachment protein of Rhizobiaceae." Plant Mol Biol **24**(1): 171-183.
- Tao, Y., P. K. Rao, et al. (2004). "Expression of plant protein phosphatase 2C interferes with nuclear import of the Agrobacterium T-complex protein VirD2." Proc Natl Acad Sci U S A **101**(14): 5164-5169.
- Tarn, W. Y., K. R. Lee, et al. (1993). "The yeast PRP19 protein is not tightly associated with small nuclear RNAs, but appears to associate with the spliceosome after binding of U2 to the pre-mRNA and prior to formation of the functional spliceosome." Molecular and Cellular Biology **13**(3): 1883-1891.
- Thanassi, D. G., J. B. Bliska, et al. (2012). "Surface organelles assembled by secretion systems of Gram-negative bacteria: diversity in structure and function." FEMS Microbiol Rev **36**(6): 1046-1082.
- Tinland, B., Z. Koukolikova-Nicola, et al. (1992). "The T-DNA-linked VirD2 protein contains two distinct functional nuclear localization signals." Proc Natl Acad Sci U S A **89**(16): 7442-7446.
- Toki, S. (1997). "Rapid and efficient Agrobacterium-mediated transformation in rice." Plant Molecular Biology Reporter **15**(1): 16-21.
- Tomlinson, A. D., B. Ramey-Hartung, et al. (2010). "Agrobacterium tumefaciens ExoR represses succinoglycan biosynthesis and is required for biofilm formation and motility." Microbiology **156**(Pt 9): 2670-2681.
- Toro, N., A. Datta, et al. (1989). "The Agrobacterium tumefaciens virC1 gene product binds to overdrive, a T-DNA transfer enhancer." J Bacteriol **171**(12): 6845-6849.

- Tu, H. (2010). "A global profile of yeast genes involved in Agrobacterium-yeast gene transfer." National University of Singapore.
- Tzfira, T. and V. Citovsky (2006). "Agrobacterium-mediated genetic transformation of plants: biology and biotechnology." Curr Opin Biotechnol **17**(2): 147-154.
- Tzfira, T., M. Vaidya, et al. (2001). "VIP1, an Arabidopsis protein that interacts with Agrobacterium VirE2, is involved in VirE2 nuclear import and Agrobacterium infectivity." The EMBO Journal **20**(13): 3596-3607.
- Uetz, P., L. Giot, et al. (2000). "A comprehensive analysis of protein-protein interactions in *Saccharomyces cerevisiae*." Nature **403**(6770): 623-627.
- Valentine, L. (2003). "Agrobacterium tumefaciens and the plant: the David and Goliath of modern genetics." Plant Physiol **133**(3): 948-955.
- van Attikum, H., P. Bundock, et al. (2001). "Non-homologous end-joining proteins are required for Agrobacterium T-DNA integration." EMBO J **20**(22): 6550-6558.
- van Attikum, H. and P. J. Hooykaas (2003). "Genetic requirements for the targeted integration of Agrobacterium T-DNA in *Saccharomyces cerevisiae*." Nucleic Acids Res **31**(3): 826-832.
- Van Larebeke, N., G. Engler, et al. (1974). "Large plasmid in *Agrobacterium tumefaciens* essential for crown gall-inducing ability." Nature **252**(5479): 169-170.
- Wagner, V. and A. Matthyse (1992). "Involvement of a vitronectin-like protein in attachment of *Agrobacterium tumefaciens* to carrot suspension culture cells." Journal of Bacteriology **174**(18): 5999-6003.
- Wahl, M. C., C. L. Will, et al. (2009). "The Spliceosome: Design Principles of a Dynamic RNP Machine." Cell **136**(4): 701-718.
- Wang, Q., J. He, et al. (2005). "Interactions of the Yeast SF3b Splicing Factor." Molecular and Cellular Biology **25**(24): 10745-10754.

- Warkocki, Z., P. Odenwälder, et al. (2009). "Reconstitution of both steps of *Saccharomyces cerevisiae* splicing with purified spliceosomal components." Nature Structural and Molecular Biology **16**(12): 1237-1243.
- Wilkinson, K. D. (2000). "Ubiquitination and deubiquitination: Targeting of proteins for degradation by the proteasome." Seminars in Cell and Developmental Biology **11**(3): 141-148.
- Will, C. L. and R. Lührmann (2011). "Spliceosome structure and function." Cold Spring Harbor Perspectives in Biology **3**(7): 1-2.
- Wilson, T. E. (2002). "A genomics-based screen for yeast mutants with an altered recombination/end-joining repair ratio." Genetics **162**(2): 677-688.
- Winzler, E. A., D. D. Shoemaker, et al. (1999). "Functional characterization of the *S. cerevisiae* genome by gene deletion and parallel analysis." Science **285**(5429): 901-906.
- Yang, Q. (2013). Molecular analysis of the role of yeast mitochondrial protein QCR7p in *Agrobacterium*-yeast DNA transfer.
- Zambryski, P., H. Joos, et al. (1983). "Ti plasmid vector for the introduction of DNA into plant cells without alteration of their normal regeneration capacity." EMBO J **2**(12): 2143-2150.
- Zhou, S. and S. D. Hayward (2001). "Nuclear localization of CBF1 is regulated by interactions with the SMRT corepressor complex." Molecular and Cellular Biology **21**(18): 6222-6232.
- Zhu, Y. (2003). "Identification of Arabidopsis rat Mutants." Plant Physiology **132**(2): 494-505.
- Zhu, Y., J. Nam, et al. (2003). "Agrobacterium-mediated root transformation is inhibited by mutation of an Arabidopsis cellulose synthase-like gene." Plant Physiology **133**(3): 1000-1010.

- Zhu, Y., J. Nam, et al. (2003). "Identification of Arabidopsis rat mutants." Plant Physiol **132**(2): 494-505.
- Ziemienowicz, A. (2001). "Odyssey of agrobacterium T-DNA." Acta Biochim Pol **48**(3): 623-635.
- Ziemienowicz, A., B. Tinland, et al. (2000). "Plant Enzymes but Not AgrobacteriumVirD2 Mediate T-DNA Ligation In Vitro." Molecular and Cellular Biology **20**(17): 6317-6322.
- Zupan, J. R. and P. Zambryski (1995). "Transfer of T-DNA from Agrobacterium to the plant cell." Plant Physiol **107**(4): 1041-1047.